UNIVERSITEIT VAN PRETORIA
UNIVERSITY OF PRETORIA
YUNIBESITHI YA PRETORIA

Characterisation of the pre-invasion glycophosphatidylinositol-anchored surface proteins of *Plasmodium falciparum* merozoites

by

Tarryn Lee Venter

A dissertation submitted in fulfilment of the requirements for the degree

Magister Scientiae

in

Pharmacology

in the

Faculty of Health Sciences

at the

University of Pretoria

Supervisor: Prof. A.D. Cromarty

Department of Pharmacology, University of Pretoria

Co-supervisor: Prof. L.M. Birkholtz

Department of Biochemistry, University of Pretoria

2017

Acknowledgements

I would like to acknowledge and give sincere thanks to the following people for their assistance, support and understanding throughout the duration of this study:

- My supervisor, Prof. Duncan Cromarty for his support, guidance and belief in me during my postgraduate years
- My co-supervisor, Prof. Lyn-Marie Birkholtz for her advice and guidance
- Dr Stoyan Stoychev for his technical assistance and expert advice
- The staff and students at the Department of Biochemistry and the Department of Pharmacology for their friendship and encouragement
- The Council for Scientific and Industrial Research (CSIR) for the use of their proteomic facilities
- The National Research Foundation (NRF) for their financial assistance
- My parents, Charmaine and Eddy for their understanding and love throughout this journey
- Alan and Bev Gould for their constant love and support
- Ryan Gould for being there unconditionally, and his continuous motivation, patience and belief in me
- My heavenly father for always keeping me in the palm of his hand

Table of Contents

Declaration

University of Pretoria

Faculty of Health Sciences

Department of Pharmacology

I, Tarryn Lee Venter,

Student number: 29223492

Subject of study: Characterisation of the pre-invasion glycophosphatidylinositol-anchored surface proteins of *Plasmodium falciparum* merozoites

Declaration

1. I understand what plagiarism entails and am aware of the University's policy in this regard.
2. I declare that this dissertation is my own original work. Where someone else's work was used (whether from a printed source, internet or any other source) due acknowledgement was given and reference was made according to departmental requirements.
3. I did not make use of another student's previous work and submit it as my own.
4. I did not allow and will not allow anyone to copy my work with the intention of presenting it as his or her own work.

Signature: 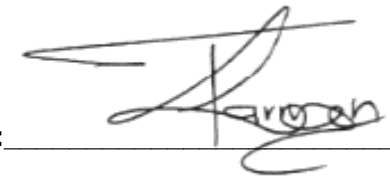

Abstract

Plasmodium falciparum is a protozoan parasite responsible for causing the most severe form of malaria in humans. This species is responsible for over 90% of malaria mortalities which occur predominantly in Africa. An increase in drug resistant parasites in recent years is threatening the progress made against malaria and thus new antimalarial drugs and vaccines are needed to combat this disease.

During the intraerythrocytic phase, merozoites egress from mature schizonts to invade new uninfected erythrocytes. Glycophosphatidylinositol (GPI) -anchored proteins cover most of the exterior surface of the merozoite prior to invasion, while other GPI-anchored proteins are released onto the merozoite surface through apical organelle secretions. These proteins are involved in interactions with erythrocytes and are thought to be vital to erythrocyte invasion. GPI-anchored proteins have also been implicated as a cause of pathogenic symptoms and activation of immune components. These proteins are then released or cleaved to enable merozoite entry into the erythrocyte. Several enzymes are thought to be involved in their cleavage including the serine proteases subtilisin-like proteases (SUB) 1 and 2, and phosphatidylinositol-phospholipase C (PI-PLC); GPI-anchored proteins are also generally sensitive to phospholipase A_2 (PLA_2). Cleaved proteins are released into the host blood system, while uncleaved proteins are carried into the erythrocyte during invasion.

Merozoites have a limited period in which they retain invasive capacity. A previous lack of available techniques that are specifically adapted to merozoite analysis has resulted in an incomplete understanding of invasion and GPI-anchored protein involvement in invasion. This study aimed to determine how GPI-anchored proteins on the merozoite surface are altered in the invasive phase, and explore the possibility of using merozoite GPI-anchored proteins as potential drug targets to block erythrocyte invasion.

Optimised methods of *in vitro* parasite culturing which produce highly synchronised merozoites was essential to this study. Parasite culturing techniques were optimised by utilising low haematocrit cultures with frequent culture splitting and optimised synchronisation. The “Malarwheel” is a tool that was developed for this research to provide a means for scheduling sorbitol treatments and MACs isolations. This tool and optimised culturing methods enabled large volumes of highly synchronised invasive merozoites to be harvested. Four compounds (vanadate, edelfosine, dioctyl sodium sulfosuccinate (DSS), and gentamicin) suspected to interfere with GPI-anchored cleavage or processes were screened on intraerythrocytic stages and merozoites.

Antimalarial and anti-invasive properties of these compounds were screened by modified malaria SYBR Green I-based fluorescence (MSF) assay and merozoite invasion assays (MIA) respectively. DSS and gentamicin showed limited potential as antimalarials or as anti-invasive agents. Vanadate and edelfosine both showed antimalarial and anti-invasive activity, while edelfosine was the most potent anti-invasive agent at physiological concentrations.

The merozoite GPI-anchored proteome was analysed by sodium dodecyl sulphate-polyacrylamide gel electrophoresis (SDS-PAGE) followed by complete gel lane analyses conducted by liquid chromatography-tandem mass spectrometry (LC-MS/MS) on soluble and pelleted merozoite proteins in samples from either invasive or non-invasive merozoites. Thirteen known or predicted GPI-anchored proteins were identified in samples. Several changes were identified in merozoite GPI-anchored proteins between the invasive phase and after its completion, and minor differences were observed following treatment with edelfosine. Edelfosine showed partial inhibition of erythrocyte invasion, however, the primary cause of inhibition cannot be directly related to interferences with GPI-anchored proteins. These results suggest that GPI-anchored proteins are controlled by various complex processes, and are cleaved or processed by diverse mechanisms during the invasive phase. These mechanisms may be controlled by multiple signals which effect proteins or groups of proteins in specific ways. These signals may be influenced by “checkpoints” during invasion processes including the time period after egress from schizonts, and possibly the recognition of erythrocyte targets.

These methods and results provide a foundation for future research to enable culturing of *P. falciparum* parasites specifically for merozoite research, and to identify merozoite proteins active during the invasive phase. These results confirm and challenge previous ideas reported in literature on the GPI-anchored processes of merozoites and further characterise less studied GPI-anchored proteins. The results suggest that the processes controlling GPI-anchored proteins may be more complex than previously thought. These results form a basis to further identify and characterise GPI-anchored proteins in the aim to develop antimalarial medications and vaccines that target merozoites and their GPI-anchored processes.

Keywords: Malaria, *Plasmodium falciparum,* merozoite, erythrocyte invasion, cell culture, MACs Isolation, MSF assay, Merozoite invasion assay, SDS-PAGE, electrophoresis, LC-MS/MS, proteomics

List of Abbreviations

°C	Degree Celsius
%	Percentage
µL	Microliter
µM	Micromolar
µm	Micrometre
2DE	Two-dimensional gel electrophoresis
ACN	Acetonitrile
ACT	Artemisinin based combination therapy
ALP	Alkyl-lysophospholipid
AM	Artemether
AMA1	Apical membrane antigen 1
AQ	Amodiaquine
ART	Artemisinin
AS	Artesunate
ASP	Apical sushi protein
AT	Atavaquone
ATP	Adenosine triphosphate
BCA	Bicinchoninic acid
BSA	Bovine serum albumin
CCM	Complete culture media
CL	Clindamycin
CM	Culture media
cm^2	Centimetres squared
CO_2	Carbon dioxide
CQ	Chloroquine
C-terminal	Carboxyl-terminal
$CuSO_4$	Cupric sulphate
CyRPA	Cysteine-rich protective antigen
D	Doxycycline
DBL	Duffy binding-like
DDA	Data-dependent acquisition
DDT	Dichlorodiphenyltrichloroethane

DHA	Dihydroartemisinin
DHFR	Dihydrofolate reductase
DHPS	Dihydropteroate synthase
DIA	Data-independent acquisition
DMSO	Dimethyl sulfoxide
DNA	Deoxyribonucleic acid
DPM1	Dolichol-phosphate mannosyltransferase polypeptide 1
DSS	Dioctyl sodium sulfosuccinate
DTT	Dithiothreitol
DV	Digestive vacuole
E64	*trans*-Epoxysuccinyl-L-leucylamido(4-guanidino) butane
EBA	Erythrocyte binding antigen
EDTA	Ethylenediaminetetraacetic acid
EGF	Epidermal growth factor
ER	Endoplasmic reticulum
ETOH	Ethanol
FA	Formic acid
FDR	False discovery rate
GAMA	GPI-anchored micronemal antigen
GlcNAc	N-Acetylglucosamine
GlcNAc-PI	N-Acetylglucosamine-phosphatidylinositol
GlcN-PI	N-Glucosamine-phosphatidylinositol
GPA	Glycophorin A
GPC	Glycophorin C
GPI	Glycophosphatidylinositol
GTP	Guanosine-5'-triphosphate
HABP	High affinity binding peptide
HEPES	4-(2-hydroxyethyl)-1-piperazineethanesulfonic acid
hpi	Hours post invasion
HPLC	High performance liquid chromatography
hr	Hour
IAA	Iodoacetamide
IC_{50}	Inhibitory concentration causing 50% inhibition

ICAM1	Intracellular adhesion molecule 1
ICM	Incomplete culture media
IL	Interleukin
INF-c	Interferon-c
IP	Inositol phosphate
IP_3	Inositol 1,4,5-triphosphate
IRS	Indoor residual spraying
ITN	Insecticide treated net
KCl	Potassium chloride
kDa	Kilodaltons
kV	Kilovolts
L	Litre
LC-MS/MS	Liquid chromatography tandem mass spectrometry
LLIN	Long lasting insecticidal net
LM	Lumefantrine
MACs	Magnetic-activated cell sorting
man	Mannose
MCV	Mean corpuscular volume
MEOH	Methanol
mETC	Mitochondrial electron transport chain
mg	Milligram
MIA	Merozoite invasion assay
min	Minute
mL	Millilitre
mM	Millimolar
MQ	Mefloquine
msec	Millisecond/s
MSF	Malaria SYBR green I-based fluorescence
MSP	Merozoite surface protein
N_2	Nitrogen
Na_2CO_3	Sodium carbonate
NaCl	Sodium chloride
$NaHCO_3$	Sodium bicarbonate
NaOH	Sodium hydroxide

ng	Nanogram
NH_4HCO_3	Ammonium bicarbonate
NKT	Natural killer T cells
nm	Nanometre
NO	Nitric oxide
NQ	Naphtoquine
N-terminal	Amino-terminal
O_2	Oxygen
P	Pyrimethamine
PBS	Phosphate buffered saline
PEtN	Phosphoethanolamine
Pf	*Plasmodium falciparum*
*Pf*CRT	*P. falciparum* chloroquine resistance transporter
*Pf*MDR1	*P. falciparum* multidrug resistance 1
*Pf*Rh	*P. falciparum* reticulocyte binding-like homolog
*Pf*Ripr	*P. falciparum* Rh5-interacting protein
PG	Proguanil
pH	Negative logarithm of the hydrogen ion concentration
PI	Phosphatidylinositol
PIG	Phosphatidylinositol n- acetylglucosaminyltransferase
PIP_2	Phosphatidylinositol 4,5-bisphosphate
PI-PLC	Phosphatidylinositol-Phospholipase C
PLA	Phospholipase A
PO_4^{3-}	Phosphate
PPQ	Piperaquine
PQ	Primaquine
PVM	Parasitophorous vacuolar membrane
PYR	Pyronaridine
QN	Quinine
RAMA	Rhoptry-associated membrane antigen
RON	Rhoptry Neck Protein
rpm	Revolutions per minute
RPMI	Roswell Park Memorial Institute
RSLC	Rapid separation liquid chromatography

S	Sulfodoxine
SDS-PAGE	Sodium dodecyl sulphate-Polyacrylamide gel electrophoresis
sec	Second/s
SEM	Standard error of the mean
SH	Sulfhydryl
SOV	Sodium orthovanadate
SP	Sulfadoxine plus pyrimethamine
SUB	Subtilisin-like protease
T	Tetracycline
TCA	Trichloroacetic acid
TNF-α	Tumour necrosis factor-α
Tris-HCl	Tris-(hydroxymethyl)aminomethane hydrochloride
UV	Ultraviolet
V	Volts
v/v	Volume per volume
VCAM-1	Vascular cell adhesion molecule 1
w/v	Weight per volume
WHO	World Health Organization
x*g*	Gravitational force

List of Figures

Chapter 1

Chapter 2

Chapter 3

List of Tables

Chapter 1

Chapter 2

Chapter 3

Chapter 1: Introduction

"The damage this disease does is quite incredible… The parasite has been killing children and sapping the strength of whole populations for tens of thousands of years… Now we can chart a course to end it."

Bill Gates

1.1 Introduction to malaria

Malaria is a disease caused by the protozoan *Plasmodium* parasite that is prevalent in tropical and subtropical regions around the world. Having affected generations of people for thousands of years, malaria has had debilitating effects on public health and economic development in endemic countries.[1] Throughout history, at least 40% of global populations have been at risk of contracting malaria. While numerous control and eradication methods have actively been employed to reduce the incidence of malaria, history has shown that this disease is complex and "intelligent" in the fact that it has often adapted its molecular pathways to evade elimination.

The emergence of insecticide resistant vectors and drug resistant parasites threatens any progress made against eliminating malaria. With a lack of effective malaria vaccines available and with a decrease in drug efficacy, there is a need to find new antimalarial targets. An ideal new antimalarial drug would need to combat parasitic pathways different to those inhibited by current treatments, and target an essential process within the parasite's lifecycle in order to prolong a compounds effective lifespan and ultimately, lead to malaria elimination.

1.2 Lifecycle of *Plasmodium falciparum*

There are over 100 species of *Plasmodium* which infect many animals such as reptiles, birds, and various mammals. Five species of *Plasmodium* are recognised to infect humans, these are: *P. falciparum, P. ovale, P. malariae, P. vivax,* and *P. knowlesi* (a zoonotic form of malaria).[2] Of these species, *P. falciparum* is the most virulent of the species, causing the most severe malaria symptoms, and accounting for over 90% of global malaria mortalities which occur predominantly in Sub-Saharan African regions.[3, 4] For these reasons, *P. falciparum* will be focused on in this study. *P. vivax* is also an important species to take note of, as it has greater resilience to changing temperatures and higher altitudes and is the most widely geographically distributed parasite, being found in all regions where malaria is endemic.

The *Plasmodium* parasite has two separate host organisms, spending part of its lifecycle within the female *Anopheles* mosquito and part within a vertebrate host. The parasite has multiple stages within both the sexual and asexual replicative cycles (Figure 1.1). The parasite is transmitted through the bite of an unknowingly infected female *Anopheles* mosquito while taking a blood meal from a vertebrate.

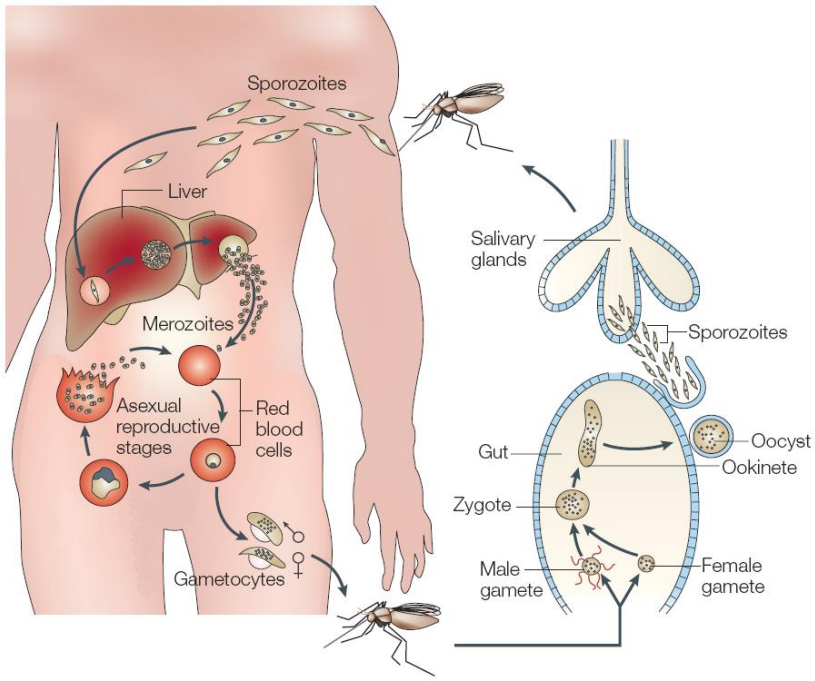

Figure 1.1: The complete lifecycle of the *Plasmodium* parasite. The malaria parasite has two separate host organisms spending part of its lifecycle within the female *Anopheles* mosquito and part within a vertebrate host; the parasite undergoes sexual and asexual replicative stages. (Adapted from Harper *et al.* 2005[5] with permission)

As the mosquito bites to take a blood meal, it expels the contents of its salivary glands which contains several hundred sporozoites[6] into the subcutaneous capillaries of the new host. These sporozoites travel though the circulatory system where only a few successfully reach the liver where they invade hepatocytes. The hepatic phase of malaria lasts for 10–14 days during which no typical malaria symptoms are experienced, therefore the presence of the parasite is unknown to the host. During this time, the parasites differentiate and undergo mitosis and 13–14 rounds of deoxyribonucleic acid (DNA) synthesis and nuclear division (schizogony) which results in tens of

thousands of nuclei. These nuclei lead to the production of liver stage merozoites. Once the hepatocytes have been saturated with merosomes (vesicles containing merozoites) these are released into the circulatory system and rupture releasing merozoites.

Merozoites target and invade erythrocytes to commence the intraerythrocytic phase of the parasite lifecycle.[7] Erythrocytes are prime targets of the *Plasmodium* parasite as they lack a nucleus and organelles, and provide the parasite with a space and nutrients to replicate in a secure location hidden from the host's immune defences. The *P. falciparum* intraerythrocytic cycle lasts 48 hours (hrs) during which the merozoite develops sequentially into a ring stage followed by trophozoite and then schizont stages (Figure 1.2). The ring stage progresses from 0–22 hrs post invasion (hpi). Characteristic of the ring stage is the typical stained ring shape which when stained can be seen with light microscopy. Here, the parasite begins to feed on the erythrocyte contents and metabolises the erythrocyte's haemoglobin to use the amino acids for growth and development.

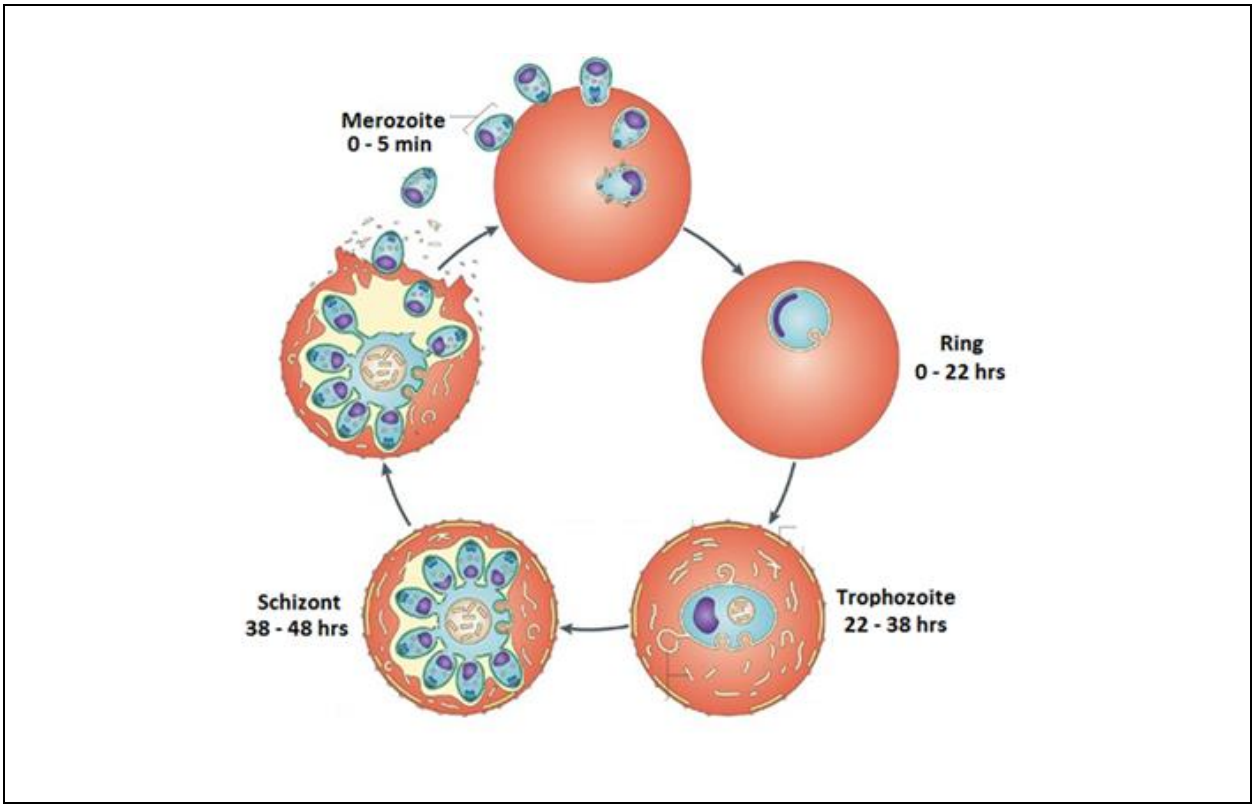

Figure 1.2: The asexual intraerythrocytic lifecycle of the *Plasmodium* parasite. The merozoite invades erythrocytes and progresses over a 48 hr period into ring, trophozoites and schizont stage. (Adapted from Haldar *et al* .2006[8] with permission)

The metabolism of haemoglobin results in an iron containing by-product called haeme to accumulate in the parasite. Haeme is toxic to the parasite, but the parasite has developed the ability to neutralise haeme by converting it into a non-toxic crystalline product called haemozoin. By the time the parasite reaches the end of the trophozoite stage, which progresses from 22–38 hpi, it would have used approximately 80% of cytosolic haemoglobin.[9, 10] The heamozoin crystals produced during the intraerythrocytic lifecycle accumulate within a large parasitic food vacuole and combine to produce a large heamozoin crystal. The heamozoin crystal contains sufficient amounts of ferric iron obtained from the degraded haemoglobin to impart paramagnetic properties to the crystal.

During the trophozoite stage, DNA replication occurs in an endomitotic fashion, where the chromosomes do not condense and the nuclear envelope remains intact throughout mitosis, and these only divide once all DNA synthesis has been completed.[7, 11] DNA replication does not occur synchronously, and because the cell does not divide after each nuclear division, multinuclear cells develop which contain significantly different numbers of nuclei between parasites. These nuclei then separate into daughter merozoites during schizogony. Parasites of the same clonal line may develop between 2-3 fold the number of merozoites (8-24 merozoites in the 3D7 strain) from a singly infected erythrocyte.[11]

Schizont phase (38-48 hpi) commences with the production of merozoite rough endoplasmic reticulum (ER), free ribosomes, mitochondria and plastids, and large lipid vacuoles that are used for the development of the parasite membrane and other lipids. Merozoites develop around a parasite centre where the apical organelles develop. Many of the secretory apical organelles develop from vesicles that bud off from the nuclear envelope. Once the merozoites have matured, a protein coat is added to the merozoite surface. Several minutes preceding the release from schizonts the spaces within the parasitophous vacuole become filled with a “fuzzy” material known to include several parasite antigens.[12, 13] Biochemical and enzymatic alterations destabilise the mature schizont’s cytoskeleton causing it to swell under osmotic pressure and burst to release the mature invasive merozoites.[14, 15]

The majority of merozoites which invade new erythrocytes continue growing in the asexual replicative cycle, while others develop into gametocytes to commence the sexual phases of *Plasmodium* replication. Merozoites produced from a single schizont will differentiate either into all male or all female gametocytes.[16] Gametocyte production is induced by a switch that occurs when environmental conditions such as glucose and other nutrient supplies being to diminish,[17, 18]

thus inferring that the parasite prepares to be transferred to a new host. Commitment to gametocyte development is initiated during the parasite's preceding intraerythrocytic phase. Mature male and female gametocytes (maturing over approximately 8-12 days) are taken up by a mosquito during a blood meal.[17, 19] The gametocytes fertilise to form zygotes and then continue into ookinetes that develop into oocysts within the mosquito's gut lining. These oocytes grow and develop producing several thousand haploid sporozoites that burst out and migrate to the mosquito's salivary glands. These sporozoites are then released into a new host during a blood meal to recommence a secondary host phase of the lifecycle.

1.3 Clinical features of malaria

The clinical symptoms of malaria are experienced during the intraerythrocytic phase, and initially occur in 48 hr cycles corresponding to time at which merozoites egress from schizonts and invade new erythrocytes. Uncomplicated malaria symptoms are attributed to antigens released by the parasite and the immune system's reaction to these toxins by mass cytokine release. Although there may be various components involved in malaria pathogenesis and production of inflammatory cytokines, glycophosphatidylinositol (GPI) –anchored surface proteins have been proposed to be the primary parasite component responsible for malaria symptoms.[20, 21] Malaria initially presents itself as uncomplicated malaria expressing episodic flu like symptoms such as fever, chills, and headaches, muscle aches along with nausea, vomiting, abdominal pain and diarrhoea. The chances of developing malaria complications are increased in children below the age of five, pregnant woman and malaria naïve individuals.

Severe malaria is the result of the disease manifestations that generally involve the central nervous, pulmonary, renal and haematopoietic systems. There are several combining factors which result in severe malaria. First, a parasitaemia greater than 5% with a compounding parasite load destroys masses of healthy oxygen transporting erythrocytes causing severe anaemia. Second, expression of parasitic adhesion molecules on late stage trophozoite infected erythrocytes enables these erythrocytes to adhere to endothelial cells in capillaries of organs. Rosettes of parasitised erythrocytes form where several parasites conjoin around a central parasite; this results in microvascular obstructions which may occur in single or multiple organs such as the placenta of pregnant women, lungs, heart, liver or brain. Microvascular obstructions may have severe repercussions alone, for example, obstructions in the brain results in cerebral malaria which is manifested by altered levels of consciousness, focal neurologic deficits and seizures. Third, the GPI antigens released from the parasite activates macrophages and natural killer T cells (NKT) cells to produce nitric oxide (NO) and many inflammatory cytokines such as

tumour necrosis factor (TNF-α), interleukin-1 (IL-1), interleukin-6 (IL-6), interferon–c (IFN-c), interleukin-12 (IL-12) that are able to induce expression of intracellular adhesion molecule-1 (ICAM-1), and vascular cell adhesion molecule-1 (VCAM-1).[20, 22] Although cytokines normally improve the clinical outcomes of the infections, the excess production of cytokines (particularly TNF-α) is responsible for the clinical symptoms and results in severe pathological fever, and vascular damage in the lungs and brain, cachexia and acidosis.[23-25] The antigens are insulin mimetic which exacerbates hypoglycaemia. Hypoglycaemia would already be evident due to the parasite's continuous utilisation of host glucose. Severe malaria is ultimately the combination of major pathologies brought on by the parasite and the sometimes counterproductive effect of the host's immune system. If left untreated 90% of severe malaria cases would result in death. However, even in cases where optimal treatment is received, between 15 and 25% of severe malaria episodes result in fatalities.[26, 27, 28]

1.4 Eradication efforts and malaria incidence

Since 2000, malaria has been classified as one of the top priority communicable diseases in need of urgent interventions to reduce the unacceptably high global incidence and mortality rates.[29] This is a result of unsuccessful 20th century eradication efforts where the controversial insecticide dichlorodiphenyltrichloroethane (DDT) was at the forefront of vector control. Malaria was successfully eradicated from Northern America, Europe and Australia by the late 1950s, however, interventions failed in Africa, Asia, and the South and Central Americas leaving behind insecticide resistant vectors. The number of reported malaria cases in 2000 was 262 million which lead to approximately 839 000 recorded deaths.[30]

Many organisations such as the World Health Organization (WHO), large financing corporations, and government institutions of endemic countries have joined forces to roll out global initiatives against malaria. The strategy to reduce malaria incidence has focused on 3 key areas: vector control, chemoprevention, and case management.[4] Vector control is done predominantly through distribution of insecticide treated nets (ITNs) or long lasting insecticidal nets (LLINs) and indoor residual spraying (IRS).[31] Chemoprevention is where antimalarial drugs are given to suppress intraerythrocytic stage parasites. This is predominantly used in pregnant women, infants and young children up to the age of 5 years, and malaria naïve travellers going to malaria areas.[4] Malaria case management is the control of infection which requires diagnostic testing followed by antimalarial treatment predominantly using Artemisinin Combination Therapies (ACTs). By targeting the separate entities that make up this disease, there has been progress made towards malaria elimination.

By 2015 the number of incidences reduced to 214 million globally reported cases of malaria and 438 000 deaths, this is an 18% and 48% decrease in cases and deaths respectively since 2000. The regions of Sub-Saharan Africa are most severely affected and account for 88% of all malaria events and 90% of malaria deaths[4] (Figure 1.3). However, the number of malaria cases represented here from 2000 and 2015 are from reported cases that have been documented by the WHO, there are however, numerous malaria events from poor and rural regions that go unreported or undiagnosed and the actual number of malaria events is estimated to be double the number of the reported cases.[32]

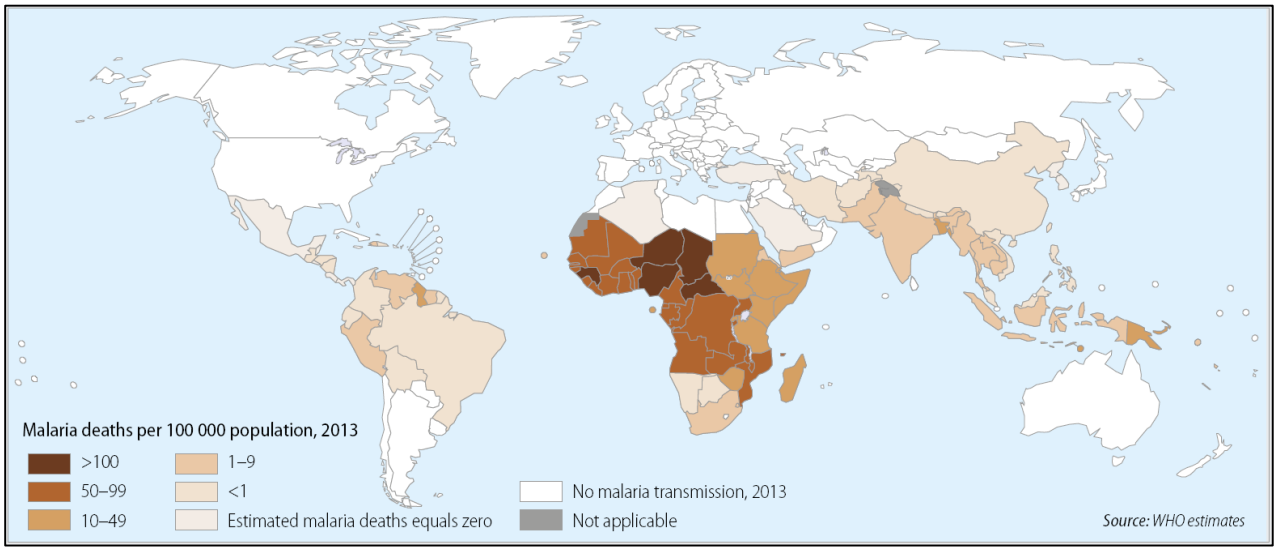

Figure 1.3: Global distribution of malaria deaths per 100 000 population in 2013. Africa accounts for the majority of malaria deaths followed by South-East Asia and the Eastern Mediterranean. (World malaria report 2014[30])

Although significant progress has been made there are several challenges that further complicate the fight against malaria and threaten to reverse the progress achieved. Many countries that face malaria also face other large challenges; conflicts, social unrest, increasing economic burdens, and other diseases which may become prioritised, such as the Ebola outbreak in 2014 and 2015. These all cause shifts of attention away from malaria resulting in weakened and strained sustainable control strategies. Increases in global temperature may also influence the vectors movements allowing for resurgence in areas that had made progress against malaria. This suggests that vector and disease control remain highly important for low transmission countries, and regions neighbouring malaria areas. The malaria vectors has also adapted to years of exposure to insecticide treatments by developing drug resistance to many of the compounds

commonly used against it. The malaria vector has adapted its biting patterns; previously being known to bite only at night, it has now been found to bite earlier in the evenings during times when people are outdoors or not protected by mosquito nets. These challenges in eradication efforts are further compounded by a decrease in effective medications caused by the parasites increasing development of drug resistance.

1.5 Antimalarial medications and drug resistance

There are several compound classes that are used against malaria for chemoprophylactic and treatments purposes. According to the WHO, the medications prescribed globally during 2015 are classified within the following five classes: quinolines (with sub-classes for 4-aminoquinolines, arylaminoalcohols, and 8-aminoquinolines); antifolates; sesquiterpene lactones; respiratory chain inhibitors and certain antibiotics (Table 1.1). The majority of malaria medications used within these classes are derivatives of core structures, modified to make medications that are more soluble and demonstrate a greater bioavailability, and in some cases these were produced to cause less side effects. Because malaria symptoms are associated with the intraerythrocytic phase - and this is the stage where diagnosis generally occurs - the majority of medications currently used to treat malaria are active against these stages, specifically ring, trophozoite, and schizont stages. There are currently no recognised medications that are active against merozoites. Primaquine is the only prescribed medication that is active against liver stage parasites and gametocytes. Despite these being the prescribed medications used against malaria, the parasite has shown varying degrees of drug resistance to the majority of these medications.[33]

The development of drug resistance is a gradual process where the parasite is exposed to drug concentrations that fall below therapeutic levels. This gives parasites an opportunity to mutate by adapting molecular pathways to reduce their sensitivity to a given drug or drug class. Mutations that increase the parasites survival are carried into successive parasite generations while susceptible parasites are “phased-out” over time.[33, 34] This leads to strains of drug resistant parasites that are initially localised to specific geographical regions before spreading to other areas and across borders. Drug resistance begins with changes to susceptibility and *in vivo* prolongation of parasite clearance times, which gradually leads to full blown resistance. However, the number of mutations needed for resistance to develop varies from drug to drug and is influenced by the specific parasite strain affected. Certain compounds only require a single point mutation to develop resistance, while others may require multiple mutations.

Table 1.1: Antimalarial medications activity and resistance. Antimalarial medications listed used in 2014 according to the WHO drug policy. List of drugs mentioned were obtained from the World Malaria Report 2015 edition.

Drug Class	Drug name	Activity	Resistance	Resistance Identified
4-Aminoquinolines	**Chloroquine (CQ)**	Accumulates in the digestive vacuole (DV) binds to haematin (haeme dimer) inhibiting polymerisation of haeme to haemozoin. This causes a build up of haeme monomers which are toxic to the parasite and results in permeabilisation of the parasite membrane[35, 36] Active against the erythrocytic late stages Half-life of 60 days[35]	Resistance is characterised by point mutations in two genes in *P. falciparum:* Chloroquine resistance transporter (*pfcrt*) lysine to threonine at codon 76 (K76T) CQ expelled 40 to 50 times faster than sensitive parasites[37] Multidrug resistance 1 (*pfmdr1*)[38] asparagine to tyrosine at codon 86 (N86Y) The mutant allele N86Y is found in isolates from all continents[39]	1950s[40]
	Amodiaquine (AQ)	Similar mechanism to CQ[35, 36, 40] Half-life of 9-18 days[35]	AQ and CQ show cross resistance[33] however other mechanisms involved as some CQ resistant parasites remain susceptible to AQ[35]	1970s[41]
	Piperaquine (PPQ)	Similar mechanism to CQ: accumulates in the DV and is a potent inhibitor of haeme polymerisation.[35] Possesses bisquinoline dimers with 4 positive charges which decreases drug expulsion and its steric bulk is suspected to prevent it from fitting into the binding site of *Pf*CRT allowing activity against CQ-resistant parasites[35] Half-life of 35 days[35]	Resistance develops when used as monotherapy due to long half-life[40] therefore used in ACTs. Possible affiliations with *Pf*CRT mutations remain to be confirmed[35]	1980[40]
	Pyronaridine (PYR)	Inhibits haemozoin production, and glutathione-dependent haeme degredation[42] High potency against *P.falciparum*, and CQ-resistant strains[42] Mannich-base schizontocide[40] Half-life of 12-14 days	*In vitro* assays revealed presence of PYR-resistant strains. Cross resistance with CQ and AQ in certain regions. More than one resistance mechanism suspected as some CQ resistance strains are PYR sensitive[40]	1980s[42]
	Naphtoquine (NQ)	Novel CQ-like partner drug used in ACTs with long half-life and slowness of onset, single dose treatment	Cross resistance to CQ identified in *P. berghei* mouse models[43]	N/A[43]
Arylaminoalcohols	**Quinine (QN)**	Accumulate in the parasite's DV and can inhibit the detoxification of haeme[35, 44] Importance in severe episodes[44] Schizonticidal[45] Half-life of 8-10 hrs[35]	Cross resistance with MQ and resistance occurs in monotherapies[35, 44] Multiple genes influencing susceptibility, currently including: *pfmdr1*, *pfcrt*, *pfnhe1* - all of them encoding for transporter proteins[35, 39]	late 1950s[44] 1980s[39]
	Mefloquine (MQ)	Binds to haeme and inhibits haeme detoxification, although it is expected to have an additional mode of action[35, 44] High activity against most CQ resistant plasmodium strains[44] Schizonticidal[45] Half-life of14-18 days[35]	Cross resistance with QN and resistance occurs in monotherapy Resistance associated with *pfmdr1* N86Y[46] leading to overexpression of membrane transporter[35]	1990s[44]
	Lumefantrine (LM)	Interfere with the haeme digestion[44] displays *in vitro* synergism with AM Less side effects than halofantrine Highly lipophilic - Oral bioavailability increased with high fat meal Schizonticidal[45] Half-life of 3-5 days[35]	*In vitro* cross resistance with LM, MQ and halofantrine[47] Parasites with *Pf*MDR1 N86Y associated with reduced susceptibility, and parasites with the wild type copy of *Pf*CRT mutation in Africa and Asia indicating alternative mechanism of resistance[35, 48]	2000s[48]
8-Aminoquinolines	**Primaquine (PQ)**	Binds to *Pf*CRT and inhibits CQ transport, possible synergistic action between the two antimalarials and a reversal of CQ resistance[35] Active against the liver and sexual intraerythocytic stages - only approved therapy for liver stage hypnozoites in *P .vivax* Half-life of 4-9 hrs	Unconfirmed resistance[49]	N/A

Drug Class	Drug name	Activity	Resistance	Resistance Identified
Sesquiterpene lactones	**Artemisinin (ART)**	Contain a unique trioxane structure with endoperoxide bonds which are believed to be cleaved by intraparasital iron-II sources to yield carbon centered radicals. Suspected that these radicals unspecifically modify multiple targets like proteins and haeme in the DV or inhibit an ER-located calcium pump *P. falciparum* Ca^{2+} transporting ATPase 6 (*Pf*ATP6). Due to the low solubility of ART, several semi-synthetic derivatives are used clinically[35] Act predominantly against the late ring stages[44] Half-life of 0.5-1.4 hrs[35]	Confirmed resistance caused by point mutations in *kelch* protein in the propeller region beyond amino acid position 441.[50, 51] Reported reduced sensitivity associated with *pfmdr1* gene in West-African isolates, and single point mutation in the *pfatp6* gene[35, 44]	2000s[50]
	Dihydroartemisinin (DHA)	Similar activity to ART DHA is the active metabolite of AM and AS and is manufactured as an oral antimalarial drug in China.	Confirmed resistance caused by point mutations in *kelch* protein in the propeller region beyond amino acid position 441[50]	2000s[50]
	Artesunate (AS)	Similar activity to ART Unstable drug which rapidly converts to active ingredient DHA. When taken orally, is almost entirely hydrolysed to DHA and so has equivalent therapeutic efficacy[44]	Confirmed resistance caused by point mutations in *kelch* protein in the propeller region beyond amino acid position 441[50] Resistance associated with *inubp1* polymorphisms encoding a deubiquitination enzyme in *P. chabaudi* (rodent malaria parasite)[35]	2000s[50]
	Artemether (AM)	Similar activity as ART	Confirmed resistance, same as ART	2000s[50]
Antifolates	**Sulfadoxine (S)**	Inhibit folate synthesis by acting as a competitive inhibitor of 4-aminobenzoic acid or as a false substrate to inhibit the step mediated by dihydropteroate synthase (DHPS)[44] Not a potent antimalarial as a monotherapy – used in combination with P Act against intraerythrocytic stages Combination of S+P has a half-life of 4-5-days	Resistance develops more rapidly when used alone Specific gene mutations encoding for resistance to DHPS has been identified and have reduced lifespan of SP in many regions[33]	1970s[33]
	Pyrimethamine (P)	Inhibits folate synthesis by inhibiting the step mediated by dihydrofolate reductase (DHFR)[33]	Resistance develops more rapidly when used alone Specific gene mutations encoding for resistance to DHFR has been identified and have reduced lifespan of SP in many regions[33]	1970s[33]
Respiratory chain inhibitors	**Atavaquone (AT)**	A coenzyme Q analogue it inhibits the mitochondrial electron transport chain (mETC) and leads to a rapid breakdown of the mitochondrial membrane potential. It binds to the ubiquinone binding side of the cytochrome bc1 complex and blocks the movement of an iron-sulfur cluster containing a protein domain which is normally involved in electron transport[44] thus inhibiting dihydroorotate dehydrogenase, which is an essential enzyme for pyrimidine biosynthesis[35] Activity against intraerythocytic stage parasites Half-life of 2-3 days[35]	Resistance confirmed in use as monotherapy Mutations in the quinone binding site of the cytochrome b gene Y268C, Y268N, are suggested to be associated with AT resistance are to be confirmed[52]	1990s[52]
	Proguanil (PG)	Unknown mode of action, but is proposed to inhibit a still-unidentified mitochondrial membrane protein that maintains the mitochondrial membrane potential when the mETC is blocked. Synergistic with AT, reduces development of resistance in combination[53] but causes treatment failure when used alone[53]	Resistance associated with single mutations in the recrudescent isolates	1990s[52]
Antibiotics	**Doxycycline (D)**	Interfere with protein biosynthesis machinery of the mitochondrion and/or the apicoplast[44] Activity on these organelles as they are prokaryote-like. Potent antimalarial that can be used for both treatment and prophylaxis[33] Half-life of 18-22 hrs	No clinically relevant resistance has been noted[44]	N/A
	Clindamycin (CL)	Similar mechanism as D Less effective than D and T and shows high recrudescence rates[33] Half-life of 2-3 hrs	No clinically relevant resistance has been noted[44]	N/A
	Tetracycline (T)	Similar mechanism as D Potent antimalarial that can be used for both treatment and prophylaxis[33] Half-life on 6-12 hrs	No clinically relevant resistance has been noted[44]	N/A

South-East Asia is known as the “cradle of resistance” for antimalarial medications. Drug resistance was first identified within this region for several antimalarial medications. Chloroquine (CQ), sulfadoxine-pyrimethamine (SP), and artemisinin (ART) have all been recommended as the first-line treatment for uncomplicated *P. falciparum* infections within their respective eras. CQ was prescribed from 1946 and rapidly became overused as it was fast acting, inexpensive and had a low side effect profile. Drug resistance emerged in South-East Asia in the late 1950s[33, 34] and gradually spread across Asia and into Africa which has limited its current use to only a few areas. A similar geographical spread of resistance occurred with SP after resistance was identified in South-East Asia in the 1970s.[33, 34] The Chinese-discovered medication, ART and its derivatives, showed strong antimalarial activity, and replaced other compounds to become the first-line antimalarials in the 1990s. However, in 2009 drug resistance was identified at the border of Thailand and Myanmar. This region is susceptible to the development of drug resistance for three main contributing factors. First, the warm and wet tropical regions are prime conditions for the malaria vector to thrive. Second, like many other poverty stricken areas, this region lacks medical facilities and so patients treat malaria by self-medication which may be done inadequately. With a lack of medical advice, poor drug compliance to the standard 7 day course of treatment can result in only partial parasite clearance.[34, 54] Third, the parasite strains in this region do not interbreed, thus once mutant parasites arise the lack of genetic diversity produces a population of clone-like parasites which contain the resistant characteristics. Parasite resistance to ART has been confirmed in South-East Asia, and other evidence indicates that it may be developing independently in some African regions.[50] The spread of drug resistance occurs slowly through the migration of people and vectors. Figure 1.4 demonstrates the spread of ART resistance between 2013 and 2014.

The WHO has recommended Artemisinin Combination Therapies (ACTs) as the first-line treatment of uncomplicated *P. falciparum* malaria as a means to combat drug resistance and prolong the efficacy of antimalarials. ACTs use two antimalarials with different mechanisms of action; fast acting ART derivatives are combined with partner drugs that have long half-lives.[55] The list of current medications used to treat malaria in African and South-East Asian regions is shown in Table 1.2. ART or derivatives quickly reduce the parasite load, leaving the long half-life partner drug with a much smaller parasite population to eliminate. ACTs have had a major contribution to the reductions in global malaria morbidity and mortality since their implementation.[33, 55] The idea of using two antimalarials is that parasites showing resistance to one compound would be removed by the partner drug, and thus minimise the risk of selecting

resistant parasites to either of the medications.[33, 48] However, a complication arises as ART derivatives have short half-lives and are rapidly removed from the circulatory system. The long acting partner drug's concentration falls to sub-therapeutic levels over time, leaving the remaining compound vulnerable to parasite recrudescence and selection of resistant parasites from new infections.[48, 56] Recent studies have noted the failure of ACTs are increasing rapidly with some regions in South-East Asia reporting half of confirmed malaria cases showing treatment failure.[57]

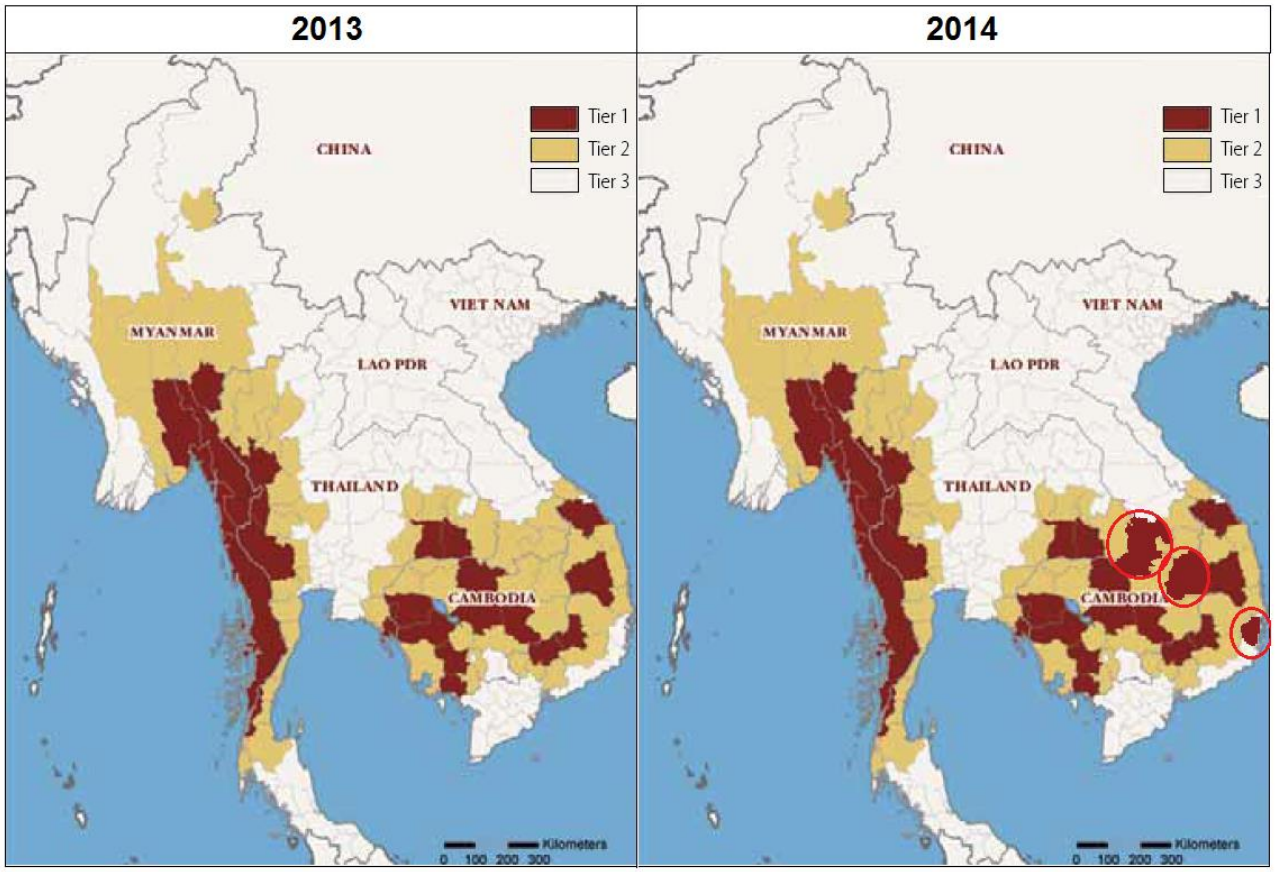

Figure 1.4: Resistance of *P. falciparum* to ART and its derivatives in South-East Asia between 2013 and 2014. Resistance to ART and its derivatives are increasing, with a larger geographical spread seen in 2014 in comparison with the previous data recorded from 2013. Circled areas representing the change in areas with confirmed resistance Tier 1) areas where there is credible evidence of ART resistance; Tier 2) areas with significant inflows of people from Tier 1 areas, including those immediately bordering Tier 1 areas; Tier 3) areas with no evidence of ART resistance and limited contact with Tier 1 areas. (Adapted from the World Malaria Report 2013[58] and 2014[30]).

Table 1.2: The antimalarial drug policy for treatment in Africa and South-East Asia. Antimalarial medications used in malarial treatment in Africa and South-East Asia according to the Malaria drug policy 2014 as determined by the World Health Organization.[4]

Species	***P. falciparum***				***P. vivax***
	Uncomplicated unconfirmed	**Combinations for uncomplicated malaria**	**Combinations for severe malaria**	**Prevention during pregnancy**	**Treatment**
Africa	AM+LM; AS+AQ	AM+LM; AS+AQ; QN+CL; QN+D	AS; QN; AM; QN+AS; AS+D; QN+D	SP; CQ+PG	CQ; AS+AQ+PQ; CQ+PQ; AM+LM; AM+LM+PQ
South-East Asia	CQ	AM+LM; AS+SP+PQ; AS+AQ; DHA-PPQ+PQ; AM; AS+MQ; DHA-PPQ; PQ; AM+LM+PQ	AM; QN; AS; QN+D	-	CQ+PQ; AS+AQ; DHA-PPQ

Key: AM- Artemether; AQ- Amodiaquine; ART- Artemisinin; AS- Artesunate; AT- Atovaquone; CL- Clindamycin; CQ- Chloroquine; D- Doxycycline; DHA- Dihydrartemisinin; LM- Lumefantrine; MQ- Mefloquine; NQ- Naphroquine; PG- Proguanil; PPQ- Piperaquine; PQ- Primaquine; PYR- Pyronaridine; QN- Quinine; SP- Sulfadoxine-Pyrimethamine.

The extent of drug resistance and its continual development highlights the crucial need to develop new avenues of malaria prevention, treatment and cure. This would most likely need to be in the form of new antimalarial drugs and antimalarial vaccines. There are no vaccines available to prevent malaria. Although the concept of an effective malaria vaccine is feasible, the reason contributing to why there has not been an available vaccine is because of a lack of discovered vaccine targets, and a lack of parasite antigens that are highly conserved across strains. An ideal vaccine should be able to provide complete immunity against the disease or prevent severe malaria and death. Vaccine development may best be attempted against parasite life stages that are exposed to immune components in the serum, thus potential targets could be antigens of sporozoites, gametocytes, or merozoites (egressing from hepatocytes or erythrocytes). A potential drug or vaccine would need to target a process that is vital to the survival of the parasite in the aim of a significant reduction of invasion events.

1.6 The merozoite and invasion

Merozoite invasion of erythrocytes is essential for the reproduction of the asexual intraerythrocytic phase and the development of the malaria disease. The merozoites are exposed to the immune components between egress and invasion which has considered them to be an attractive target for vaccine and drug development.

There have been very few well-defined drug targets discovered against merozoites, and the current understanding of this lifecycle stage is incomplete because there has been a lack of suitable methods to study merozoites and their activities.[59] The current understanding of merozoites has been learnt through invasion studies on either *P. knowlesi* (which is less virulent than *P. falciparum* and differs in regards to mechanisms of invasion) or on merozoites which have lost invasive capacity.[60-62] However, the exploration of merozoite optimised parasite culturing methods coupled with techniques such as magnetic isolation, flow cytometry, and proteomics are opening new avenues to examine merozoite invasion and related activities.[63, 64]

Merozoites are well structured for invasion; they are ovoid shaped and contain apically located secretory organelles that secrete proteins required for invasion (Figure 1.5). Measuring between 1-1.2 µm, merozoites are the smallest of the *Plasmodium* lifecycle stages. The complete exterior is surrounded by a “fuzzy” layer that includes many proteins, a small proportion of these proteins are integral membrane proteins or peripherally-associated proteins, while the majority of these are attached as GPI–anchored proteins to the plasma membrane.[13, 14, 65, 66]

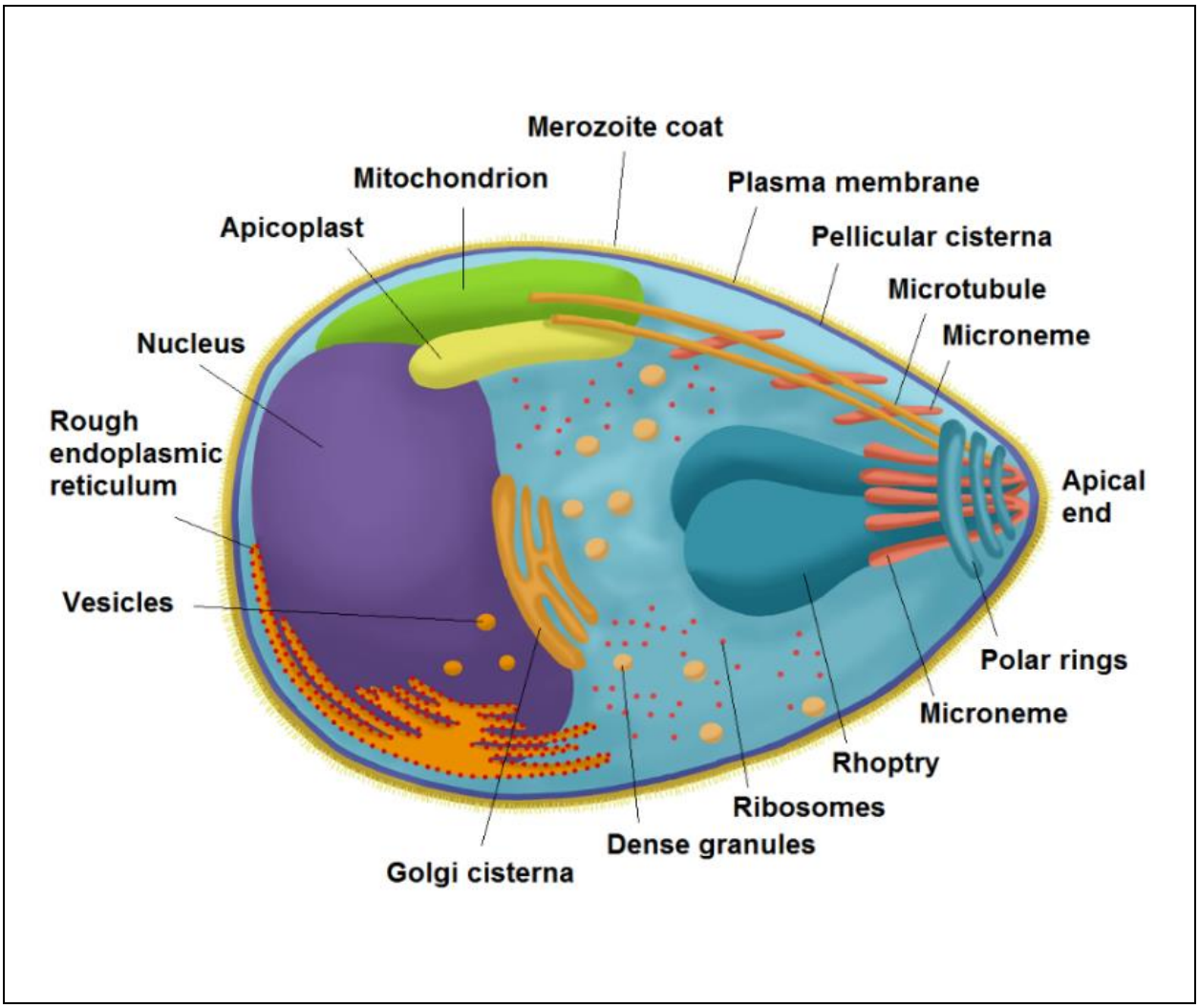

Figure 1.5: The merozoite structure. Mature invasive merozoite with organelles and protein coat required for invasion of uninfected erythrocytes. A cytoskeleton gives the merozoites shape with several organelles are anchored to it. The nucleus is situated at the basal end while secretory vesicles (involved in invasion) are located towards the apical end.

Once merozoites egress from schizonts they have a short period in which they maintain invasive capacity. *In vitro* studies have demonstrated that merozoites have an invasive half-life of approximately 5 minutes (min) at 37°C with approximately 85% of invasion events completed within 10-15 min of mixing merozoites and erythrocytes.[63] While a small percentage of merozoites remain invasive after this time point, all invasive capacity is lost approximately 120 min after egress. The process of erythrocyte invasion by merozoites is a rapid and systematic process which can occur within ±60 seconds (sec) after the initial recognition of erythrocytes.[67, 68] This process of merozoite invasion can be broken down into five chronological steps (Figure 1.6) which will be discussed.

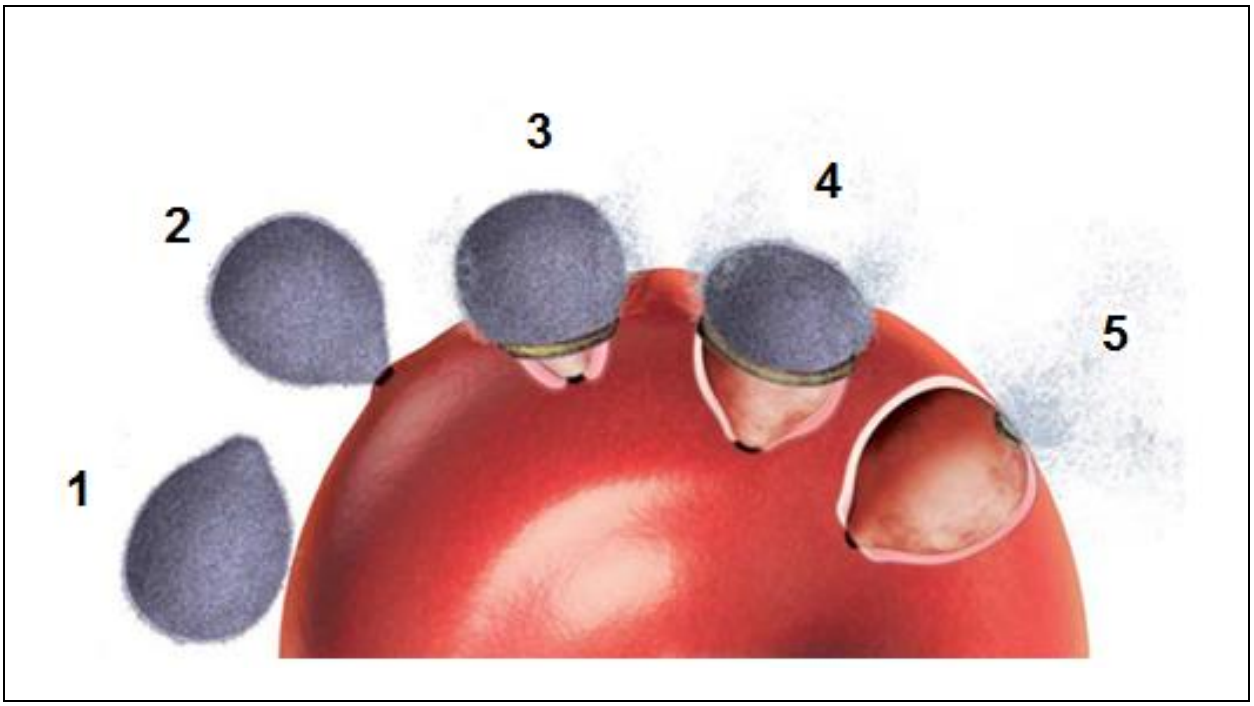

Figure 1.6: Merozoite invasion of erythrocytes. Steps of invasion: 1) Initial recognition of erythrocytes by GPI-anchored proteins and reorientation; 2) Irreversible attachment; 3) Formation of a tight junction; 4) Invasion of erythrocyte; 5) Resealing within a parasitophorous vacuole. (Cowman *et al.* 2006[14] with permission)

1.6.1 Initial recognition of erythrocytes and reorientation

Once a merozoite has egressed from a schizont it must first distinguish erythrocytes from other cells. Initial interactions with erythrocytes are weak and reversible as the parasite has not yet committed to invasion. These interactions occur along any point of the merozoite membrane with the erythrocyte and extend over relatively long distances.[14] The primary recognition and attachment to erythrocytes are thought to be predominately caused by merozoite GPI-anchored surface proteins, which surround the exterior of the merozoite surface membrane.[69, 70] The initial interactions between merozoite and erythrocyte are vital to invasion,[71] showing marked decreases in invasion when these processes have been knocked out.[69] Merozoites appear to 'roll' along the erythrocyte, interacting with its surface proteins and dissociating repetitively causing deformations in the erythrocytic cytoskeletal structure at each association.[65, 68] Once the merozoite has attached to the erythrocyte it orientates its apical region to direct specialised apical secretory organelles (micronemes, rhoptries and dense granules) towards the erythrocyte surface in preparation for invasion. The GPI involvement is discussed further below.

1.6.2 Irreversible attachment

Irreversible attachment occurs between the apical end of the merozoite and the erythrocyte, this takes approximately 10 sec.[68] The binding of the merozoite to the surface is dependent on one of two known invasion pathways which mediate commitment to invasion and trigger subsequent events leading to entry. Irreversible attachment utilises either erythrocyte binding antigen (EBA) or reticulocyte binding-like homologous (*Pf*Rh) protein families.[72, 73, 74] These pathways utilise either sialic acid dependent or sialic acid independent antigens respectively. Sialic acid dependent pathways make use of the duffy binding-like (DBL) protein family including EBA-175, -140, and -181 which bind to glycophorin A (GPA), glycophorin C (GPC) and an unknown glycosylated receptor respectively. Sialic acid which is present on these receptors is essential to bind to cysteine-rich dual DBL domains found within the N-terminus of DBL proteins. The sialic acid independent pathway utilises the *Pf*Rh proteins. *Pf*Rh1 binds to unknown glycosylated erythrocyte receptors where evidence is lacking on whether *Pf*Rh2a, *Pf*Rh2b and *Pf*Rh4 directly bind to erythrocytes.[75] The sialic acid dependent and independent ligands mediate specific routes of invasion, however, although these pathways are important to invasion they have been demonstrated to be redundant as the disruption of corresponding genes causes the parasite to utilise alternative antigens for invasion resulting in no effect on invasion rates.[75]

1.6.3 Formation of a tight junction

The merozoite forms a tight junction between its apical end and the erythrocyte membrane. After the release of rhoptry proteins, rhoptry neck protein 2 (RON2) anchors into the erythrocyte membrane, this is followed by binding of apical membrane antigen 1 (AMA1) (which is present on the merozoite surface after release from the micronemes at egress) to form a link between the host and merozoite.[73] These complexes form a ring shaped junction creating a space into which the merozoite can move as it invades and establishing the parasitophorous vacuole and parasitophorous vacuole membrane (PVM).[73]

1.6.4 Invasion of erythrocytes

The merozoite moves into the erythrocyte through the tight junction increasing the size of the parasitophorous vacuole and simultaneously sealing itself off from the external environment and erythrocyte cytoplasm. The invasion process is driven by a single headed myosin chain which is attached to an inner membrane complex. Actin filaments concentrate around the tight junction ring and trail the RON complex providing a substrate with which the myosin can interact and generate a propelling movement which pushes the merozoite further into the parasitophorous

vacuole.[74, 76, 77] During the invasion process the GPI-anchored proteins which line the merozoite surface appear to be shed and released into the host's circulatory system.[13, 69, 78, 79]

1.6.5 Resealing within a parasitophorous vacuole

Once the merozoite has completed entry it seals itself inside the erythrocyte by fusion of the parasitophorous vacuole and erythrocyte membranes.[14, 73, 74] The entry into the erythrocyte causes no damage or apparent physical changes to the host cell, thus once the parasite has entered and sealed itself inside the erythrocyte it is well concealed, evading identification by host immune and complement systems. The antigens released from the merozoite surface during invasion are left as decoys within the circulatory system to be identified by immune components and causing immunological flairs, thus aiding in the merozoite "disappearance" and allowing it to continue development into intraerythrocytic ring stage.

1.7 The GPI-anchor

Glycophosphatidylinositols (GPI) are glycolipids found abundantly on the surface of most eukaryotic cells.[80] GPIs are found either as free GPIs unlinked to either proteins or lipid membrane, or may be found anchored to a lipid membrane with a protein attached as a posttranslational modification. The structure comprises of a hydrophobic phosphatidylinositol (PI) group containing two long chain fatty acids that anchor into the membrane lipid bilayer, the inositol of the PI group links to a carbohydrate core via a phosphoethanolamine (PEtN) bridge linking to the C-terminal of a mature protein in anchored forms.[80] GPIs represent approximately 95% of the total carbohydrate presence on merozoite surface, while N- or, O-glycosylation, and mannosylation are found at very low levels.[22, 23, 81, 82]

The biosynthesis of GPIs in mammals and protozoans follow similar pathways with a highly conserved basic glycan structure seen between the species (Figure 1.7).[83] Biosynthesis commences on the cytoplasmic side of the ER membrane in both mammals and protozoa, where an N-acetylglucosamine (GlcNAc) is transferred to PI on the membrane, resulting in N-acetylglucosamine- phosphatidylinositol (GlcNAc-PI) which is N-deacetylated to generate N-glucosamine-phosphatidylinositol (GlcN-PI). The GlcN-PI flips position into the luminal side of the ER. During this process the sn-2 position of the inositol is acylated with an unsaturated fatty acid. In *P. falciparum* three mannose (man) molecules are added to form the glycan chain, followed by a single PEtN residue on the third mannose to form a conserved trimannosyl-glucosaminyl moiety with a final 1,2-linked mannose being attached to the mannosyl residue distal to the glucosamine residue.[83, 84] Thus, the complete *P. falciparum* GPI structure is defined as PEtN-6(Manα1-

2)Manα1-2Manα1-6Manα1-4GlcNα1-6(acyl-2)*myo*-Inositol-1-P-(*sn*1,2diacyl)-glycerol.[81] The mammalian glycan core can be variously modified with additional groups or side chains containing PEtNs, mannose, galactose, sialic acid or GlcNAc which are not found on *P. falciparum* anchors.[80, 85] In contrast to mammalian GPI-anchors which have several variations to the glycan core modifications and lipid moieties, the structure of GPI-anchors in *P. falciparum* have essentially the same conserved structure. After protein attachment the molecule is then transported to the Golgi apparatus,[84] where in *P. falciparum* unsaturated acyl chains of the inositol and diacylglycerol moieties are thought to be removed and replaced usually with palmitic acid or myristic acid.[83]

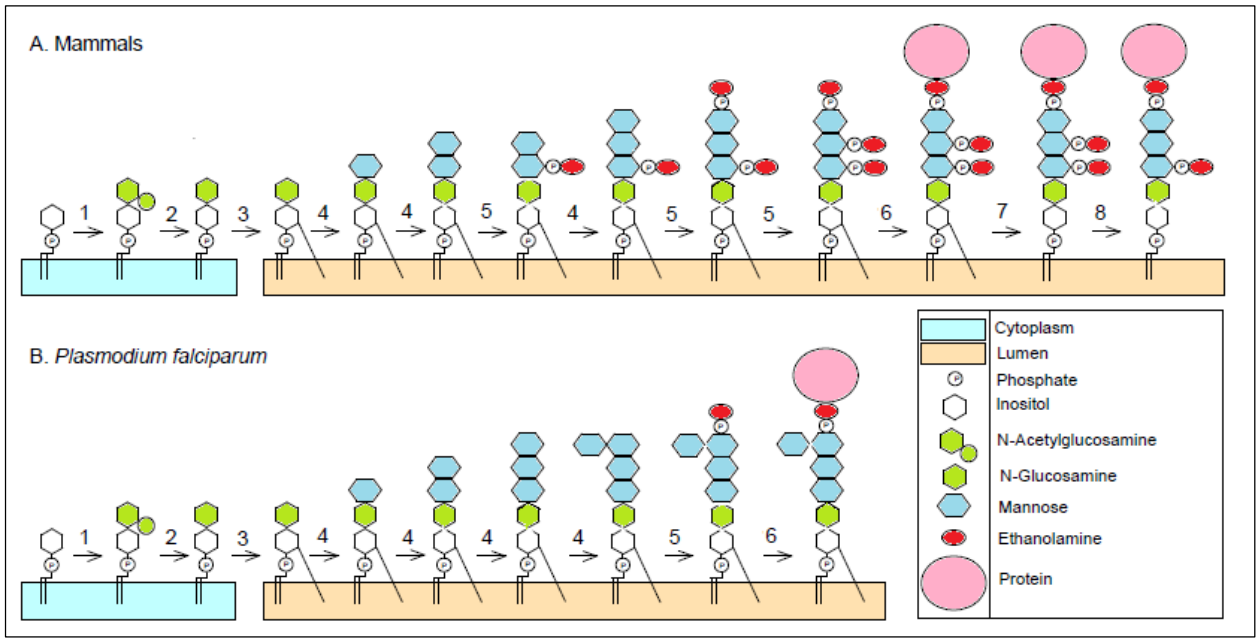

Figure 1.7: Biosynthesis and structure of the GPI-anchor. Reactions that occur in A) mammals and B) *P. falciparum*: 1)Transfer of GlcNAc to PI by phosphatidylinositol n-acetylglucosaminyltransferase (PIG-A); 2) GlcNAc deacetylation by N-acetylglucosaminyl phosphatidylinositol deacetylase (PIG-L) followed by flipping of GlcN-PI into the luminal side of ER); 3) acylation of inositol by inositol acyltransferase (PIG-W); 4) mannosylation using dolichol-phosphate mannosyltransferase polypeptide 1 (DPM1) and GPI mannosyltransferase I-III (PIG-M, -V, -B) for respective mannosylations; 5) addition of PEtN; 6) attachment of GPI to protein by GPI transamidase; 7) inositol deacylation; 8) removal of the second PEtN.

The palmitate on inositol and the second PEtN are removed in some mammalian cases,[84] although this has not yet been described in *P. falciparum*. The GPI-anchored proteins are transported from the ER to the Golgi apparatus and then presented on the external cell surface.[86]

The GPI-anchor's primary function is to anchor the protein to the merozoite surface, however, it also imparts a range of properties to the protein and performs a number of roles. The GPI-anchor may be involved in signal transduction acting as an intermediary between the exterior of the cell and internal molecules associated with transmembrane signal transduction partners, such as protein tyrosine kinases, integrins, and heterotrimeric guanosine-5'-triphosphate (GTP)-binding protein, as well as allowing for signal transduction by the anchored proteins themselves. The GPI-anchor is also thought to be involved in cellular functions including sorting and localisation of proteins, protein secretion, cell membrane properties, cell adhesion, cell–cell communication, receptor–ligand interactions, modulation of immunological properties, control of protein conformation and proteolytic processing.[85]

P. falciparum merozoite GPI-anchored surface proteins vary structurally and range in size with masses from 20-200 kDa.[86] Only a limited set of proteins are selected for this kind of anchorage with 19 GPI-anchored proteins having been identified or predicted on the merozoite and 30 GPI-anchored proteins in total predicted in *P. falciparum* parasites from all lifecycle stages.[65, 87]

GPI-anchored surface proteins include MSP1, 2, 4, 5, 8, 10, the Cys6 protein family (*Pf*12, *Pf*38, *Pf*92, *Pf*113), the serine protease P76 and Cysteine-rich protective antigen (CyRPA)[88, 89]. Other GPI-anchored merozoite proteins include *Pf*34, Rhoptry-associated membrane antigen (RAMA), apical sushi protein (ASP), apical asparagine rich protein (AARP), GPI-anchored micronemal antigen (GAMA) and two others.[20, 22, 90] These proteins include rhoptry, and microneme associated and a non-localised protein.

There are several known mechanisms by which GPI-anchors and its associated proteins may be processed. First, the serine proteases, subtilisin-like proteases (SUB) 1 and 2 process some GPI-anchored proteins at different times during the invasive period. Second, GPI-anchored proteins have shown sensitivity towards treatment with exogenous phospholipase A_2.[83] Third, most eukaryotic GPI-anchors are regulated through protein cleavage by phosphatidylinositol phospholipase C (PI-PLC).[86] The enzyme PI-PLC cleaves the protein from the anchor releasing the protein into the extracellular space. In *P. falciparum* the palmitic or myristic acid on the inositol ring affects cleavage by PI-PLC, while only one GPI-anchored protein on the merozoite surface has shown sensitivity towards PI-PLC to date.[89] This is the uncharacterised P76 serine protease involved in invasion, its direct role, the proteins which it may affect, and reasons for different processing compared to other proteins are undetermined. In addition, PI-PLC is involved in potent second messenger signalling and releases inositol 1,4,5-triphosphate (IP_3) which is involved in the control of intracellular Ca^{2+} levels.[91] Invasion is Ca^{2+} dependent and release of this cation may

be implicated in the processing of GPI-anchored proteins involved in invasion. Finally, GPI-anchored proteins are attached to the merozoite surface which contain additional signalling and networking properties implicated in the correct functioning of the GPI-anchor and associated protein.[92] The potential to inhibit the cleavage, or activity of GPI-anchored proteins could be lethal to the parasite as these processes are thought to be essential to the parasites invasion and therefore survival and reproduction.[93]

1.8 Method selection to assess the merozoite proteome

1.8.1. Method selection

As merozoite invasion occurs rapidly with *P. falciparum* parasites, the extent of protein involvement and proteomic alterations occurring during this time period remain to be further characterised and understood. There have been minimal studies conducted which characterise the changes to the merozoite surface proteins over time. Protein cleavage from the surface of the merozoite, and how the protein cleavage may affect invasion and the active lifespan of the merozoite is yet to be fully understood. The GPI-anchored proteins have vital roles in invasion, but some of the proteins remain to be further characterised. It has not been determined how proteins change after merozoite egress with time nor the effects of compounds that influence the processing or activities of the GPI-anchor.

Previous research to assess *P. falciparum* invasion has generally been limited to merozoites which are no longer invasive. In addition, screening of potential invasion inhibitory compounds would be assessed by conducting “invasion assays” that would be initiated with late trophozoites or schizonts. These assays would overlook the effects that the compound would have on late stage parasite progression, merozoite egress, and on the subsequent cycles’ ring formation and thus were not specific to invasion. Boyle *et al.*[63] was the first researcher to develop a method that looks specifically at invasion and assesses compounds effects on invasion by only exposing the invasive merozoite to potential inhibitory compounds for the duration that the merozoite retains invasive capabilities.

With a lack of known invasion inhibitory compounds, the pre-screening of compounds with potential anti-invasive properties is conducted using standard growth inhibitory assays to assess relative inhibitory concentration ranges. In this study, four compounds were assessed and these are discussed below. The Malaria SYBR Green I-based Fluorescence (MSF) assay is a method used for high throughput antimalarial drug screening. The MSF assay is a cost saving and robust method, which is a reliable alternative to previous inhibitory assays which assessed viability

through uptake of radioactive substances.[94] Using the MSF assay, parasite inhibition is assessed using fluorescence by measuring parasite DNA proliferation within erythrocytes; using this technique total double stranded DNA concentration is assessed after the lysis of infected erythrocytes and so is unable to quantify DNA proliferation in individual cells.

Flow cytometry is used to assess invasion inhibition in merozoite invasion assays (MIAs). Flow cytometry is a laser based cell sorting technique that is able to analyse thousands of particles per second. Flow cytometry uses dyes to stain DNA, the fluorescence of the DNA in each individual cell is measured to create a histogram of cells that fit into a predefined set of parameters. This information can be used to quantitatively assess cell cycle and proliferation. The advantage of flow cytometry is that is has multiple applications that can be adapted and tailored to the research question.[63, 95]

Proteomic techniques used in this study are sodium dodecyl sulphate-polyacrylamide gel electrophoresis (SDS-PAGE) followed by liquid chromatography-tandem mass spectrometry (LC-MS/MS). The combination of these two methods has long proven to obtain in-depth understandings of various proteomes, by characterising protein expression and post-translational modifications, thus leading to improved analyses of protein-protein interactions. These result in functional and structural proteomics, typically used for drug discovery and drug target identification and validation. SDS-PAGE is used to separate proteins into bands based on their apparent mass. When analysing whole organisms there may be multiple proteins within a single visualised band i.e. multiple proteins with same or similar apparent masses; thereby, limiting the ability definitively state which protein/s are present in the band and require mass spectrometric analysis to identify proteins based on the peptide sequence. “Bottom-up” protein analysis refers to the characterisation of proteins by analysis of peptides derived from the protein through proteolysis. When bottom-up is performed on a mixture of proteins it is called shotgun proteomics. By using shotgun proteomic techniques proteins in complex mixtures can be identified using a combination of high performance liquid chromatography (HPLC) combined with mass spectrometry. The derived peptide mixture is fractionated and subjected to LC-MS/MS analysis. Peptide identification is achieved by comparing the tandem mass spectra to a protein database and assigning peptide sequence to proteins. To quantify the proteins label-free quantification is used here. Label-free method is used to determine the relative amount of protein based on signal intensity or spectral counting. In spectral counting, the total number of tandem mass spectra that match peptides to a particular protein is used to measure the abundance of proteins in a complex mixture.

1.8.2 Compounds selected

1.8.1 Vanadate

Vanadium is a water soluble trace element which is found naturally in mammals at concentrations that have no effect on physiological functions. The oxidation state of vanadium is dependent on the concentration of the element found in solution. At low concentrations vanadate is predominantly found in the pentavalent redox state as monomeric sodium orthovanadate (SOV) (Figure 1.8). As the concentration increases vanadate dimer and decamer species are formed. The oxidation state of vanadium influences separate profiles of enzyme inhibitory activity. Monomeric vanadate may behave as a phosphate analogue thereby causing enzymatic inhibition.[96] Several enzymes are known to be inhibited by monomeric vanadate including serine proteases,[96] P-type and calcium ATPases,[97, 98] protein tyrosine phosphatases, while tetrameric vanadate inhibition profile includes PI-PLC,[99] and enzymes involved in glycolysis.[100]

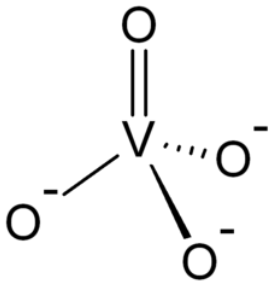

Figure 1.8: Structure of vanadate.

1.8.2 Edelfosine

Edelfosine (1-octadecyl-2-O-methyl-glycero-3-phosphocholine) (Figure 1.9), is a synthetic alkyl-lysophospholipid (ALP). Edelfosine has been found to have activity in mammalian and protozoan species including *Leishmania*[101] and *Schistosoma.*[102] Edelfosine has been found to incorporate into membranes, interact with lipid rafts of cell membranes and accumulate on cell surfaces.[103, 104] This drug modifies plasma membrane lipid composition resulting in selective association or/and displacement of crucial proteins.[104] Edelfosine has previously been proposed to affect their organisation and disrupt pathways including signalling, phospholipid metabolism,[105] inhibition of PI-PLC,[106] influence on Ca^{2+} flux,[107] and activation of macrophages.[105] The characteristics of this amphiphilic compound would suggest that it could be active on surface membranes of *P. falciparum.*

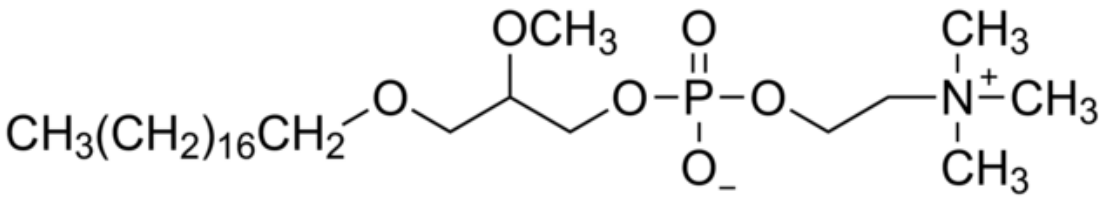

Figure 1.9: Structure of edelfosine.

1.8.3 Dioctyl sodium sulfosuccinate

Dioctyl sodium sulfosuccinate (DSS) is an anionic surfactant with a sulfonate head group (Figure 1.10). DSS has been shown to have an effect on proteolytic enzymes where the compound predominantly causes either substrate-inhibitor interactions by causing substrate depletion involving the primary substrate sites, or causing inhibition by interaction between the enzyme and the inhibitor molecules.[108] DSS has been shown to inhibit trypsin, casein and PI-PLC.[99] DSS is expected to have an effect on cell surfaces and surface proteins.

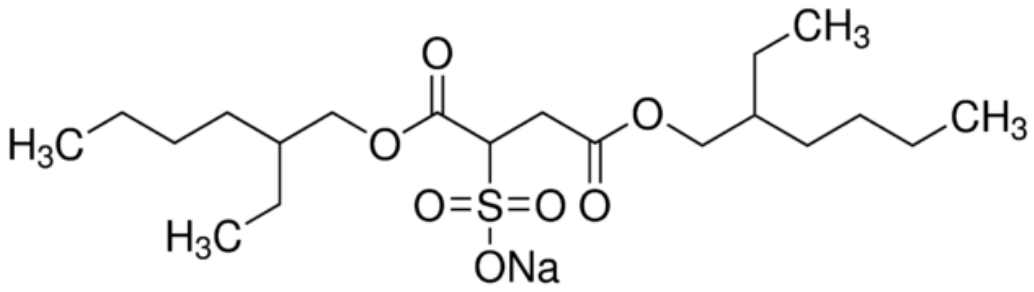

Figure 1.10: Structure of dioctyl sodium sulfosuccinate.

1.8.4 Gentamicin

Gentamicin (Figure 1.11) is an aminoglycoside antibiotic which is active against a wide range of bacterial infections including gram-negative bacteria and some gram-positive bacteria.[109] Gentamicin acts by preventing bacterial protein synthesis, however, also has an effect on the metabolism of phosphatidylinositols.[110, 111] Gentamicin has been shown to inhibit separate

phospholipases including an acidic phospholipase, PI-PLC, β-lysophopholipase, and phospholipase A1 and A2.[112-115]

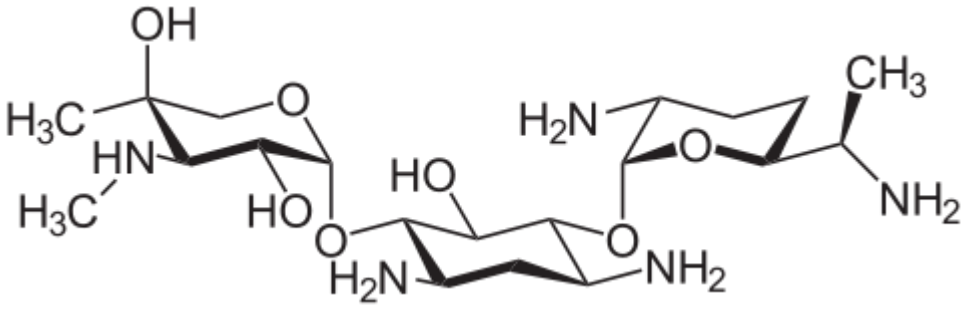

Figure 1.11: Structure of gentamicin.

1.9 Summary and study rationale

Despite large scale attempts over many years to eradicate this ancient disease, malaria still affects millions of people around the globe. Progress has been made against malaria in recent years with the introduction of integrated eradication efforts that focus on vector transmissions, chemoprevention and cure. These have led to significant reductions in infection rates, and mortality, however, as with previous eradication efforts, this progress is threatened by the emergence of insecticide resistant vectors and drug resistant parasites. With a lack of malaria vaccines available and with a decrease in drug efficacy, there is a need to find new antimalarial targets. An ideal new antimalarial drug would need to combat parasitic pathways which differ to those that current treatments inhibit, and target multiple essential process within the parasite's lifecycle including parasite transmission. This multiple stage control is required to prolong a compounds effective lifespan and significantly contribute to malaria elimination.

There are currently no antimalarial medications or vaccines that target the merozoite or erythrocyte invasion. This is essentially because of incomplete understandings of the invasion pathways and the interactions that occur between the antigens of the merozoite and erythrocyte receptors. There is also a lack of understanding of the modifications to and pleiotropic roles of the many antigens involved during the invasive process; this includes mechanisms in which antigens activate pathogenesis.

Previous research has shown that after initial contact with an erythrocyte different receptor-ligand pathways are utilised to invade erythrocytes. These are the sialic acid dependent and sialic acid independent pathways. The parasite is capable of switching between these pathways by changing protein utilisation. The changes that occur in the parasite protein expression are not regulated during the transcription process and are controlled by an unknown mechanism.[116] Knock out studies involving these pathways have proven them to be redundant with merozoites employing alternative pathways when challenged thus not affecting the rates of invasion.

Prior to invasion the merozoite recognises an erythrocyte using GPI-anchored merozoite surface proteins that engage in initial interactions that ultimately lead to erythrocyte invasion. These initial interactions are suggested to be vital to invasion. Blocking or interfering with these interactions or functionality of the proteins could result in severely hindered invasion.

The merozoite has a short five minute invasive half-life and cell entry occurs rapidly once in direct contact with an erythrocyte. However, during the short time period between merozoite egress and complete erythrocyte invasion the merozoite is exposed to host antibodies and immune cells. Merozoite GPI anchored proteins are involved in invasion and simultaneously contribute to malaria symptoms. The GPI-anchoring structure has been found to be well conserved with minimal polymorphisms, reconfirming that merozoite GPI-anchors could be considered attractive targets for vaccine and drug development. By inhibiting GPI-anchor related processes and activities the symptomatic profiles and invasion rates can potentially be reduced, improving the chance for immune system to recognise and inactivate the invasion thereby preventing disease progression. In light of the previous limitations of available techniques, the processes involving the biology and proteomics need to be better characterised and understood. Characterising the proteomics of viable merozoites and the changes undergone could lead to a better understanding of mechanisms involved in this process and would facilitate a more targeted approach to vaccine and drug development.

1.10 Study aim

The aim of this study was to determine how GPI-anchored proteins on the merozoite surface are altered during the invasive phase, and explore the possibility of using merozoite GPI-anchored proteins as potential drug targets against malaria.

1.11 Objectives

- To optimise parasite culturing methods to have highly synchronised parasites specifically for harvesting large numbers of invasive merozoites.
- To isolate large volumes of schizonts by magnetic-activated cell sorting, and isolate invasive merozoites.
- To assess inhibitory effect of vanadate species, edelfosine, dioctyl sodium sulfosuccinate and gentamicin on intraerythrocytic phases and assess their potential to inhibit invasion.
- To optimise SDS-PAGE gel electrophoresis of merozoite surface proteins.
- To optimise and conduct LC-MS/MS on selected merozoite proteins isolated from SDS-PAGE gel bands.
- To analyse selected proteins using proteomic software for the characterisation of the merozoite proteome.
- To assess the changes that occur within the GPI-anchored proteome during invasive merozoites to that of non-invasive merozoites, in treated and untreated samples.

Chapter 2: Parasite Biological Aspects

2.1 Methodology

2.1.1 *P. falciparum* culture: Optimised culturing techniques

The aim of this part of the study was to culture large quantities of highly synchronised *P. falciparum* parasites, and isolate late stage parasites to obtain protein from pure stage defined populations of invasive merozoites.

2.1.1.1 Parasite culture

The cultivation of healthy parasites requires fresh blood cells from healthy individuals. Approximately 450 mL (millilitres) of venous blood from consenting volunteers was collected into sterile, non-pyrogenic SO Fenwal AFRO193 blood bags (Adcock Ingram, Midrand, RSA). The blood bags contained acid citrate dextrose and adenine anticoagulant solution. Bags were well mixed by gentle inversion and stored in this bag overnight at 4°C for diffusion of anticoagulant and prevention of coagulation. The blood was transferred to sterile 50 mL centrifuge tubes and kept at 4°C until use with a maximum storage time of 2 weeks. The blood was centrifuged at 2500x*g* (Boeco C-28A centrifuge, Hamburg, Germany) for 5 min and serum was removed using a suction pump. The blood was washed 2-4 times in an equivalent volume of phosphate buffered saline (PBS) by centrifugation at 2500x*g* for 10 min to remove all traces of leukocytes. This was essential as leukocytes are capable of destroying parasites.[117] All constituents of PBS were purchased from Sigma (St Louis, MO, USA) and made up as follows: 137 mM sodium chloride (NaCl), 2.7 mM potassium chloride (KCl), 10 mM phosphate (PO_4), at pH 7.4. Incomplete culture media (ICM) (Roswell Park Memorial Institute (RPMI) 1640 media (Sigma, St Louis, MO, USA), supplemented with 0.2% (*w/v*) D-glucose (Sigma, St Louis, MO, USA), 0.2 mM hypoxanthine (Sigma, St Louis, MO, USA), 0.024 mg/mL gentamicin (Sigma, St Louis, MO, USA), buffered with 25 mM Hydroxyethyl piperazine ethanesulfonic acid (HEPES) (Sigma, St Louis, MO, USA) and 23.81 mM sodium bicarbonate (Merck, Darmstadt, Germany) per litre of MilliQ water (double distilled, de-ionised, 0.22 µM filter sterilised) was added to the washed erythrocytes to make a 50% haematocrit suspension which was maintained at 4°C when not in use.

The laboratory adapted *P. falciparum* 3D7 parasites were cultured using optimised methods. Parasites were cultured in sterile 225 cm^2 sealed tissue culture flasks (Sigma, St Louis, MO, USA) using complete culture media (CCM) (ICM with the addition of 0.5% Albumax II (Invitrogen, Life Science Technologies, Waltham, MA, USA). Albumax II is an alternative to human serum and eliminates the requirement for blood type compatibility[118] without affecting the preparation of

parasite antigens that occur naturally with human serum.[117] Culture media was replaced daily and cultures were assessed by thin blood smears. Cultures were transferred from flasks into 50 mL tubes and centrifuged for 2 min at 2000x*g* and placed in a water bath at 37°C during the time that the thin blood smears were being assessed. Care was taken to prevent parasite exposure to temperatures below 37°C for any time longer than the time it takes to change media, as temperature fluctuations retard the proliferation process. After assessing the blood smear the culture pellet was resuspended in pre-warmed CCM and returned to culture flasks. The volume of media required for a 24 hr period was determined by the following formula[119]:

$$\text{Volume (mL)/24 hours} = 0.005\ (\mu\text{L of packed erythrocyte volume})\ (\%\ \text{parasitaemia})$$

Trophozoite and schizont cultures were given additional media (above calculated volume) as the parasitaemia would increase before the subsequent media change, this was done to prevent a shortage of nutrients and to avoid parasite stress. Cultures were gassed for 30 sec with a special gas mix containing 5% carbon dioxide (CO_2), 5% oxygen (O_2) and 90% nitrogen (N_2) (Afrox, Germiston, RSA) and incubated at 37°C in a shaking incubator rotating at 60 revolutions per minute (rpm).

Thin blood smears were prepared and dried using a low heat hair dryer, smears were fixed in 100% methanol (MeOH) (Merck, Darmstadt, Germany) for approximately 20 sec. The smears were placed in a 1:5 dilution of Giemsa Azur Eosin methylene blue (Merck, Darmstadt, Germany) and distilled water solution for 5 min to stain the smears. Slides were viewed under oil immersion light microscopy at 1000x magnification (Nikon AFXDX microscope, Melville, NY, USA) to assess parasite proliferation and general condition.

The percentage parasitaemia was determined by counting approximately 1000 cells (100 cells in ten different fields on the side) and dividing the number of infected erythrocytes by the total number of erythrocytes. The parasites “age” was also evaluated and was determined by the hours post invasion (hpi). This was used to determine the synchronisation status of the parasites.

The Malarwheel (Figure 2.1) was developed during this research and was made specifically for the purpose of this merozoite study. The Malarwheel was developed in order to schedule parasites into times to synchronise early stage, and for isolation of late stage parasites. The outer numbered wheel (largest) demonstrates the 48 hr lifecycle of the parasite and demonstrates the

hpi recommended for sorbitol synchronisation and magnetic based cell sorting (MACs) isolation (outermost wheel). The centre wheel represents two 24 hr day periods which demonstrates the time (24 hr clock) and the two days that constitute a full intraerythrocytic lifecycle. By aligning the outer and centre rings (parasite age and time), the estimated time at which synchronisation, isolation and merozoite egress will occur can be predicted. The inner wheel also represents the 48 hr lifecycle but with the corresponding number of 48 – t (time in hrs) to determine the amount of time until the next event/egress.

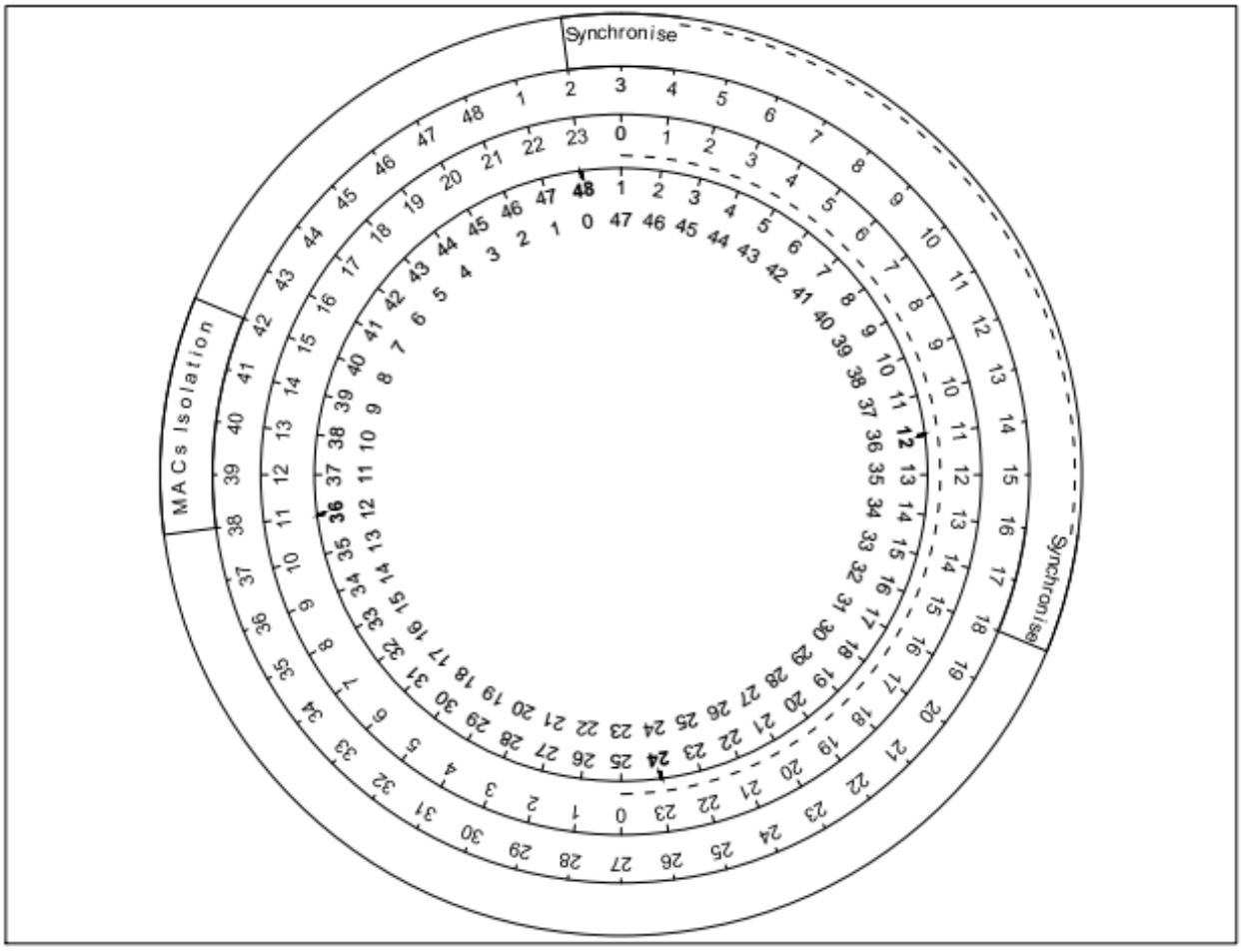

Figure 2.1: The Malarwheel. The tool developed to determine the synchronisation and isolation schedule of parasite cultures. The outer wheel (largest wheel that is numbered) demonstrates the 48 hr lifecycle of the parasite with the hpi recommended for sorbitol synchronisation and MACs isolation. The centre wheel represents two 24 hr day periods. By aligning the outer and centre rings (parasite age and time), the estimated time at which synchronisation, isolation and merozoite egress will occur can be predicted. The inner wheel represents the 48 hr lifecycle (as the other circle does) but with the corresponding number of 48 – t (time in hrs) to determine the time until merozoite egress.

2.1.1.2 Synchronisation

Synchronisation of *P. falciparum* parasites was done using a combination of sorbitol treatment and MACs isolation to obtain parasites within a 2-3 hr window of a defined point. Sorbitol penetrates into low density parasitised erythrocytes (parasites >20 hpi) causing cell lysis by altering osmotic conditions. Uninfected erythrocytes and ring stage parasites remained unaffected and continued to grow.[120] Parasites were incubated in a 5% (*w/v*) D-sorbitol for 15 min at 37°C using 1 mL packed culture cells to 15 mL of sorbitol. Parasites were synchronised for a maximum of 15 min to avoid sorbitol toxicity. Cultures were centrifuged for 5 min at 2000x*g* and washed in fresh media to remove any remaining contaminating sorbitol. Sorbitol treatment was performed at 2-4 hpi and 16-18 hpi (as shown on the Malarwheel). Cultures were synchronised using sorbitol treatment for 3 consecutive cycles in conjunction with MACs synchronisation as needed and then allowed to replicate normally for several cycles. This process was repeated several times for approximately one month period until stable cultures grew which would retain synchronisation. Cultures were then allowed to replicate untreated with frequent splitting of cultures and only treated with sorbitol periodically as determined by the daily assessment of thin blood smears.

2.1.1.3 MACs isolation

Magnetic activated cell sorting (MACs) and parasitised erythrocyte isolation was used to purify cultures to obtain a population of >95% schizonts in a narrowly synchronised window. These could either be introduced to new uninfected red blood cells – thus used as a synchronisation technique, or could be used to obtain highly synchronised merozoite populations.

Haemozoin is strongly drawn towards a magnetic field and accumulates in parasites >38 hpi. These magnetic properties are used to separate schizonts from uninfected and parasitised erythrocytes <38 hpi.

Highly synchronised parasites of 38-44 hpi were prepared using 1 mL of packed culture pellet in 15 mL ICM. The MACs column (Miltenyi Biotek, Biocom Biotech) was prepared by washing consecutively with 100% ethanol (EtOH), triple distilled water, and pre-warmed ICM. The wash steps ensure sterility, while removing air bubbles within the column (which could decrease isolation yield). The parasite culture was passed through the MACs column while mounted in the magnet (Figure 2.2), trophozoites and schizonts would remain trapped within the iron wool of the column while erythrocytes and earlier stage parasites would pass through unretained. The column was washed with ICM to elute parasites that do not contain haemozoin, and then removed from

the magnetic field and washed again to elute schizonts. The remaining culture present in the flow through and wash were combined, centrifuged for 2 min at 2000x*g* and passed through the column a second time. This was repeated so that cultures were passed through the MACs column a total of 3 times.

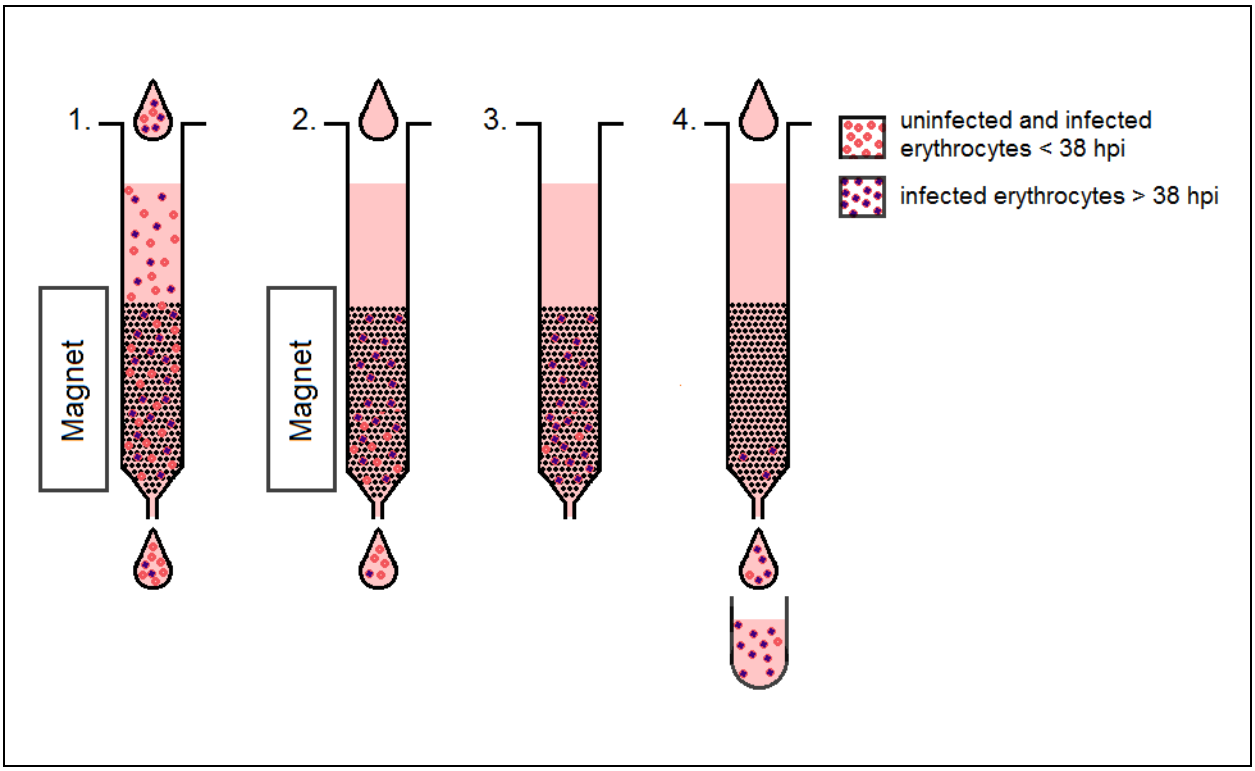

Figure 2.2: Diagram of the magnetic activated cell sorting (MACs) isolation procedure. 1) Parasite culture was pipetted into the MACs column. Schizonts were drawn towards the magnet and remained within the column. The initial eluent was referred to as the "flow through". 2) Uninfected erythrocytes and parasites <38 hpi were removed by washing with ICM. The eluent here was called the "wash". 3) The column containing infected erythrocytes >38 was removed from the magnetic field. 4) Schizonts were isolated by washing from the column with ICM.

Schizonts were incubated for 6-10 hrs in CCM sufficient for a 24 hr period as determined by the formula of Radfar *et al*.[119] The excess media was given to avoid parasite stress, as parasite stress would retard maturation rate. Isolated parasites were treated with 10 µM of cysteine protease inhibitor *trans*-epoxysuccinyl-L-leucylamido(4-guanidino) butane (E64) (Sigma, St Louis, MO, USA), which has been reported to prevent mature schizont rupture by directly blocking proteases from lysing membranes,[121] thereby allowing slower maturing parasites an opportunity to "catch-up".[63] The schizonts were determined to have undergone complete schizogony once the PVM was indistinguishable from the erythrocyte membrane, if it contained a single haemozoin crystal,

and had clearly separated merozoites.[122] Once schizonts had matured sufficiently, E64 was removed by washing using E64 free media and centrifugation for 2 min at 2000x*g*. If the MACs isolation had been undertaken for synchronisation purposes then parasites were used to innoculate uninfected erythrocytes and allowed to incubate. For assessment of proteins from invasive merozoites; a volume of fresh CCM was added to schizonts and these were filter purified using 1.2 µm Acrodisc filters (Pall, Vienna, Austria) to rupture schizonts and isolate merozoites.

2.1.2 MSF assays: Exploring the inhibitory potential of selected compounds

The aim of assessing the inhibitory effect of vanadate species, dioctyl sodium sulfosuccinate, edelfosine and gentamicin on the intraerythrocytic phases and their potential to inhibit invasion was to screen the inhibitory potential of these compounds by determining the IC_{50} and to determine stage specific and temporal effects which were to be correlated with the proteomic analysis.

2.1.2.1 MSF assays

The test design used here was a modification of methods employed for high throughput drug screening on new potential candidate antimalarial compounds.[123] The malaria SYBR Green I-based fluorescence (MSF) assay was used to find the concentration range, and parasite stages where compounds are most effective against intraerythrocytic parasites. SYBR Green I intercalates with DNA by binding to the minor groove in double stranded DNA. The dye exhibits very little fluorescence when unbound but fluorescence greatly increases upon binding to DNA.

Parasites were cultured and synchronised as described above**.** Prior to conducting the assay parasite cultures at the different parasite development stages were adjusted to a 2% haematocrit, 1% parasitaemia and maintained at 37°C until plates were ready for the parasite culture. Compounds were all purchased from Sigma (St Louis, MO, USA) and prepared as follows: Sodium orthovanadate (SOV) was dissolved in PBS and was stored at room temperature when not in use. DSS and edelfosine were prepared freshly by dissolving in CCM. Gentamicin stock solution (84 mM) was stored at 2–8°C and diluted directly into CCM. Gentamicin is typically added to all culture media (CM) during the time that CM is made in order to maintain sterility, so all CM contained 50 µM gentamicin prior to experimentation, taking this into account, the concentrations of gentamicin described represents the total concentration in CCM (Gentamicin present from making media plus newly added). Chloroquine diphosphate (negative control) was dissolved in PBS and frozen at -20° when not in use. To provide and maintain sterility compounds were filter

sterilised using 0.2 µm filters (Pall, Acrodisc, Washington, NY, USA), and diluted to 2 fold the required concentrations in CCM.

All assays were conducted under sterile conditions using sterile flat bottomed 96 well plates. To account for possible edge effects, all wells on the edges of the plates were filled with 200 µL of deionised water. A volume of 100 µL of compound at the test concentrations was plated followed by 100 µL of parasite culture, untreated controls were given CCM in place of the compound, and this resulted in a final 1% haematocrit still with 1% parasitaemia in wells. Plates were incubated under static conditions at 37°C using the same gas mixture as above. Initial parasitaemia of 1% was chosen as the lower quantitation limit of SYBR green is 0.5% parasitaemia, thus allowing for accurate fluorescence quantitation.[124] A low initial starting parasitaemia and haematocrit also ensures sufficient nutrients for the incubation period.

The assays that were conducted to determine IC_{50} utilised synchronised ring stage parasites of 6-12 hpi for a fixed 96 hr incubation period. After IC_{50} had been determined the stage specific effects were assessed by conducting assays on either rings (starting at 6-12 hpi) or late trophozoites (starting at 30-36 hpi) for 24, 48, 72 and 96 hr incubation periods.

After incubation, cells which had settled at the bottom of wells were resuspended, and a volume of 100 µl of parasite culture was removed from assay plates into new 96 well plates, combined with 100 µL of 0.2 µL/mL 10 000x SYBR Green I (Invitrogen, Life Science Technologies, Waltham, MA, USA) in lysis buffer (20 mM Tris; pH 7.5; 5 mM Ethylenediaminetetraacetic acid (EDTA); 0.008% (*w/v*) saponin; 0.08% (*v/v*) Triton X-100) and incubated in the dark for 1 hr at room temperature. Fluorescence was measured using a Fluoroskan Ascent FL microplate fluorometer (Thermo Fisher Scientific, Waltham, MA, USA) excitation at 485 nm and emission at 538 nm.

The IC_{50} was determined as the concentration at which compounds inhibit the *in vitro* proliferation of parasites by 50%. Parasite proliferation was expressed as a percentage of untreated controls. The assays were performed in triplicate and were repeated for three independent biological assays (n=3) unless otherwise stated. Data analysis was conducted on GraphPad Prism (Version 5) software to determine the IC_{50} by generating non-linear dose response regression curves. Further comparisons of stage specific effects were done by MS Excel 2013 for standard error of mean in conjunction with GraphPad. Kruskal-Wallis test followed by Dunn's post-hoc pairwise comparisons of each sample set against the others. This analysis was conducted using GraphPad Prism (Version 5) and significance was set at $P < 0.05$.

2.1.3 Merozoite invasion assays: Exploring the inhibition of selected compounds on merozoite invasion

The aim was to first isolate highly synchronised and viable merozoites that invade new uninfected erythrocytes and second, to evaluate the effects of selected compounds on merozoite invasion of erythrocytes.

2.1.3.1 Merozoite invasion assays

Merozoite Invasion Assays (MIAs) require large numbers of highly purified merozoites which retain invasive capacity. A volume of 1 mL packed highly synchronised schizonts was used at an 18% parasitaemia (or equivalent) to provide a high merozoite to erythrocyte ratio. Parasites were isolated by MACs isolation as previously described to yield >95% schizont infected erythrocyte isolates from the parasite cultures.

Fresh uninfected erythrocytes were diluted to a 10% haematocrit in CCM and maintained at 37°C until use. Concentrations of the four test compounds assessed were selected as the IC_{50} for each, as determined by MSF assays or IC_{50}'s from literature, 100 µM was assessed for all compounds as a standard for comparison, and 2 mM vanadate was assessed as at this concentration vanadate would predominantly be in tetrameric form.[99] Compounds were prepared in CCM just prior to schizont rupture, this was done to reduce the amount of protein binding for edelfosine and DSS. Compounds were diluted to 10 fold the required concentration. A volume of 5 µL of each test compound high concentration stock was plated onto sterile flat-bottomed 96 well plates, and placed on plate warmer to maintain a constant 37°C temperature.

Once schizonts had matured sufficiently, cultures were washed twice to remove E64, cultures were washed by centrifugation at 2000xg using CCM at 37°C. Schizonts were resuspended in 2.5 mL pre-warmed CCM at 37°C and filtered using a 1.2 µm filter. The filtrate contained both merozoites and haemozoin crystals.

A volume of 40 µL of merozoite suspension was immediately added to each well, followed directly by 5 µL of the uninfected erythrocytes to produce a final 1% haematocrit in each well. The plated merozoites and erythrocytes were mixed for 10 min by gentle agitation. MIA plates were incubated for 50 min at 37°C under static conditions using the 5% O_2 5% CO_2 and 90% N_2 special gas mix. Merozoites plus erythrocytes suspensions were exposed to the test compounds for a total of 60 min, which would normally account for the majority of the invasion events. Prolonging compound exposure could risk an effect on ring stage parasites. Following the incubation period, compounds and remaining non-invaded merozoites were removed from erythrocytes by washing twice with

CCM and centrifugation at 200x*g* for 2 min (Thermo Scientific SL 16R (Thermo Fisher Scientific, Waltham, MA, USA)). Fresh CCM was added to maintain a 1% haematocrit. Compounds were incubated for approximately 40 hrs for parasite DNA proliferation to occur, but not longer than this to avoid including parasites from a second replicative cycle.

Flow cytometry was used to determine the percentage of invasion. Cultures from MIAs were fixed in 1 mL of 0.025% glutaraldehyde (Sigma, St Louis, MO, USA) for 45 min, and stored at 4°C. These samples were used for flow cytometry analysis within one week. Fixed cells were washed twice to remove the excess glutaraldehyde using 1 mL of PBS and centrifuged for 5 min at 500x*g*. Samples were made up to 100 µL in PBS, and then parasite DNA was stained using 10 µL of a 1:1000 dilution of SYBR Green I for 45 min in the dark at room temperature. After incubation the samples were centrifuged for 5 min at 500x*g* and washed once with 500 µL PBS. Samples were made to a final volume of 400 µL in PBS prior to flow cytometric analysis. A minimum of 2.4 x 10^5 cells were analysed for each sample using a FACS FC500 Series (Beckman Coulter, Brea, CA, USA) equipped with an air-cooled argon laser with fluorescence emission collected in the FL-1 channel (Green signal, FITC channel) with 488 nm excitation, 525 nm emission. FlowJo v9.1 (Tree Start, Ashland, OR, USA) was used to analyse the data. Invasion rates of inhibitor treated samples were compared to the invasion rates of the untreated control. Statistical analysis was conducted using the non-parametric Kruskal-Wallis test followed by Dunn's post-hoc pairwise comparisons of each sample set against the others. This analysis was conducted using GraphPad Prism (Version 5) and significance was set at $P < 0.05$. At least three independent biological assays (n=3) were conducted in triplicate for all compounds.

2.2 Results

2.2.1 *P. falciparum* culturing techniques

Standard *P. falciparum* culturing methods typically used for research on other intraerythrocytic stages were inadequate for merozoite assessments. These resulted in insufficient volumes of merozoites with culture synchronisation windows too wide for optimum assessments. Standard culture methods recommend a 5% haematocrit which caused parasite stress at >4% parasitaemia. Parasite stress was initially evident by the appearance of condensed dark staining parasites which caused desynchronisation and a decreased rate of development, this resulted in retardation of merozoite egress with diminished numbers of rupturing schizonts. If continued at this haematocrit, crisis level would be reached where parasite death and severe reduction in new ring stage production would result. Using standard methods parasite crisis level was reached at 5–12% parasitaemia (Figure 2.3). Using optimised methods the formula of Radfar *et al.*[119] was used to determine a daily haematocrit based on packed cell volume and parasitaemia. This allowed parasites to replicate within a normal 48 hr lifecycle without parasite stress, and retain synchronicity. The cultures were frequently split to maintain high replication rates and to rapidly increase parasite quantity before experimental procedures took place. Using the methods described here synchronised healthy cultures were obtained with parasitaemias reaching as high as 34%.

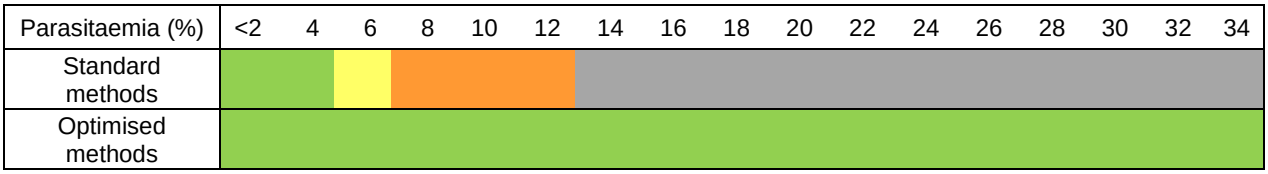

Figure 2.3: Parasite stress observed using standard culturing techniques and optimised culturing techniques. Parasite stress is indicated by colours: green- no stress; yellow- mild stress; orange- high to crisis level; grey- non attainable.

Sorbitol alone did not produce adequate synchronisation at high parasitaemias[125] and resulted in a 4-6 hr synchronous window as determined by hpi assessment of thin blood smears during routine culturing. MACs isolation was used to separate schizonts from faster replicating parasites that had progressed to early ring stage, and exclude slower growing younger trophozoites. The incorporation of MACs isolation improved the synchronisation window to 2-3 hrs (Figure 2.4). Parasites may replicate at different rates despite synchronisation methods, resulting in smaller percentages of parasites remaining in different synchronisation windows. In cultures treated with sorbitol alone 20% of parasites had a 2-3 hr synchronous window, 60% in 4-6 hr window and 20%

in >6 hr window. Using the combination of sorbitol and MACs 80% of parasites were within 2-3 hr window, 15% within 4-6 hrs and 5% had a synchronisation window of >6 hrs. Cultures initiated from freshly thawed parasites needed several cycles to reach a steady growing state and did not replicate at rates described here. Approximately one month of daily culturing with intermittent repeated cycles of sorbitol treatment (with occasional MACs synchronisation) was required for parasites to retain synchronisation. Parasites undergoing regular sorbitol treatment also did not replicate at these rates and therefore parasites were allowed to proliferate for several cycles without any sorbitol synchronisation treatment prior to isolations for experimental purposes.

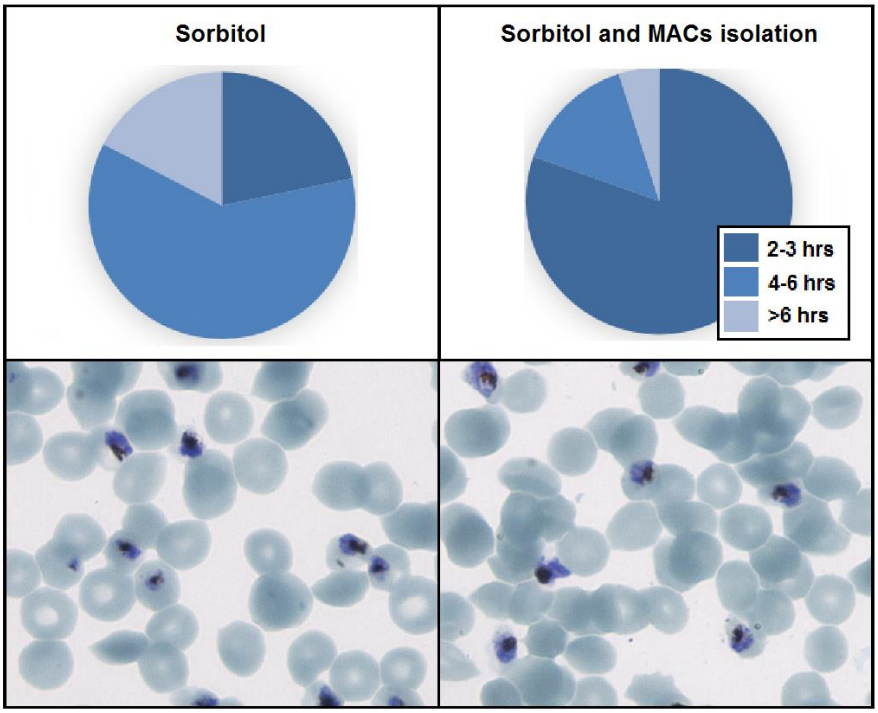

Figure 2.4: Comparison of synchronisation techniques. Merozoite research requires a narrow synchronous window. Sorbitol treatment resulted in a synchronous window of 4-6 hrs, while sorbitol treatment combined with MACs isolation was found to be superior and decreased the synchronous window to 2-3 hrs. The hpi of the parasites is determined by the size, shape and staining characteristics of the parasites. Parasites synchronised using the combination of sorbitol and MACs resulted in parasites with similar staining patterns, while parasites treated with sorbitol alone showed parasites of varying sizes, inferring a larger window of synchronisation.

After passing the culture through the MACs column once (as with standard techniques) schizonts were still observed in the flow through fraction. Cultures were passed through additional times to increase merozoite and proteomic yield. After cultures had been passed through the column 3 times no remaining schizonts were visible in the flow through (Figure 2.5). The proteomic yield of

merozoites increased 1.5 and 1.8 fold for 2 and 3 times through the MACs column respectively as determined by proteomic quantitation assays (details not discussed here).

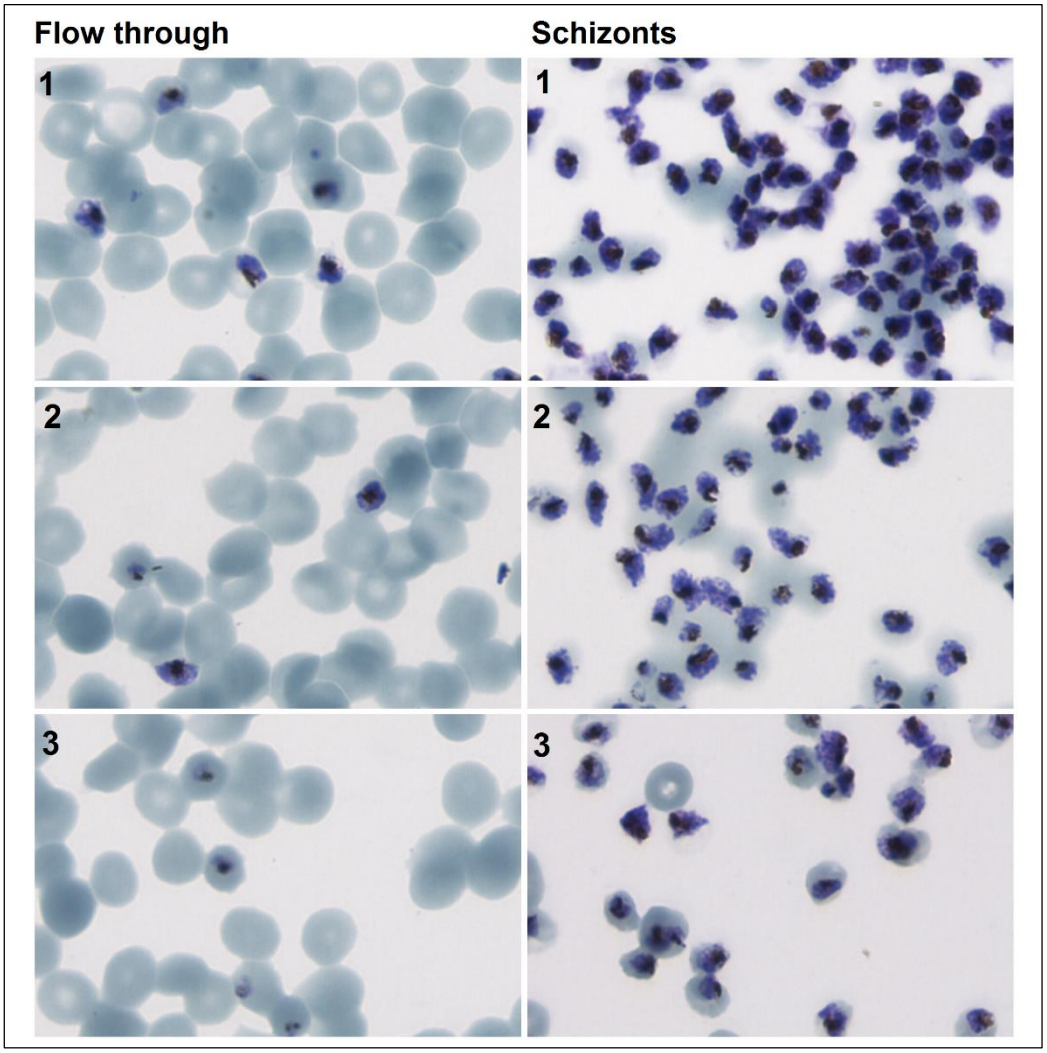

Figure 2.5: The flow through and schizont isolations of *P. falciparum* 3D7 cultures. Late stage parasite cultures had been passed through the MACs column additional times where no schizonts were evident after the cultures had been passed through the column 3 times. Numbers are indicative of the times that the culture was passed through the MACs column.

The optimised methods described here resulted in cultures with fast replicative rates which retained synchronicity (Figure 2.6). These methods increased the parasite volume rapidly to enable several MACs isolations every 2-4 days, in comparison to standard culturing methods where 1-2 MACs isolations were conducted in one month period. New cultures were initiated every 3-4 months to prevent phenotypic variation that occurs from long term culturing.[126]

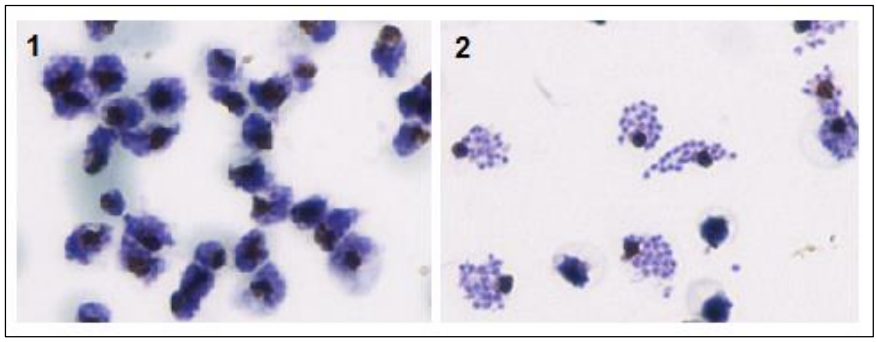

Figure 2.6: Highly synchronised *P. falciparum* 3D7 cultures after MACs isolation. 1) Late stage parasite population; 2) Mature schizonts prior to rupture.

2.2.2 MSF assay

2.2.2.1 MSF assay: IC_{50} determination

The results described here for MSF assays are separated into two sections, first for IC_{50} determination, and second for stage specific effects with a speed of action component. The inhibitory effects of the selected compounds (vanadate, edelfosine, DSS and gentamicin) was determined on intraerythrocytic *P. falciparum* 3D7 strain by conducting MSF assays on ring stage parasites.

A parasite culture of 1% parasitaemia at 1% haematocrit was used for each assay and incubated with inhibitors in standard static culturing conditions for 96 hrs. After the incubation period, SYBR-green was added to quantify the parasite's DNA proliferation by fluorescence and determine the inhibitory potentials. IC_{50} values of 10 µM, 50 µM, 200 µM and 5 mM were obtained for vanadate, edelfosine, DSS and gentamicin respectively (Table 2.1). Dose-response curves depicting the antimalarial efficacy are represented as a percentage of the control (Figure 2.7).

Table 2.1: IC_{50} values of selected compounds as determined by MSF assays on *P. falciparum* 3D7 strain ring stage parasites after 96 hrs of incubation in static conditions. Data representative of three independent experiments (n=3) with standard error of mean (SEM) represented.

Compound	**IC_{50} ± SEM**
Vanadate	9.7 µM ± 1.18
Edelfosine	46.9 µM ± 13.6
DSS	205.9 µM ± 13.1
Gentamicin	5.4 mM ± 0.74

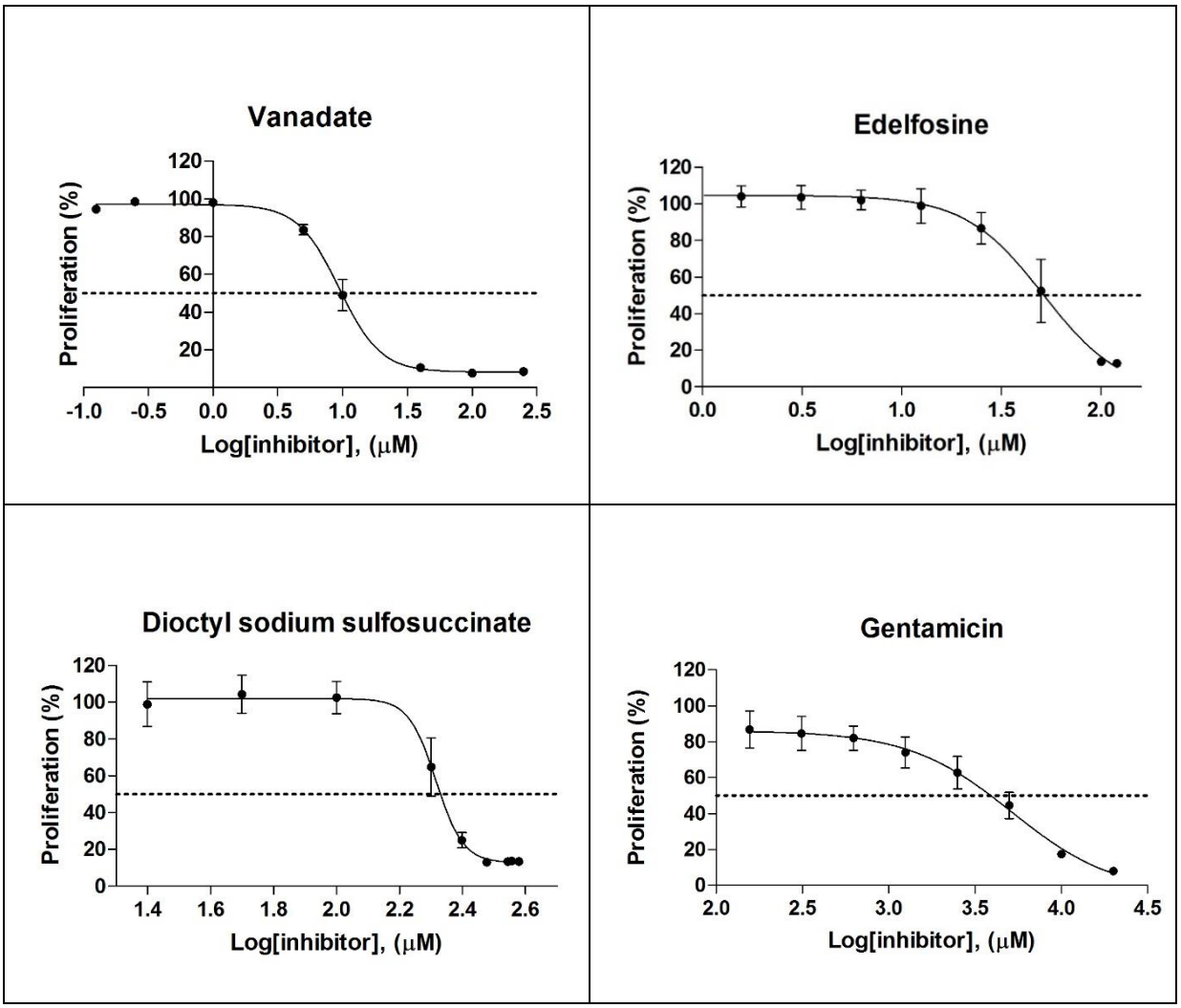

Figure 2.7: Dose-response curves of selected compounds tested against intraerythrocytic ring stage *P. falciparum* 3D7 parasites for 96 hrs to determine IC_{50} by vanadate, edelfosine, DSS and gentamicin. Data representative of three independent experiments (n=3) with error bars representing the SEM. Points without visible error bars contain bars within points.

2.2.2.1 MSF assays: Stage specific effects

MSF assays were conducted on either ring or late trophozoite stage parasites for 24, 48, 72, and 96 hr incubation periods (Figure 2.8). The rationale to perform the stage specific assays was to give an indication on whether early or late stage parasites were more sensitive to the test compounds, as this could indicate additional mechanisms of inhibition. Ring assays conducted for 24 hr incubation periods were initiated with parasites of 6-12 hpi and ended with parasites between 30-36 hpi, during this assay rings developed into trophozoites. In contrast, the 24 hr trophozoite assays were initiated at 30-36 hpi and ended with parasites 6-12 hrs post erythrocyte egress. During this assay parasites progressed from trophozoite stage through schizogony, merozoite invasion and concluded with young rings. The duration of the assays covered a period between 0.5-2 complete cycles. The resulting graphs of the MSF assays are overlaid for each time period (Figure 2.9a and 2.9b).

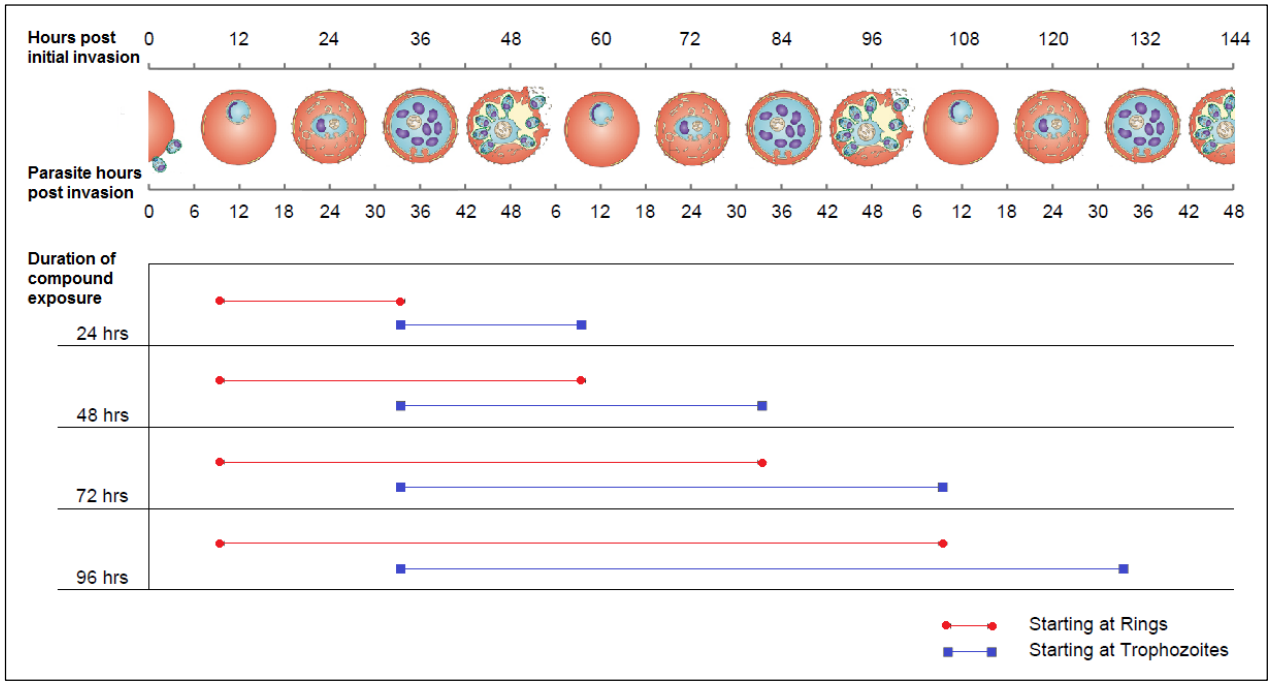

Figure 2.8: Temporal and stage specific MSF assay analyses. MSF assays were conducted on parasites commencing in ring phase (red) or trophozoites (blue) for 24, 48, 72, and 96 hrs. The image of the life cycle at the top shows the developmental stages in which the parasites were during exposure to the compounds (Lifecycle images were obtained and adapted from Maier *et al.* 2009[127] with permissions).

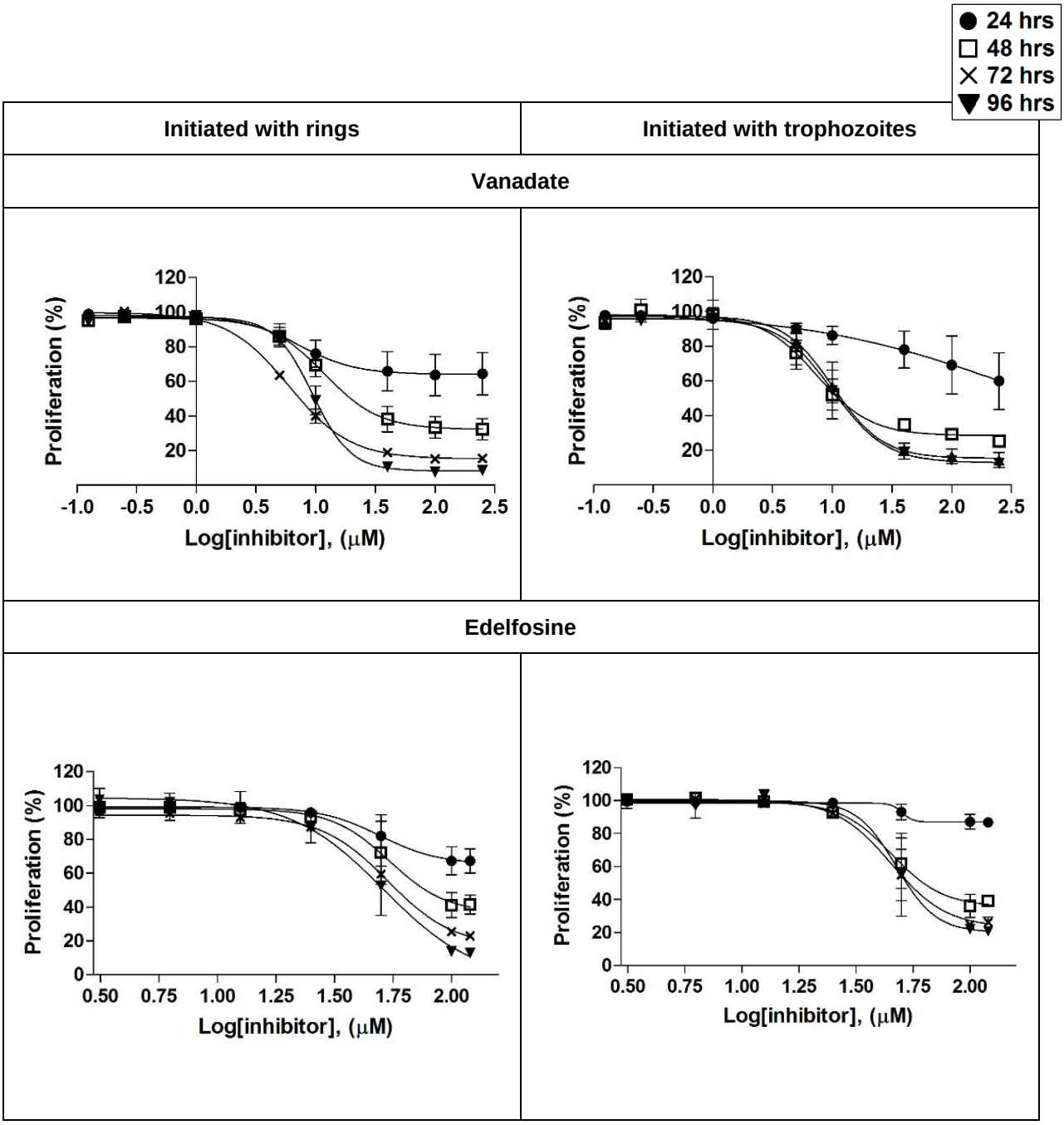

Figure 2.9a: The results of temporal and stage specific MSF assays overlaid for the separate time points assessed for vanadate and edelfosine. Graphs without visible error bars are contained within the point. Data representative of n=3 for vanadate, with n=2 for edelfosine (assays were conducted in triplicate).

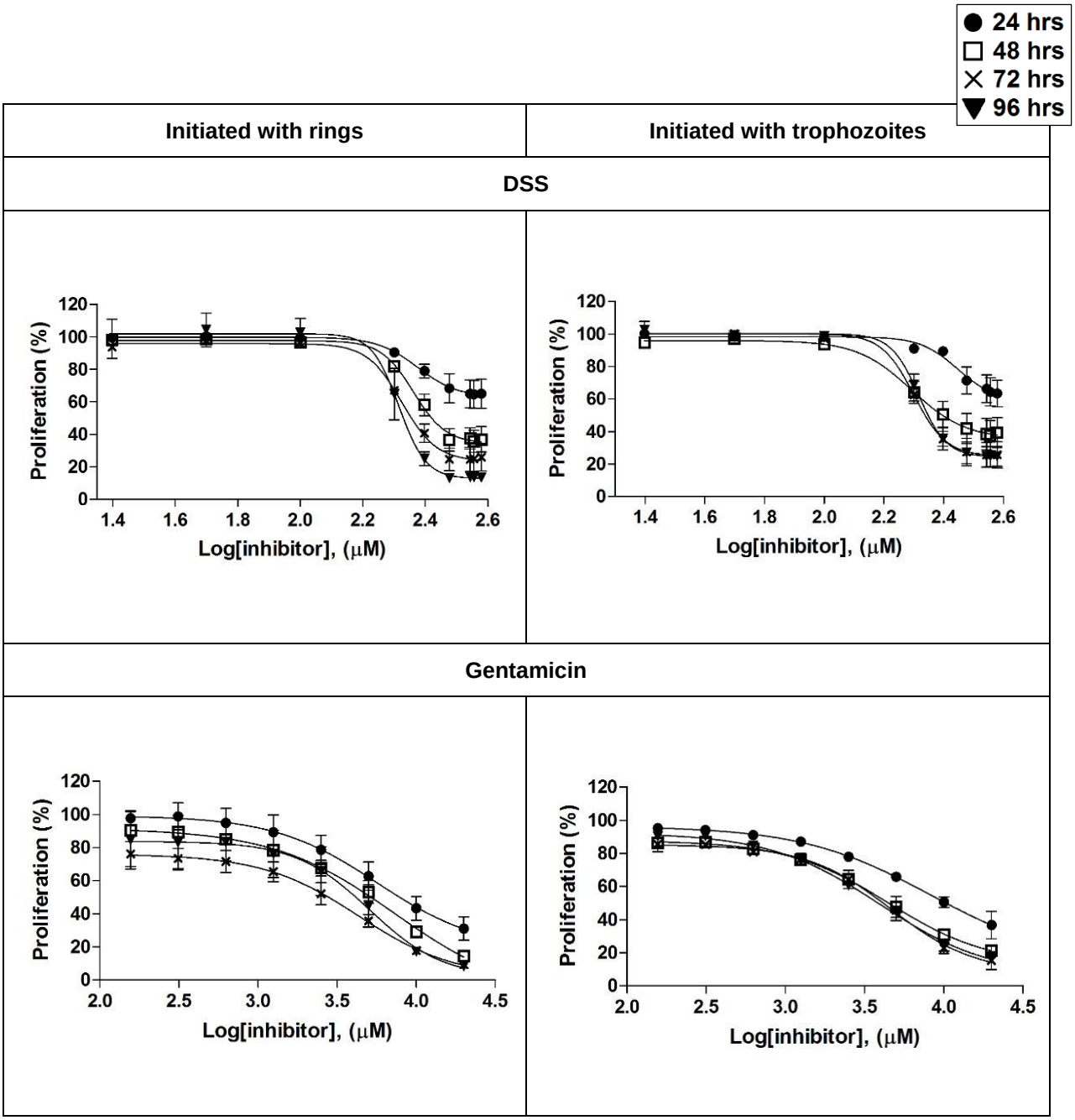

Figure 2.9b: The results of temporal and stage specific MSF assays overlaid for the separate time points assessed for DSS and gentamicin. Graphs without visible error bars are contained within the point. Data representative of n=3 for DSS and gentamicin (assays were conducted in triplicate).

The IC_{50} values found at 24, 48, and 72 hrs supplemented the standard 96 hr assays by providing a broad indication of the speed and stage at which the compound worked. The speed at which compounds act were determined by the time taken to reach a stable IC_{50} value (normally determined as the IC_{50} value at 96 hrs of incubation). Shown in Figure 2.10, vanadate reached a stable IC_{50} of 10 µM after 24 hrs of incubation in ring assays - indicating that vanadate was probably a fast acting compound. The IC_{50} after 24 hrs of incubation starting with late trophozoites was 70 µM (7 fold higher than for the 24 hr ring IC_{50}) indicating that although vanadate is a fast acting compound it may have a preference for parasites between ring and early trophozoite stage. As the inhibitory concentration of trophozoites in 24 hr assays was significantly higher, it appeared that this compound had less effect on late stage parasites, invasion of erythrocytes, and possibly early rings. Edelfosine and DSS also reached a stable IC_{50} after 24 hr ring assays, while showing a moderate increased IC_{50} value in the 24 hr trophozoite assays which was not found to be significant, indicating that these had a fast action on parasites at both ring and trophozoites stages. Gentamicin showed an increased IC_{50} in the 24 and 72 hr trophozoite and 48 hr ring assays and did not reach an apparent stable IC_{50}, the variation and high concentrations made the determination of stage specificity and speed inconclusive.

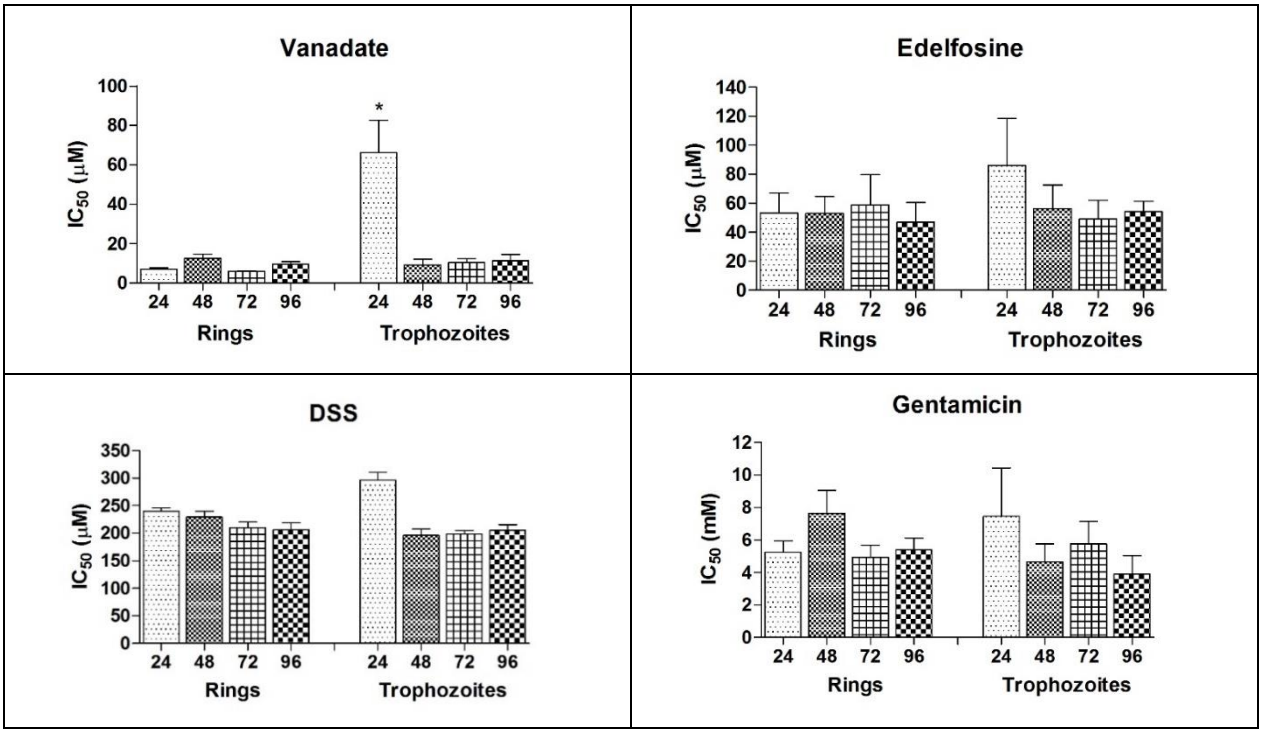

Figure 2.10: IC_{50} for determination of speed of action and stage dependent effects starting with ring or trophozoite parasites for 24, 48, 72 and 96 hrs of incubation in selected compounds. Error bars represent the SEM of n=3 assays for vanadate, DSS and gentamicin, and n=2 for edelfosine, assays were repeated in triplicate. Significance was recorded as * P <0.05

The inhibitory speed was assessed as the ratio between 24 and 96 hr assays commencing at the same initiation stage, where a stable IC_{50} had been reached. The ratio was then also used to indicate a stage specific preference. These results are summarised in Table 2.2 below.

Table 2.2: Overview of predicted stage specificity and speed of action. Ratio of 24 hr assay divided by 96 hr assay gives a suggestion as to the compound's preferred stage and speed of inhibition.

Compound	Assay commencing at stage	Ratio of 24 hr IC_{50}/96 hr IC_{50}	Predicted stage specific action	Predicted speed of activity
Vanadate	Ring	0.73 ±0.07	Rings and early trophozoites (between 6 and 36 hpi)	Fast
	Trophozoite	5.9 ±1.44*		
Edelfosine	Ring	1.14 ±0.29	No specific preference	Fast
	Trophozoite	1.59 ±0.60		
DSS	Ring	1.17 ±0.03	No specific preference	Fast
	Trophozoite	1.44 ±0.07		
Gentamicin	Ring	1.22 ±0.41	Inconclusive	Inconclusive
	Trophozoite	1.37 ±0.8		

Significance was recorded as * P <0.05

Edelfosine and DSS have a low solubility in aqueous solutions (with 5 mM and 18 mM solubility at 20°C in aqueous solutions respectively[128, 129]). The compounds were initially dissolved in dimethyl sulfoxide (DMSO) to make stock solutions. However, when edelfosine and DSS were used in combination with DMSO at non-toxic concentrations (<0.25% DMSO) erythrocyte lysis was observed in several concentrations. DMSO is amphiphilic and has been known to decrease surface tension alone and to a larger extent when combined lipophilic compounds[130, 131]. By exposing the parasitised erythrocytes simultaneously to two compounds with amphiphilic properties the compounds significantly destroyed the integrity of erythrocyte membranes causing haemolysis. Haemolysis was however, not visible when compounds were dissolved directly into CM at concentrations tested. Erythrocytes exposed to 0.5% DMSO in the absence of another compound did not show visible haemolysis. It appears that DMSO combined with the test compounds had an additive/synergistic effect leading to haemolysis. Starting solutions using edelfosine and DSS were thus made by dissolving the compounds directly in CM prior to use at concentrations soluble in aqueous solutions and filter sterilised.

2.2.3 Merozoite invasion assay

2.2.3.1 Merozoite invasion assay: Isolation of viable invasive merozoites

MIAs were initially conducted to assess the invasive potential of merozoites. Highly synchronised schizonts were isolated by MACs isolation and incubated in E64 inoculated CCM as described above. Once the parasites had sufficiently matured and began to rupture the cultures were centrifuged to pellet the schizonts. The CCM was removed and after washing, a small volume of fresh CCM was added. The whole parasite preparation was passed through a 1.2 µm filter to rupture schizonts and isolate merozoites. Visual assessments of smears showed that filtration successfully isolated merozoites from parasitised and uninfected erythrocytes. The resulting filtrate contained merozoites and haemozoin crystals. Merozoites were added to pre-warmed 37ºC erythrocyte preparations. The merozoites successfully bound to the uninfected erythrocytes and invasion occurred to recommence the intraerythrocytic cycle. This resulted in highly synchronised cultures that developed normally (Figure 2.11).

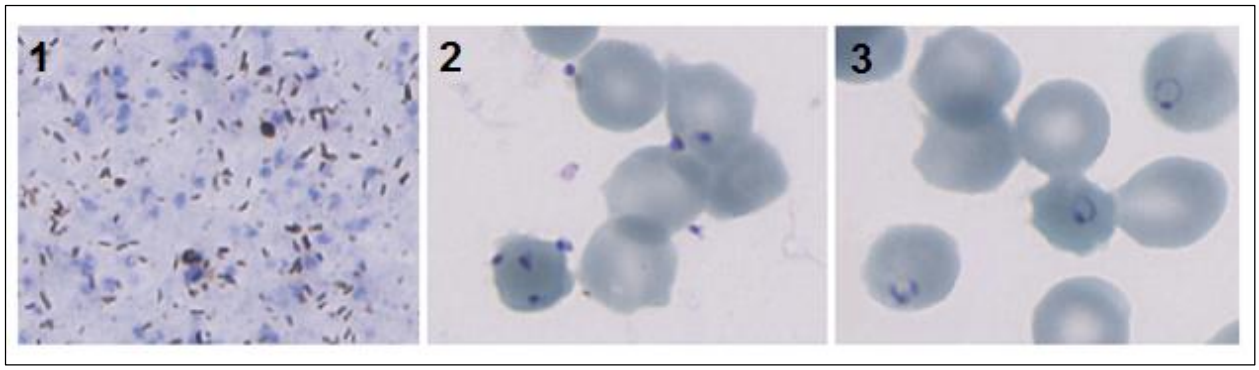

Figure 2.11: Merozoite purification and invasion of erythrocytes. 1) Purified merozoite suspensions were obtained from filtering highly synchronised E64 treated schizonts using a 1.2 µm filter. The filtrate contained merozoites and haemozoin crystals, seen as dark irregular particles. 2) Merozoites were exposed to uninfected erythrocytes and bound to commence invasion. 3) This resulted in highly synchronised cultures containing normally developing parasites.

The invasion of merozoites was assessed by flow cytometry and resulted in a 2.9% ±0.31 SEM parasitaemia of new infections at 37°C. Invasion was determined by flow cytometric analyses of untreated samples (Figure 2.12). Merozoite invasion efficiency was defined as the number of merozoites that successfully invaded new uninfected erythrocytes. The merozoite invasion efficiency was calculated by using the approximate number of erythrocytes, merozoites and percentage parasitaemia. Approximate number of erythrocytes was determined by the packed erythrocyte volume and the Mean Corpuscular Volume (MCV) of normocytic cells (90 x 10^{-15} L).[132]

The approximate number of merozoites was calculated using the number of infected erythrocytes and the average number of merozoites per schizont (17.48 merozoites per schizont in *P. falciparum* 3D7 strain (determined separately)). The formula of Boyle *et al.*[63] was used to calculate merozoite invasion efficiency:

$$\text{Merozoite invasion Efficiency} = \%\ \text{Parasitaemia(new)}\ \text{x}\ \left(\frac{\text{No. of erythrocytes(total)}}{\text{No. of merozoites}}\right)$$

High merozoite to erythrocyte ratios (100:1) were used to produce a parasitaemia acceptable for assessments by flow cytometric analyses and resulted in low 0.03% invasion efficiencies of merozoites for the untreated samples.

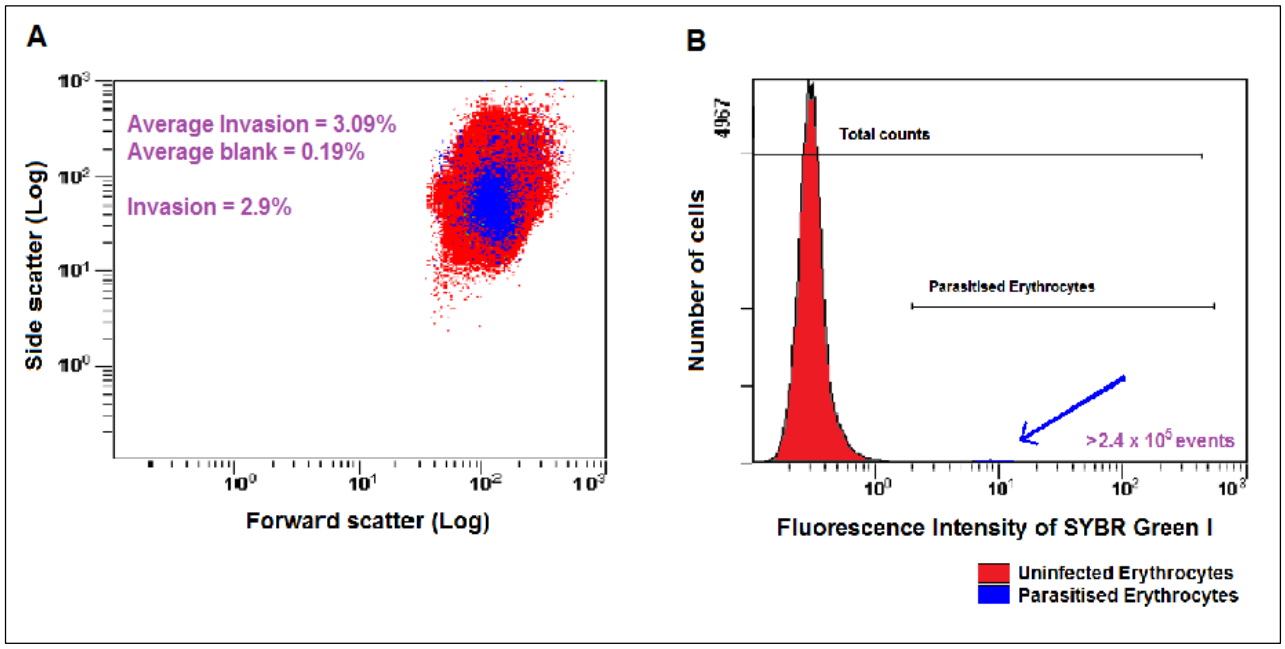

Figure 2.12: Merozoite invasion as determined by flow cytometry. A) Merozoite invasion of uninfected erythrocytes in the untreated samples as compared to the background of the negative control, the untreated samples resulted in a 2.9% ±0.31 SEM parasitaemia after 60 min incubation period of invasive merozoites with erythrocytes. B) Number of total counts and parasitised erythrocytes. The arrow points to invaded erythrocytes. A minimum of 2.4x10^5 cells were counted in each sample.

2.2.3.2 Merozoite invasion assay: Inhibition of invasion

MIAs were used to screen and assess the selected compounds inhibitory potential on invasion. Vanadate caused 14, 26 and 69% reduction of invasion at 10 µM, 100 µM and 2 mM respectively (Figure 2.13 and Table 2.3). Vanadate treatment at 2 mM caused a significant inhibition in

comparison to the untreated control. Edelfosine caused no inhibition at 10 µM, while causing 47.9, 50.7, and 56.6% inhibition of invasion at 50, 75 and 100 µM respectively. Edelfosine was the only compound of those assessed that caused a significant reduction of invasion at 100 µM. DSS demonstrated no inhibition of invasion at 100 µM. Concentrations of 200 µM and above were also assessed for DSS but these results were excluded due to haemolysis caused by the compound. Gentamicin also showed no inhibition at 100 µM and 5 mM concentrations.

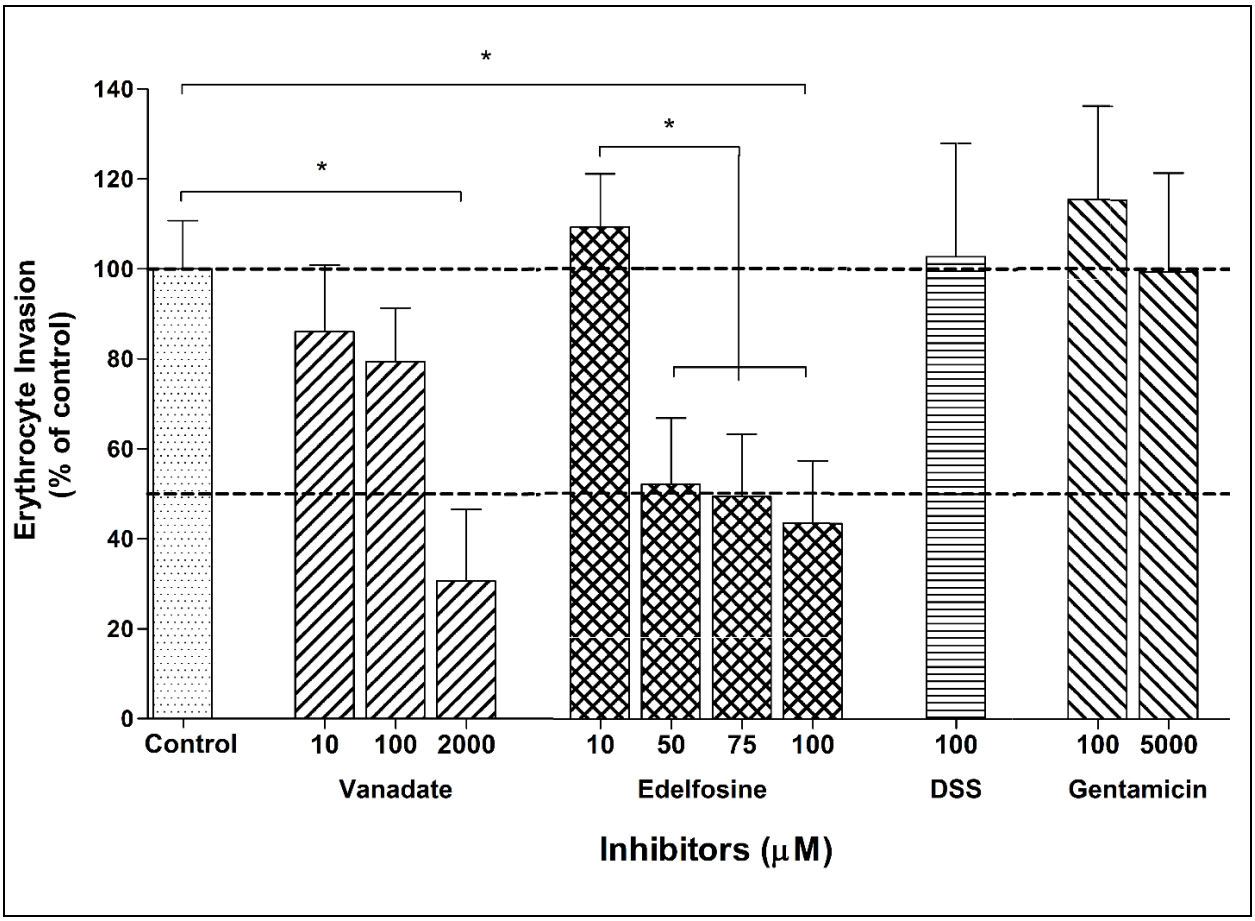

Figure 2.13: Inhibition of merozoite invasion of erythrocytes. Effects of vanadate, edelfosine, DSS and gentamicin on invasion of erythrocytes, results are expressed as a percentage of the control. Results are reported as the mean ± SEM for at least 3 independent assays.* P <0.05 in comparison to control.

Table 2.3: The effect of vanadate, edelfosine, DSS and gentamicin on merozoites invasion of erythrocytes. Summary of inhibition of invasion as percentage of the control ± SEM. * P <0.05 in comparison to control.

Compound	Concentration (µM)	Invasion inhibition (100 - % of control)
Vanadate	10	14.0 ± 14.9
	100	26 ± 10.0
	2000	69.4 ± 16.0*
Edelfosine	10	None
	50	47.9 ± 14.6
	75	50.7 ± 13.8
	100	56.6 ± 13.9*
DSS	100	None
Gentamicin	100	None
	5000	None

Variability was seen in the results, this is possibly due to differences in numbers of active merozoites that were still invasive per assay which would be affected by the timing of rupture of the schizonts. Biological variability is also expected between the parasites during separate isolations. Biological variability between erythrocytes could also result in variability in results.

Dioctyl sodium sulfosuccinate concentrations of greater than 200 µM caused haemolysis when added to erythrocytes prior to the addition of merozoites. The starting concentration of compound was 10 fold the required concentration which appeared to be above the surfactant threshold of the erythrocytes. When DSS was added after the addition of merozoites no haemoylsis was observed, however, these results were excluded as merozoites appeared to agglutinate in these samples.

2.3 Discussion

2.3.1 Optimising merozoite study techniques

With merozoite invasion being crucial to the asexual reproduction of the malaria parasite, the optimisation of a culturing method specific to produce viable merozoites is vital to be able to advance the current knowledge of merozoite processes and behaviour. Volume of culture media, number of uninfected erythrocytes, haematocrit and temperature have all been suggested as being limiting factors for parasite replication or as factors influencing replication rates and culture health. By determining the minimum volume of CCM required based on the packed-cell volume and percentage parasitaemia, cultures of up to 34% parasitaemia of viable and highly synchronised merozoites could be obtained; while using standard culturing methods parasite crisis levels were reached at 5-12% parasitaemias (which was in accordance with reported work [122, 133, 134]). The high parasitaemias achieved were comparable to that of Radfar *et al.* 2009[119] who coupled the 24 hr media formula with frequent culture splitting. High parasitaemias can be obtained using standard culture methods, however, this would require 2-3 CCM changes daily and is highly labour intensive, while the method used in this study required media changes only once per 24 hr period.

Merozoite invasion rates are sensitive to the starting parasitaemia, where invasion rates were influenced by the ratio of malaria parasites to that of erythrocytes.[122] This was observed in this study and reported by others in both routine culture and MIAs.[63, 135] High ratios of merozoites to erythrocytes (excess merozoites) result in high parasitaemias, but low invasion efficiencies. Whereas low ratios of merozoites to erythrocytes (excess erythrocytes) had high invasion rates but low final parasitaemias. Thus during routine culture the frequent splitting of cultures caused low starting parasitaemias which resulted in high invasion efficiencies and a shortened time period to obtain high parasitaemia cultures.[119, 135] However, in the setting of merozoite invasion assays, parasitaemias sufficient for flow cytometric analyses were required. Therefore, a high merozoite to erythrocyte ratio was used to increase invasion events. The high ratios resulted in low invasion efficiencies of merozoites but resulting parasitaemia was adequate for flow cytometry. The results reported here have lower invasion efficiencies compared to Boyle *et al.* 2010[63] which may be influenced by differences in virulence of *P. falciparum* strains. The resulting low invasion efficiencies seen in high starting parasitaemias may be caused by a form of competitive exclusion where interferences between merozoites become a limiting factor.[63] High parasite concentrations may also encourage entry into apoptosis.[136, 137] With cultures of high parasitaemias and/or merozoite loads this would have a continuity advantage where fewer invasion events improve the

chances of a small percentage of parasites reaching full gametocyte maturation for transmission to a new host in systems where nutrients become a limiting factor.[138, 139] During the intraerythrocytic cycles fewer invasion events occur when the nutrient supply is reduced and lower glucose levels are reported to trigger the development of sexual stages.[136] In these cases, the parasites go into parasite stress and have fewer parasites completing the sequential developmental cycles. Should merozoites behave in the same way as other intraerythrocytic stages by decreasing invasion efficiencies this would again attest to the complexity of the parasite and emphasise the importance of maintaining low haematocrit assays for increased invasion events in merozoite assays and routine culturing. High haematocrits have shown reduced invasion efficiency in merozoite invasion assays[63] and in routine cultures of intraerythrocytic stages.[125]

Maintaining optimum parasite culturing conditions in terms of temperature and correct timing of synchronisation and nutrient replacement activities are essential to obtain highly synchronised cultures of viable merozoite populations. With the *Plasmodium* parasites being sensitive to temperature, even moderate fluctuations can retard parasite progression which increases the rate at which cultures loose synchronicity.[122] Thus during routine culture the temperature was maintained at 37ºC with exposure to lower external temperatures being limited to the minimal time for media changes, and the periods during MACs isolations. The retardation of development at lower temperatures is not limited to intraerythrocytic stages, as the merozoite's invasive half-life has been shown to increase from 5 min at 37ºC to 15 min at 22ºC.[63] The increased half-life may have valuable implications in certain assays which require additional time for processing of merozoites. However, it has not been determined how this may affect the temperature sensitive protein interactions, and it was not advisable to reduce temperatures with the proteomic nature of this study.

In order to assist with the correct timing of procedures the "Malarwheel" was developed. This was a highly valuable tool that was utilised for the scheduling of procedures including routine culturing, sorbitol synchronisation and MACs isolation. Scheduling the sorbitol synchronisation for 2-4 hpi and again at 16-18 hpi reduced the synchronous window to 4-6 hrs, and combined with MACs isolation could then be further reduced to a synchronous window of 2-3 hrs. Although other techniques described have used percoll-sorbitol gradients to synchronise parasites, this has shown to not be ideal for isolation of synchronised merozoite populations suitable for downline proteomic assessment. Percoll used independently does not separate late stage trophozoites from schizonts [120] and therefore has been used in conjunction with sorbitol to narrow the

synchronous window to 3-6 hrs.[140, 141] However, this method was avoided as Percoll-sorbitol synchronisation has been shown to lower erythrocyte invasion efficiencies in a number of parasite strains,[135, 142] while improved efficiencies were seen after MACs isolations.[135, 142]

Parasite cultures were repeatedly passed through the MACs column three times which increased the parasite and protein yield. Although the additional times through the MACs column did isolate additional late stage parasites, the time at which the parasites were exposed to external temperatures was longer than if the parasites had been passed through the column once as with standard isolation. It was not determined in this study if this extended time at lower temperatures had an effect on the invasion rates by reducing parasite maturation rate. However, the addition of E64 would be expected to diminish the effect of the longer exposure period to lower temperatures. E64 is thought to permeate erythrocyte membranes through a parasite induced channel and interfere with the cysteine proteases on the cytosolic side of the erythrocyte membrane which are associated with membrane rupture.[143] As the PVM ruptures independently of cysteine proteases, the erythrocyte membrane is left surrounding the merozoite clusters.[121, 144] Protease inhibitor E64 is thought to not affect merozoites adversely, as treatment for 6-10 hrs significantly increases the quantity of merozoites obtained resulting in protease inhibitor treated solutions having higher proportions of invading merozoites in comparison to untreated.[63, 144, 145]

2.3.2 Merozoite invasion assay

The MIA is a means to assess viable merozoites for invasion kinetic studies and is a suitable technique for semi-high throughput drug screening of invasion inhibiting compounds.[63] This method contrasts other invasion studies where merozoites which have been released naturally from schizonts often result in insufficient or lack viable merozoites for conclusive studies.[146] In this study, the forceful rupture of schizonts produced large volumes of isolated merozoites which maintained invasive potential. The merozoite invasion assay differs from other assays in the sense that it specifically looks at invasion and eliminates the overlapping and interfering effects that compounds may have on other life stages from early rings up until and including schizont rupture. The results described in this study are some of the first MIAs reported on *P. falciparum* 3D7 strain parasites. Thus the ratios of merozoites to erythrocytes in MIAs would still need to be further optimised based on the virulence of this strain. By lowering the ratio of merozoites to erythrocytes additional potential invasion inhibiting compounds active within the same time period could be screened.

2.3.3 MSF assay

The MIA was supplemented by MSF assays which indicated inhibitory concentration ranges and gave a broad indication as to the lifecycle stages where the compound may have greater effects. Although not crucial for the compounds to only affect invasion, this determination would be necessary for any compound where modes of inhibition and mechanisms of action have not been well defined.[62, 147, 148] The methods used here are an adaption to those described by Le Manach *et al.* 2013[123] where the speed of inhibition was assessed using unsynchronised parasites for 24, 48, and 72 hrs, and then synchronised parasites for stage specific analyses to find the preferential stage of inhibition. A drawback with that method, particularly in the 24 hr trophozoite assay is that the assay duration does not span the full period of DNA replication (that occurs between 26 and 37 hpi[149, 150]). The lag effects seen here may be due to lower levels of DNA proliferation or decreased optimum time for chloroquine (taken up during DNA proliferation[151]) to act on parasites. It is expected that this resulted in a lower noise to background ratio in comparison to the assays of other stages and time periods, and thus lead to the visualisation of an apparent lag phase of IC_{50} values (Figure 2.10). This lag effect should not necessarily be interpreted as a lower tendency towards late trophozoites, schizonts, or early rings because the ratios between 24 and 96 hr assays were low (particularly in the edelfosine, DSS and gentamicin assays). To avoid seeing a lag effect in trophozoite assays further analyses could incorporate a wash step to remove the compound followed by a continuation of assay for a predetermined time period allowing untreated culture to continue proliferating to take additional replicated DNA noise over background into account. In addition to this, a control drug whose primary mode of action does not involve DNA replication could be used in place of chloroquine. Further analyses using the recommendations noted above would need to be carried out to confirm each compounds stage specific effects. However, because of the low ratio seen between the 24 and 96 hr trophozoite assays it cannot be excluded that the drugs are fast acting compounds which is highly important in merozoite invasion studies.

2.3.4 Inhibitory effect of selected compounds

Vanadate demonstrated the lowest inhibitory concentrations in MSF assays. In contrast to the lag effect seen in the other compounds tested, vanadate appeared to have a marked affinity towards late ring and early trophozoites and not schizonts, and/or early rings. This was noted by the significantly higher concentrations required to inhibit these life stages in the 24 hr trophozoite assays. Vanadate showed its maximum inhibitory effect at 100 µM in MSF assays (excluding 24 hr trophozoite assays), with 26% invasion inhibition at the same concentration in MIAs. At the

concentrations assessed in MSF assays vanadate would predominately be in monomeric state.[99] As vanadate has a number of phosphate transfer related inhibitory properties and can penetrate into parasitised erythrocytes, the primary inhibition caused by monomeric vanadate is probably not directly related to GPI-anchored proteins or other proteins involved in invasion. Monomeric vanadate would most likely then affect other processes for example; SOV has been found to bind to ATPases causing their inhibition in other cell lines at comparable concentrations.[97, 152-154] The activity of Ca^{2+} and Na,K-ATPases increases from 12-18 hpi during the progression of the parasite lifecycle, where they act by increasing intracellular levels of cations and decrease the efflux of ions.[98] The increased intracellular cations are required for essential processes.[155] In addition, SOV has been found to inhibit serine subtilisin proteases by 10 and 25% at ~10 and 100 µM respectively in blood cells of ascidians.[96] SOV's inhibition shown by Guerrieri *et al.* [96] was comparable to that of MIAs at the same concentrations. During merozoite invasion subtilisin-like proteases process GPI-anchored proteins. The inhibition of these proteins can only be speculated upon in this research, although this could suggest an explanation for the increased concentrations of monomeric vanadate required for inhibition in 24 hr trophozoite assays and MIAs. The concentration of the vanadate tetramer spontaneously rises sharply from 2 mM vanadate in solution and this tetramer is a potent PI-PLC inhibitor.[156] The greatest inhibition seen in MIAs was in the 2 mM vanadate assays where 70% inhibition occurred. The high concentrations of vanadate could also be expected to cause other toxic effects. These results suggest that vanadate is more likely to affect other intraerythrocytic stages and pathways with an effect on invasion being secondary or indirect.

The results for the *Plasmodium* parasite sensitivity to edelfosine exposure reported here are the first evidence of *in vitro* activity of edelfosine against *P. falciparum* parasites. Previous research has found that edelfosine has a time dependent effect on *Schistosoma* inhibition; approximately 50% inhibition occurred at concentrations of 80 µM after 24 hrs, and 20 µM after 72 hrs.[157, 158] In this study, a time dependent effect of edelfosine was not identified in MSF assays as the inhibitory concentrations were comparable across the times and stages assessed (50% inhibition at 50 µM, with the maximum inhibition seen at 100 µM). These results suggests that the effect of edelfosine may not be time dependent in *P. falciparum* rings, trophozoites and schizonts. In addition, MIAs demonstrated ±50% inhibition of invasion at 50 µM edelfosine, and ±60% inhibition at 100 µM. The fact that the inhibition seen from 24-96 hrs in MSF assays was comparable to that seen after 1 hr in MIAs may indicate the specificity of edelfosine to inhibit merozoite invasion. With the surface constituents of merozoites being vital to the invasion process, these results would suggest agreement with previous work which found the compound's primary effect to be on the surface

membranes and their associated proteins. Based on the differences in inhibition of invasion vs. intraerythrocytic parasites it can be suggested that separate mechanisms of inhibition are involved corresponding to the different stages of protozoan life cycle. Edelfosine affects proteins on the cell membrane including enzymes of phospholipid metabolism as well as enzymes involved in transduction signals which would have an indirect inhibitory effect on RNA and protein synthesis resulting in parasite death[101]. As protein synthesis occurs during the intraerythrocytic stages, the majority of protein synthesis would be completed during schizogony in preparation for merozoite invasion, as primary energy use of the merozoite would be expected to go towards the invasion processes. ALPs also effect the phospholipid formation which could be due to depleting phosphatidylinositol 4,5-bisphosphate (PIP_2) as the substrate for inositol phosphate (IP) formation or enhancing the breakdown of IPs.[106] Thus it can be expected that inhibition of protein, RNA and phospholipid synthesis could be important mechanisms involved in inhibition seen in ring, trophozoite and schizont stages. The inhibition of merozoite invasion may be due to the inhibition of surface proteins involved in signalling that initiate successive steps in the invasion process which may or may not be GPI-anchored proteins. Previous research showed edelfosine to exert a 50% inhibition of PI-PLC at 10 µM in human renal systems.[106] However, at these concentrations no inhibition of invasion was observed in MIAs, although the concentrations required for inhibition could be influenced by species, cell line and assay differences. Edelfosine showed inhibitory effect on merozoite invasion within physiological concentrations which is expected to primarily involve the merozoites surface proteins, thus in this research, the potential invasion inhibitory activity of the compound shall be further characterised against *P. falciparum.*

Dioctyl sodium sulfosuccinate (DSS) has previously been shown to inhibit proteolytic enzymes of the cell surfaces, however, the extent of this has not been well characterised.[108] The concentrations required for inhibition by DSS in both MSF and MIA assays were above physiologically attainable concentrations. As with other compounds assessed, DSS appeared to have the lag effect in the 24 hr trophozoite assay. At concentrations higher than those assessed in MSF assays, DSS caused visible haemolysis of the erythrocytes showing that the erythrocytes were adversely affected by DSS which is known to have detergent type properties. It cannot be ruled out that even though no visible lysis was occurring at the concentrations tested, the inhibition may have been caused by these surfactant properties of DSS on the erythrocyte membrane integrity. In addition to this, the 100 µM tested during MIAs showed no inhibition of invasion, and higher concentrations could not be tested due to either visible presence of haemolysis or merozoite agglutination. These results would then render DSS as being unsuitable as a parasite anti-invasive agent.

Previous research has found the aminoglycoside gentamicin to have an inhibitory effect on PI-PLC at 130 µM by competitive inhibition with a possible link to calcium flux activation.[113] Gentamicin is also known to inhibit phospholipase A_2,[112, 115] with *P. falciparum* GPIs having shown some sensitivity towards phospholipase A_2.[83] The inhibition of *P. falciparum* by gentamicin has been previously described where parasite inhibition was caused by the inhibition of phospholipases, where the drug prevented the parasites from progressing into successive replicative cycles, however, the inhibitory concentrations were not specified and therefore comparisons cannot be made.[112] However, this study demonstrated a distinct lack of inhibitory effect of gentamicin seen by high IC_{50} values unattainable at physiological concentrations in MSF assays no inhibition seen in MIAs. Gentamicin is typically used at 50 µM in culture media to maintain sterility, while concentrations required for an IC_{50} in *P. falciparum* were 100 fold this concentration. The antimicrobial selectivity of gentamicin is thus not comparable to *P. falciparum* activity. Despite seeing a negative antimalarial result with this compound, these results reiterate that gentamicin is safe to use in cultures as it demonstrates no antimalarial activities even at concentrations more than 50 fold higher than the recommended concentration, and will not negatively affect parasite proliferation in routine cultures while preventing bacterial growth in CM.

Chapter 3: Merozoite Proteomics and Inhibitory Effect of Edelfosine

The aim was to characterise changes to the proteome of merozoites during and after the invasive phase in both untreated and treated samples by SDS-PAGE and LC-MS/MS analyses.

3.1 Methodology

3.1.1 Merozoite isolation and inhibitor treatment

Highly synchronised schizonts with a starting packed cell volume of 1 mL at 18% parasitaemia were isolated by repeated MACs isolation as previously described. Upon parasite maturation, schizonts were washed twice by centrifugation for 2 min at 2000x*g* with ICM at 37°C to remove the protease inhibitor, E64 and the Albumax II present in CCM. ICM was used to prevent Albumax II from overshadowing merozoite proteins in quantitation assays, on gels and in mass spectrometric analyses. Serum proteins are essential for parasite growth during intraerythrocytic stages, however, proteomic analysis could be conducted without serum proteins as they are neither essential to invasion nor enhance invasion events.[63] Schizonts were resuspended in 3.5 mL ICM, and filtered using a 1.2 µm filter. Merozoites with a background contamination of haemozoin crystals were contained in the filtrate but essentially all the erythrocyte debris was removed. Following filtration, a volume of 500 µL merozoite suspension was placed in Eppendorf tubes containing one of the invasion inhibitor test compounds or ICM for the untreated control samples. Suspensions were incubated at 37°C for 5, 15 and 120 min. The time periods were chosen as merozoites are highly invasive 5 min after egress; within 15 min most invasion events would have occurred and invasive capacity wanes[63]; after 120 min invasion is unlikely, thus characterising merozoite proteins after the invasive phase. After the incubation period the samples were centrifuged at 16000x*g* (Microfuge 16 centrifuge (Beckman Coulter, Brea, CA, USA)) for 5 min separating soluble released/cleaved proteins from insoluble and parasite bound protein. These samples were immediately placed in ice that was pre-frozen to -80°C to halt all protease activity and stored at -80°C until use. Three independent biological repeats were conducted which contained untreated controls for the same incubation periods.

3.1.2 TCA precipitation: Protein precipitation

Merozoite proteins were precipitated out of ICM using trichloroacetic acid (TCA) (Merck, Darmstadt, Germany). TCA acts in two mechanisms: first, by causing dehydration of water shells that surround hydrophobic areas of a folded protein and second, by disrupting electrostatic interactions that determine the tertiary structure of the protein. TCA was selected for protein precipitation as it precipitates proteins of low abundance, and has been found to produce well

resolved gel bands.[159, 160] Stock solution was prepared by dissolving solid TCA in deionised water to make a 100% *w/v* solution. Protein samples were thawed to 4°C and a volume of ice-cold TCA was added to the sample to produce a final 10–25% TCA concentration. Samples were incubated for 20 min at -20°C and centrifuged at 16000x*g* for 5 min. The supernatant was discarded and the pellet was washed 2–3 times by centrifugation at 16000x*g* for 5 min using 100% ice cold acetone (Merck, Darmstadt, Germany). The high concentrations of TCA coupled with washing by use of acetone also removed contaminating lipids which proteins may have been attached to, salts and phenol red found in ICM.[161] The use of acetone removes TCA while maintaining the volume of precipitated protein. Excess acetone was removed by evaporation at 60°C for 5 min.

3.1.3 BCA assay: Protein concentration determination

Merozoite proteins showed low solubility in water and PBS, but solubilised easily in sodium dodecyl sulphate (SDS) sample buffer. The bicinchoninic acid (BCA) assay was used for protein quantitation and was selected as the volume of SDS in the sample buffer does not interfere with assay reagents, unlike several other quantitation techniques.[162, 163] SDS sample buffer was made up as follows: 62.5 mM Tris-(hydroxymethyl)aminomethane hydrochloride (Tris-HCl) (Sigma, St Louis, MO, USA) at pH 6.8, 8.7% glycerol (Sigma, St Louis, MO, USA), 2% SDS (Sigma, St Louis, MO, USA). Bovine serum albumin (BSA) was used to make protein standards in a concentration range of 0.125-5 mg/mL. BSA standards were dissolved in sample buffer for a direct comparison with merozoite samples. Two stock reagents are used to make the BCA working solution which were made as follows[162, 164]: Reagent A; 1% sodium bicinchoninate (Sigma, St Louis, MO, USA), 2% sodium carbonate (Na_2CO_3) (UniLab, Mandaluyong City, Philippines), 0.16% sodium tartrate (Merck, Darmstadt, Germany), 0.4% sodium hydroxide (NaOH) (Merck, Darmstadt, Germany) and 0.95% sodium bicarbonate ($NaHCO_3$) (Sigma, St Louis, MO, USA) which was adjusted to pH 11.25 with 10 M NaOH, and Reagent B; 4% hydrated cupric sulphate ($CuSO_4$) (Rochelle, Johannesburg, RSA) dissolved in deionised water, both reagents were stored at 4°C when not in use. Working reagent was prepared by combining two solutions in a ratio of 50:1. Assays were done in round bottomed 96 well plates, a volume of 250 µL working solution and 5 µL protein standard or protein sample was used, while blank wells contained 5 µL of sample buffer, each condition was run in triplicate. Plates were gently shaken to mix working reagent and samples, and incubated for 30 min at 60°C, afterwards plates were cooled to room temperature and read at 570 nm on a ELX800 microplate reader (BioTek, Winooski, VT, USA) using Gen5 (Version 2.03.1). GraphPad Prism Version 5.00 was used to analyse the samples, by plotting the standard curve, and calculating the unknown merozoite protein concentrations using linear regression.

3.1.4 SDS-PAGE: Protein separation

Sodium dodecyl sulphate-polyacrylamide gel electrophoresis (SDS-PAGE) was used to separate proteins based on their apparent mass. Laemmli sample buffer was used to prepare protein samples: 62.5 mM Tris-HCl, 2% SDS, 10% glycerol, 0.02% bromophenol blue (Merck, Darmstadt, Germany), 5% β-mercaptoethanol (Sigma, St Louis, MO, USA); the buffer was stored at -80°C when not in use. SDS in an anionic detergent which denatures proteins into their primary structured polypeptide chains, and imparts a negative charge to proteins. SDS binds to most proteins at an almost fixed ratio which causes the protein's negative charge to relate directly to the mass of the protein (mass to charge ratio). The β-mercaptoethanol was added freshly prior to sample preparation and is used to reduce the intra and inter-molecular disulfide bonds. Samples aliquots were thawed to 4ºC and processed immediately to avoid proteolytic degradation after thawing.

A volume of protein sample was precipitated by TCA precipitation and reconstituted in Laemmli sample buffer to make a 1 mg/mL solution. The micro-tubes containing protein samples were sealed with parafilm to prevent water loss through evaporation, which would alter protein concentration. The samples were placed in a water bath on a temperature controlled hot plate with water maintained at 95°C. Both soluble and pelleted protein sample fractions were boiled for 10-15 min to allow precipitated protein to solubilise due to SDS binding. Once protein samples were removed from the waterbath, samples were centrifuged for 5 min at 16000x*g* to separate the merozoite proteins from remaining insoluble material such as nucleic acid residue.

SDS-PAGE was conducted on Bio-Rad Criterion™ TGX (Tris-Glycine eXtended) Stain-Free™ precast 12+2 wells 4-20% gradient gels. A volume of 10 µL Precision Plus Protein™ Standards Unstained (Bio-Rad, Hercules, CA, USA) was added to the wells of the first and last lanes. The standards covered a reference mass range of 10 kilodaltons (kDa) to 250 kDa (standards were stored at -20°C and thawed before use). A volume of solution equivalent to 30 µg of protein sample was added to each well. Gels were run at 60 V for 30 min, followed by 120 V until run completion in running buffer at pH 8.3 (0.1% SDS (Merck, Darmstadt, Germany), 25 mM Tris-HCl (Merck, Darmstadt, Germany), 192 mM glycine (Sigma, St Louis, MO, USA)) using a Hoefer (PS300-B) system. The completion of the run was assessed by the migration of bromophenol blue. During the electrophoretic run, the negatively charged proteins migrate towards the anode in the electrical field. The protein migration is dependent on the mass to charge ratio, thus a higher charge ratio will result in migration of proteins at a faster rate and the smaller the protein the faster it will move through the gel and the opposite is true for larger proteins. Following the gel run, the

stain free gel was placed on the Stain-Free sample tray, activated and UV visualised by Bio-Rad Gel Doc EZ Imager using Image Lab (V3.0 build 11) software. The stain free gels were placed in fixing solution (20% methanol (MEOH) (Sigma, St Louis, MO, USA) and 6% glacial acetic acid (Merck, Darmstadt, Germany) in deionised water) for 15 min and rinsed in 100 mL water. Gels were stained in QC Colloidal Coomassie Blue (Bio-Rad) for 10-20 hrs and subsequently destained by washing in deionised water for 1 hr. Coomassie binds non-covalently and reversibly to positively charged amino acids allowing detection of protein quantities as low as 3-10 ng per band.[165, 166] Coomassie has a strong affinity towards proteins, however, also weakly binds to polyacrylamide and thus gels are destained prior to visualisation. Gels were then placed on the white sample tray and protein bands were visualised using the same software mentioned above. Proteins have been known to migrate out of the lanes if gels are kept for extended periods of time. Aged gels were less likely to identify lower abundance proteins due to proteins moving out of the gel, in addition the longer a gel is kept in storage the greater possibility of acquiring contaminants such as bacterial or fungal growth. Thus once the gel had been destained and visualised it was placed in deionised water at 4ºC and prepared for mass spectrometry within one week.

3.1.5 Mass Spectrometry: Protein sequencing and analysis

Selected lanes from SDS-PAGE gel containing comparable untreated and edelfosine treated samples (100 µM) were cut out and prepared for mass spectrometry. Eight lanes were selected including the edelfosine treated and untreated lanes for both soluble and pelleted proteins for 5 and 120 min exposure times. Lanes were each cut into 10 fractions. The fraction sizes were determined by the approximate amount of protein present in the lanes (soluble protein lanes in equivalent sections and pelleted proteins in equivalent sections). The fractions were each cut into smaller 1x1 mm pieces. Gel pieces from each gel fraction were destained twice in 50 mM ammonium bicarbonate (NH_4HCO_3) (Sigma, St Louis, MO, USA) in 50% MeOH for 20 min. The use of NH_4HCO_3 weakens electrostatic interactions between the stain and positively charged amino acids, followed by 75% acetonitrile (ACN) (Merck, Darmstadt, Germany) for 20 min and dried *in vacuo*. ACN was used to disrupt the interaction between any residual Coomassie stain and proteins. Protein reduction was commenced by 60 min incubation at 60°C in dithiothreitol (DTT) (Bio-Rad, Hercules, CA, USA) followed by 10 min incubation using 100% ACN, and alkylated by incubation in 55 mM iodoacetamide (IAM) (Bio-Rad, Hercules, CA, USA) in 25 mM NH_4HCO_3 for 20 min in the dark at room temperature. Protein reduction and alkylation was carried out to disrupt disulphide bonds between cysteine amino acids and to prevent the random disulphide bridge formation, which is used to prevent peptides from binding covalently to other

peptides following proteolytic cleavage. Gel pieces were washed in 25 mM NH_4HCO_3 and dehydrated twice in 25 mM NH_4HCO_3 in 50% MeOH and then dried *in vacuo* and stored at -20°C. Proteins were digested in TrypLE Select (Gibco by Thermo Fisher Scientific, Gaithersburg, MD, USA) a sequence grade trypsin which hydrolyses peptide bonds at the C-terminal of all lysine and arginine residues. Gel pieces were digested in 10 ng/µL trypsin in 25 mM NH_4HCO_3 at 37°C overnight. Resulting peptides were extracted using 50% ACN in 5% formic acid (FA) (Merck, Darmstadt, Germany) for 25 min, this was repeated once.[167] Extracted digest solution from individual samples were combined and dried *in vacuo* and stored at -20°C. Digests were resuspended in 20 µL, 2% ACN in 0.2% FA and analysed using a Dionex Ultimate 3000 rapid separation liquid chromatography (RSLC) system (Thermo Fisher Scientific, Waltham, MA, USA) coupled to an AB Sciex 6600 TripleTOF mass spectrometer (Framingham, MA, USA). Peptides were first de-salted on an Acclaim PepMap C18 trap column (100 µm × 2 cm) for 2 min at 15 µl/min using 2% ACN in 0.2% FA, then separated on Acclaim PepMap C18 RSLC column (300 µm × 15 cm, 2 µm particle size). Peptide elution was achieved using a flow-rate of 8 µL/min with a gradient: 4-60% B in 15 min (A: 0.1% FA; B: 80% ACN in 0.1% FA). An electrospray voltage of 5.5 kilovolts (kV) was applied to the emitter. The 6600 TripleTOF mass spectrometer was operated in data-dependant acquisition mode (DDA) (Figure 3.1). Using DDA a subset of the most abundant precursor ions detected in the initial scan (MS) are selected for subsequent isolation and fragmentation in a serial manner. Chromatographic peak capacity and mass spectrometer parameters such as cycle time, number of precursor ions selected per cycle, and dynamic exclusion to minimize repeat selections of precursor ions can be selected and balanced to provide the highest quality spectra for as many precursor ions as possible.[168] Precursor MS scans were acquired from m/z 400-1500 using an accumulation time of 250 milliseconds (msec) followed by 30 MS/MS scans, acquired from m/z 100-1800 at 100 msec each, for a total scan time of 3.3 sec. Multiply charge ions (2+ - 5+, 400 -1500 m/z) were automatically fragmented in the Q2 collision cell using N_2 as the collision gas. Collision energies were chosen automatically as function of m/z and charge.

The data was submitted to the Paragon™ search engine (AB Sciex, Framingham, MA, USA) that was used for comparison of the obtained MS/MS spectra with a custom database containing sequences of *P. falciparum* (Uniprot PlasmoDb)*, Homo sapiens* (Uniprot Swissprot) and as well as a list of protein sequences from common contaminating proteins. ProteinPilot™ V4.5 software was used to analyse data using the Protein Alignment Template V2.000p (AB Sciex, Framingham, MA, USA) to collate these results. ProteinPilot is limited in the sense that it identifies the spectral count of each peptide as the total amount of the peptide within the full length of the gel lane, and

does not separate the total spectral count into the individual mass ranges (gel fractions that the lane was cut into during sample preparation). To identify the spectral count in the separate mass fractions PeptideShaker V0.41.1 was used to further analyse data in association with the data presented in the Protein Alignment Template. Only proteins with identification confidence threshold above ≥ 99.9% were reported.

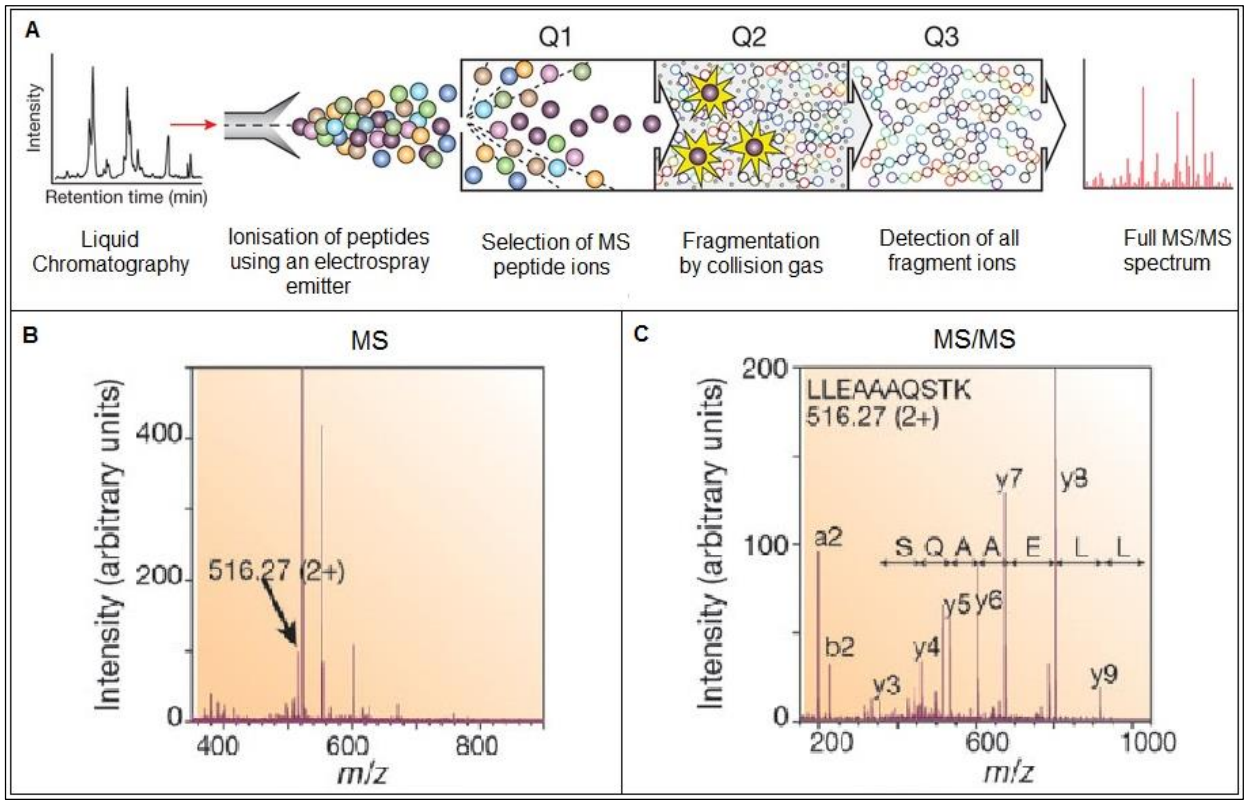

Figure 3.1: Mass spectrometric analysis using data-dependent acquisition (DDA). In preparation for mass spectrometric analysis gel fractions were excised and prepared by destaining, reduction, alkylation, digestion and extraction. A) Following sample preparation liquid chromatography was conducted. The peptides were loaded on a reverse-phase column attached to the liquid chromatography system and eluted via electrospray ionisation to yield gas-phase ions. Many peptides (tens to hundreds) elute within a very narrow time period at any given point during the chromatographic separation. During the Q1 phase, the initial full-scan of MS was acquired. Peptides of highest abundance, and those with multiple charges were selected for further analysis. This selection was based on a pre-defined set of parameters determined computationally. During the Q2 phase, the selected peptides were isolated and fragmented by collision gas. N_2 was used as it is an inert gas. At the Q3 phase all fragment ions were detected to produce a full tandem or MS/MS spectrum. The MS/MS spectra were acquired and stored for matching against protein sequence databases. The peptides and therefore the proteins making up the purified protein population could then be identified. (Adapted from Gillette *et al.* 2012[169] with permission). B) The initial full MS scan showing all peptide ions identified. A peptide showing high intensity with a charge of +2 is selected for MS/MS analysis. C) Following isolation, and fragmentation MS/MS spectrum is recorded (B and C adapted from Aebersold *et al.* 2003[170] with permission).

3.2 Results

3.2.1 SDS-PAGE

Invasive merozoites were isolated by forceful rupture from schizonts and incubated for 5, 15, and 120 min in the presence or absence of an invasion inhibitor. No new uninfected erythrocytes were present with the merozoites. Samples were centrifuged to separate cleaved or released proteins from pelleted proteins that were either non-cleaved or were still associated with the merozoite organism. A volume of 1 mL packed parasitised erythrocyte at 18% parasitaemia provided approximately 3.2 mg of protein (containing both merozoite and erythrocyte proteins). Merozoite protein samples were prepared and separated by SDS-PAGE (Figure 3.2). The various lanes from a single SDS-PAGE gel was prepared and analysed by mass spectrometry after treatment with edelfosine was chosen. This was due to the results of both the MSF and merozoite invasion assays showing edelfosine to be most potent agent against invasion. For this reason, only edelfosine will be discussed for treated sample components. Whole organism sample preparation was carried out on merozoites, thus multiple non-protein products would be present in the samples at the start of sample preparation. TCA precipitation was used to remove most contaminating non-protein products, and samples were solubilised in sample buffer (containing ionic detergents) by boiling for 10-15 min, and centrifuged to precipitate insoluble material prior to loading into wells. Despite centrifugation, contaminating insoluble material remained in the wells of pelleted sample (lanes 1-3 and lane 7-9) after gels were run. The samples were run on a Criterion TGX Stain-Free 4-20% polyacrylamide gradient gel. Gels were visualised using UV activation of the gels on the Stain-Free Tray on the Gel Doc EZ Imager using ImageLab software. Gels were subsequently stained using Coomassie blue and visualised using the White Sample Tray prior to excision and preparation for mass spectrometric analysis.

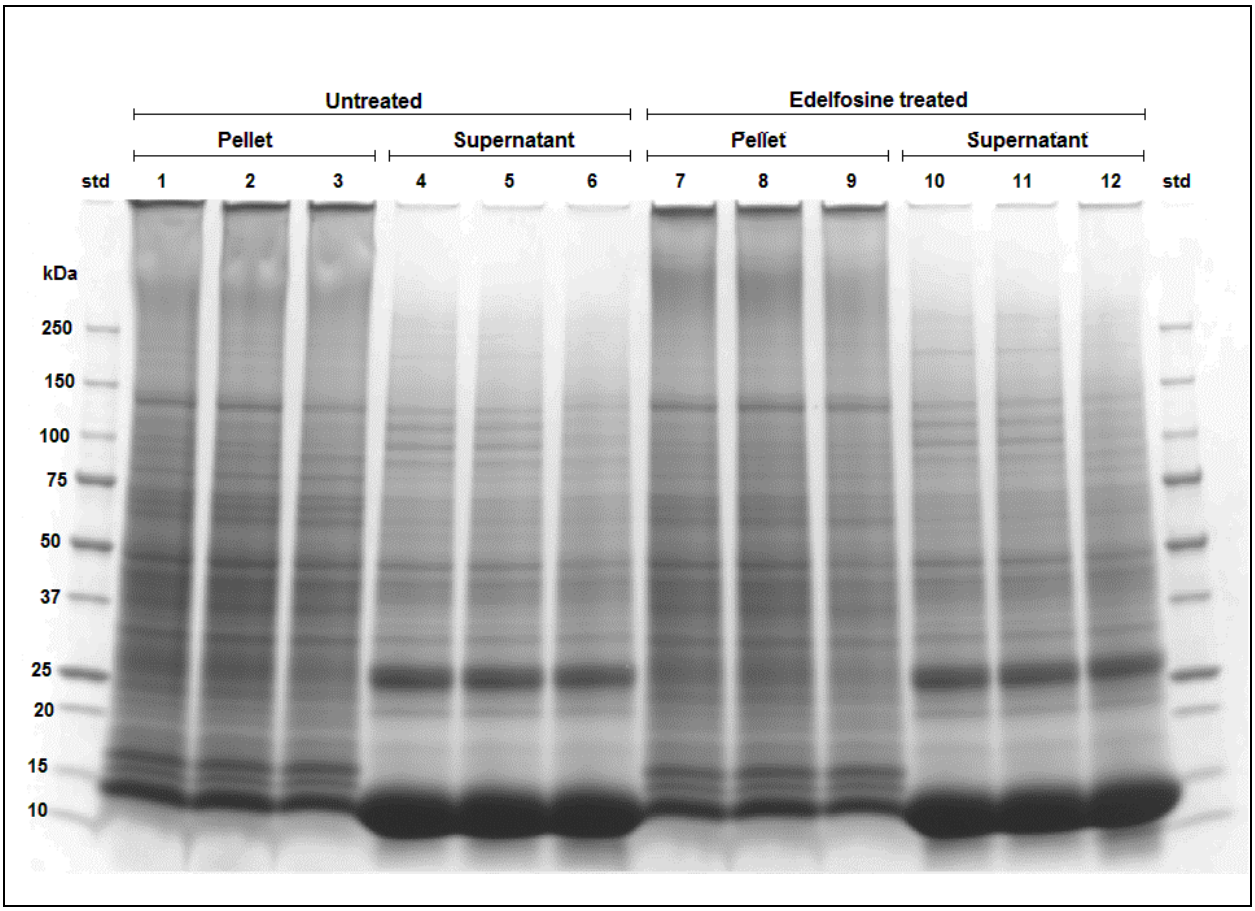

Figure 3.2: SDS-PAGE of merozoite soluble (supernatant) and pelleted proteins. Image showing proteins of untreated and edelfosine (100 µM) treated merozoite soluble and pelleted proteins at 5 min (lanes 1, 4, 7 and 10); 15 min (lanes 2, 5, 8 and 11); and 120 min (lanes 3, 6, 9 and 12) after egress by forceful rupture from schizonts. The standards (std) in outer lanes represent protein mass in kDa.

Gels had sufficiently well resolved bands in the high and low molecular mass regions and these bands showed good reproducibility between samples and between the protein fractions isolated. Soluble proteins had predominantly well resolved narrow bands with sharp edges (excluding the highly abundant 13 and 26 kDa bands that are associated with haemoglobin from the host erythrocytes). While pelleted proteins showed many bands with these same characteristics there was an increased number of bands present with broader and less defined edges. The vertical streaking in the wells above the 250 kDa mark was likely due to proteins which solubilised during sample preparation and precipitated after loading into the wells. This streaking dissipates towards the 250 kDa mark and did not appear to have significant effects on the lower molecular masses. This streaking did not have a major impact on the protein samples as few protein bands were found to be in the range above 250 kDa, in addition the purpose of the top 10% of the gel is used

primarily for protein stacking rather than protein analysis. Thus solubility of the proteins in the bands was not a significant problem but rather the solubility of sample remaining in the well. Samples are normally boiled in SDS containing sample buffer for 5 min, however, were boiled here for additional time due to solidification of the merozoite sample which occurred after TCA/acetone precipitation. The additional boiling time was used for the merozoite proteins to solubilise, once solubilised samples were centrifuged and loaded into wells. Some salts were present at the bottom of pelleted protein sample lanes causing a mild distortion of the rapidly moving bands.

Proteomic differences were identified between lanes (Figure 3.3a and 3.3b). Merozoite protein intensities appeared to decrease over time, despite equal concentrations of protein being added to each well (protein quantity compensation after BCA assays). Decreased intensities of the bands were visualised at 120 min (lanes 3 and 9) in comparison with 5 and 15 min (lanes 1, 2, 7 and 8). In the pelleted sample lanes, defined bands in the untreated 5 and 15 min lanes of 99, 175, 200, and 255 kDa the showed reduced intensity at 120 min and in the edelfosine treated lanes. While a band at 88 kDa showed increased intensity in untreated sample at 120 min in comparison with other pelleted lanes.

In the supernatant samples the majority of differences were also visualised at 120 min (lanes 6 and 12) in comparison with the 5 and 15 min samples (lane 4, 5, 10 and 11). The primary region showing differences was within the 75-150 kDa range. The 5 and 15 min lanes have five distinct bands with equivalent masses and comparable abundances, where this section on 120 min lanes had seven bands. In this section of the 120 min lanes protein abundances were lower than 5 and 15 min lanes for bands, this excludes the lower molecular mass band in this section which was visualised at ~81 kDa. The additional bands of lower abundance had a similar staining intensities as other proteins in this mass range, and would most likely be related to proteins seen within this region of the 5 and 15 min exposure lanes, where alterations have occurred, for example the proteins share amino acid sequence but one protein has undergone protein cleavage, or one may have had additional amino acid residues or differed in several key positions. There was 198 kDa band visualised in all supernatant samples which had a marked increased intensity in the edelfosine 5 and 15 min lanes in comparison to the untreated lanes and the edelfosine 120 min lane. In addition, the edelfosine 55 and 61 kDa bands showed an increased intensity in comparison to the untreated lanes.

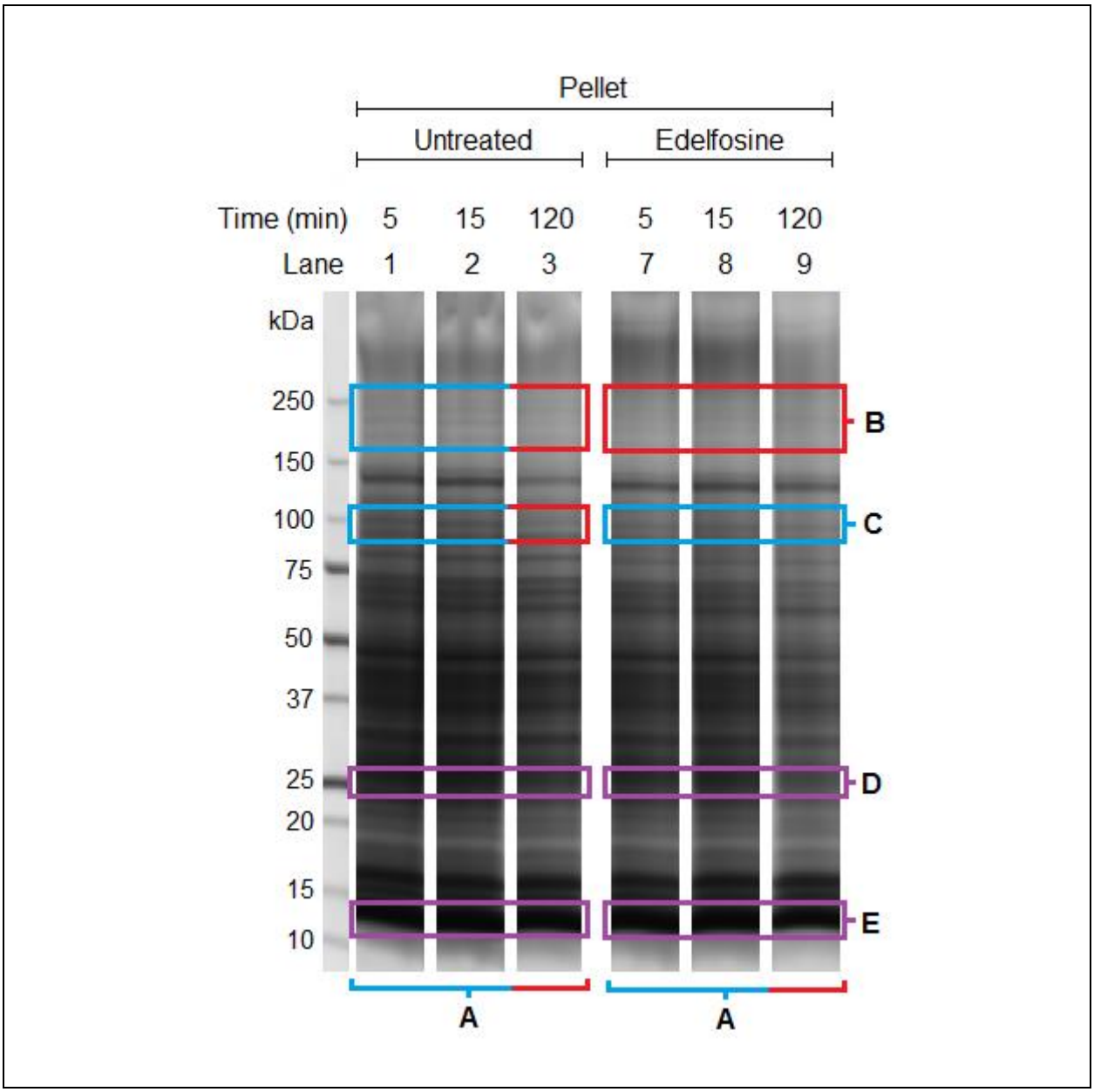

Figure 3.3a: SDS-PAGE lanes of pellet proteins indicating bands of interest and proteomic changes. A) Merozoite protein intensity appeared to decrease over time with lower band intensities showing in the 120 min lane in comparison with the 5 and 15 min lanes. B) Defined bands in the untreated 5 and 15 min lanes of 175, 200, and 255 kDa the showed reduced intensity at 120 min and in the edelfosine treated lanes. C) A band of 99 kDa in the untreated 5 and 15 min lanes showed reduced intensity at 120 min and in the edelfosine treated lanes. While a band at 88 kDa showed increased intensity in untreated sample at 120 min in comparison to other pelleted lanes. D) A 26 kDa protein which is the haemoglobin dimer E) A 13 kDa protein which is the haemoglobin monomer. Both 13 and 26 kDa bands are less abundant in pellet samples in comparison to supernatant samples. Red areas denote lanes where differences in intensity were identified in comparison with blue sectioning (typical control- i.e. untreated 5 min sample) while purple denotes bands associated with haemoglobin.

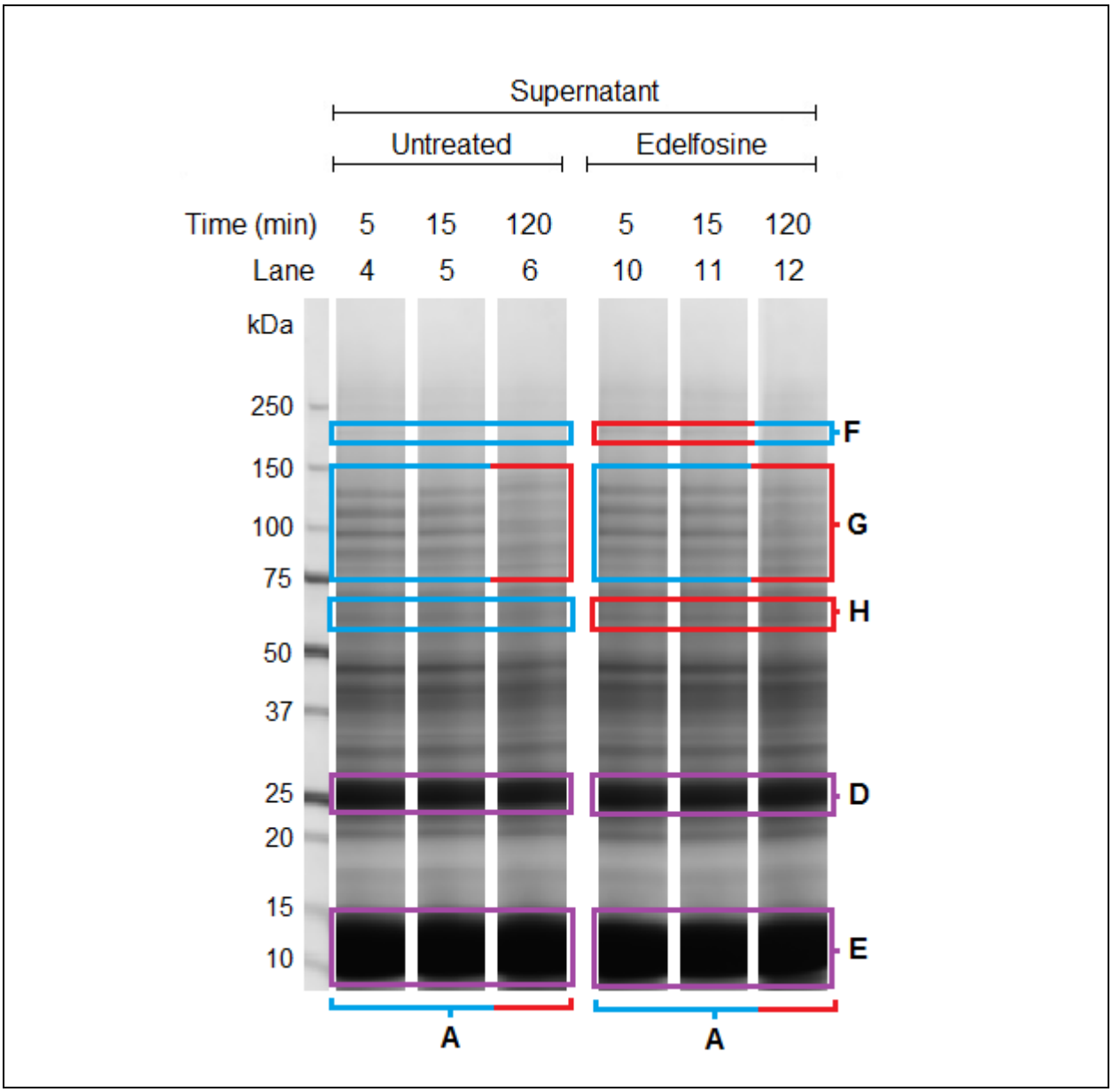

Figure 3.3b: SDS-PAGE lanes of supernatant proteins indicating bands of interest and proteomic changes. A) Merozoite protein intensity appeared to decrease over time with lower band intensities showing in the 120 min lane in comparison with the 5 and 15 min lanes. D) A 26 kDa protein which is the haemoglobin dimer. E) A 13 kDa protein which is the haemoglobin monomer. F) 198 kDa band visualised in all supernatant samples which had a marked increased intensity in the edelfosine 5 and 15 min lanes in comparison to the untreated lanes and the edelfosine 120 min lane. G) The 5 and 15 min lanes have five distinct bands with equivalent masses and comparable abundances, where this section on 120 min lanes had seven bands. In this section of the 120 min lanes protein abundances were lower than 5 and 15 min lanes for bands, excluding the lower molecular mass band in this section which was visualised at ~81 kDa. H) The edelfosine 55 and 61 kDa bands showed an increased intensity in comparison to the untreated lanes. Red areas denote lanes where differences in intensity were identified in comparison with blue sectioning (typical control- i.e. untreated 5 min sample), while purple denotes bands associated with haemoglobin.

Oversaturated bands were evident at ±13 kDa, this was predominantly evident in supernatant samples with the same mass band in the pelleted proteins but in lower abundances. The very large bands here suggest that this was a dominant protein in the sample. This was expected to be haemoglobin which has a monomeric mass of 16 kDa. Oversaturation would have masked the presence of less prevalent proteins within the 10-16 kDa range. In some cases non-covalent protein bonds may still have remained after sample preparation, as haemoglobin consists of four monomers in its native form, there may be additional bands seen corresponding to the mass of conjoined monomers. A band of 26 kDa representing the haemoglobin dimer was found in high abundance in lanes. The high abundance of these proteins caused bands to be less resolved in comparison to other bands. The haemoglobin bands were identified as mass ranges slightly below their actual mass which is not unusual for proteins.

3.2.2 Mass spectrometry: Technical aspects

The most prominent differences in lanes were seen between the 5 and 120 min lanes which are the time periods where merozoites maintain invasive viability and where invasion ability has been lost. Due to the limited visual changes between the 5 and 15 min lanes and limited resources, only 5 and 120 min samples were analysed by mass spectrometry. These lanes were sectioned and full lane mass spectrometric analysis was conducted. Some reasons for this choice were: GPI-anchored proteins and fragments would be distributed throughout the lanes as their masses range from 20-200 kDa. Protein subunits may be found in bands not corresponding to their expected absolute mass due to different modifications of proteins; and more abundant proteins could mask changes identified in bands on the gel. The selected lanes were cut into 10 fractions that were sized to distribute the relative abundance of proteins. Each fraction was destained, reduced, alkylated, trypsinised and analysed by LC-MS/MS. Proteins were identified by searching peptide sequence spectra against selected databases and analysed. A total of 1299 proteins were identified with >99.9% confidence. These proteins were each assigned a number making the master list. Proteins from each lane were assigned a number mapped to the master list to compare protein presence vs. absence in each lane analysed as well as the total sequence coverage. The majority of proteins were found in pelleted protein lanes (Table 3.1). The number of proteins identified decreased over time in both treatment and localisation groups. In comparison to untreated samples, the number of proteins found in treated samples were lower in pelleted samples, but higher in soluble samples. The differences in the number of proteins identified were minor with approximately 5% difference between untreated and the comparable edelfosine treated sample.

Table 3.1: Number of total proteins identified on SDS-PAGE gel analysed by mass spectrometry. Proteins identified with >99.9% confidence matched per lane which were aligned to make a master list.

Treatment	Untreated				Edelfosine (100 µM)			
Type	Pellet		Soluble		Pellet		Soluble	
Time (min)	5	120	5	120	5	120	5	120
Number of proteins	993	956	635	566	964	892	686	594

Label free spectral counting was used as a general indication of protein abundance and comparison between lanes and fractions. Protein quantification was assessed by spectral counting where numbers of confident peptides were used for each protein, the higher the concentration of confident peptides the higher the spectral count would be. Spectral counting was found to have greater linear correlation to absolute protein abundance than other label free methods such as peptide counting or sequence coverage.[171] Variances in the amount of protein loaded into wells would cause inaccurate representations of the spectral count, variances could be caused by biological or technical variations, and therefore the relative abundance was reported. The data was normalised to account for variations and to improve accuracy of quantitative results. Normalisation can be done by use of standards which are spiked into samples, by using a protein expected to remain constant in all samples, or by normalisation against the total spectral count identified in each lane. Here, the spectral count of GPI-anchored proteins was normalised against the total spectral count of all proteins found per lane. The full inhibitory profile of edelfosine on *P. falciparum* is yet to be characterised, inferring uncertainties in normalising against a protein identified within the sample. An improved quantitative assessment would be obtained by normalising against total lane spectral count in this research. An example of a protein and peptide spectrum with fragmented ions is shown in Figure 3.4.

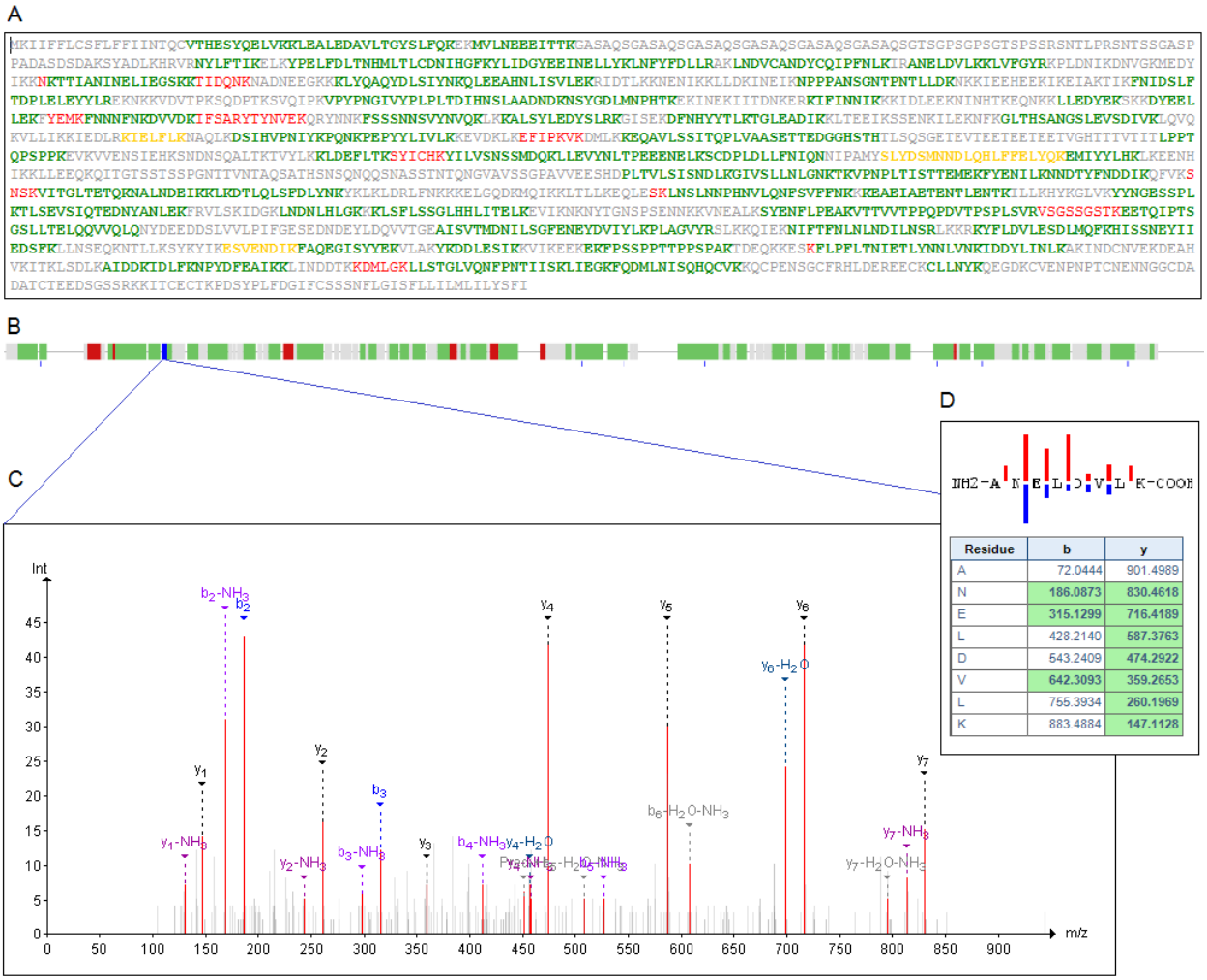

Figure 3.4: Mass spectrometry sequence coverage and spectra example. The full protein sequence of MSP1 found in untreated merozoite pellet protein sample after in-gel reduction, alkylation and trypsinisation followed my mass spectrometric analyses which was visualised using A) ProteinPilot or B) PeptideShaker. Peptide confidence is indicated by colours: green- high confidence; yellow- moderate or doubtful; red- low confidence; grey indicates peptides not found. C) A single selected peptide with a charge of +2 showing the MS/MS spectrum that was derived from MSP1 (ANELDVLK). The peptide was fragmented using collision induced dissociation which resulted in the mass spectra which contained a series of b and y ions that relies on the amino acid sequence of the peptide. Peptides are sequenced from both the N- (termed b-ions) and C-terminus (termed y-ions). Image from PeptideShaker D) Derived sequence of the peptide from the b- and y- peptide masses. Image from ProteinPilot.

GPI-anchored proteins underwent different types of modifications causing proteins to be found in mass ranges different to the full molecular mass of the protein. Some proteins were crosslinked or bonded to other proteins (where bonds were not degraded by sample preparation) causing them to be found in molecular mass ranges higher than their mass (potentially excluding cases

where cleaved proteins were crosslinked). Proteins may be cleaved in different locations along the length of the primary structure causing them to appear in lower mass ranges. Non-cleavage of GPI proteins or cleavage at the GPI anchor caused the proteins to appear at the mass of its full length in pelleted or soluble samples respectively (Figure 3.5).

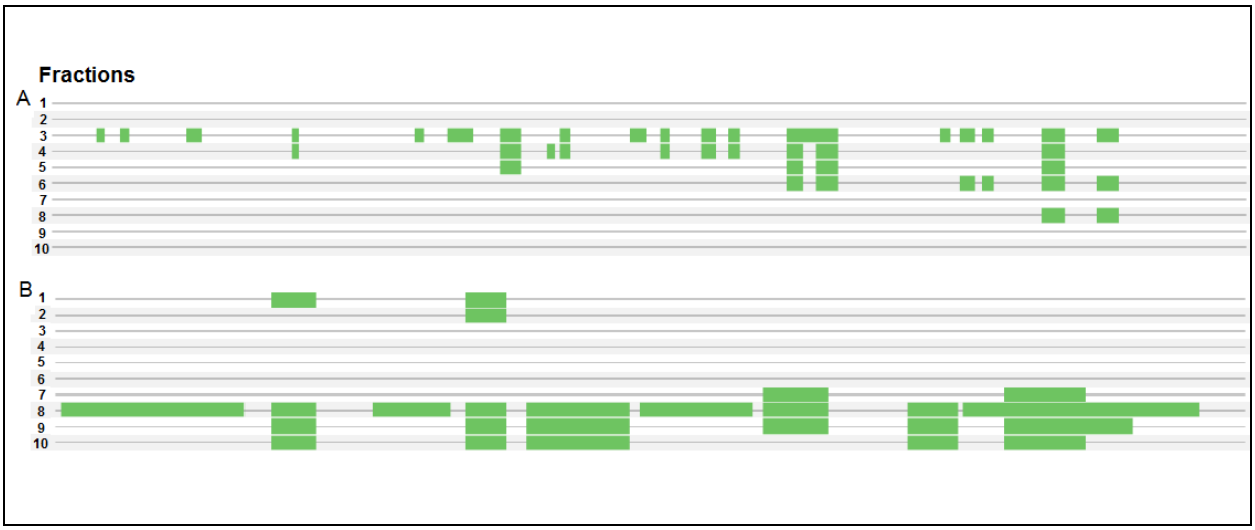

Figure 3.5: Examples of sequence coverage and protein modification. A) Sequence coverage of a 131 kDa merozoite protein. Peptides corresponding to positions across the full length of the protein are found in Fraction 3 of the gel lane (corresponding to the mass range of 75-150 kDa). The peptides in the lower weight bands (Fractions 6 and 8) demonstrate probable protein cleavage as only smaller but similar peptides locating towards the C-terminal of the same protein are found. B) Sequence coverage of a 26 kDa merozoite protein found predominantly in Fraction 8 in a mass range of 18-25 kDa. Peptides found in mass range >150 kDa (Fraction 1 and 2) suggests crosslinkages (possibly of cleaved subunits) with another protein. Images extracted from PeptideShaker software.

3.2.3 Mass spectrometry: GPI-anchored protein identification and characterisation

Thirteen merozoite GPI-anchored proteins were identified between both the soluble and pelleted protein samples (Table 3.2) these being MSP1, MSP2, MSP10, *Pf*92, *Pf*38, *Pf*12, *Pf*113, ASP, GAMA, RAMA, *Pf*34, a conserved protein and a probable protein. Several GPI-anchored proteins expected were not identified, proteins not identified were MSP4, MSP5, MSP8, AARP, CyRPA with the transcriptional sequence for P76 being uncharacterised. Proteins involved in cleavage of GPI-anchored proteins SUB1 was identified, while SUB2 and PI-PLC were not identified.

Table 3.2: GPI-anchored proteins identified in SDS-PAGE gel analysed by mass spectrometry.

Accession number	Name	Merozoite localisation	Molecular mass (kDa)	Known/ predicted GPI-anchored protein
PF3D7_0930300	MSP1	Surface	195.60	Known[65, 172]
PF3D7_0206800	MSP2	Surface	27.96	Known[65]
PF3D7_0620400	MSP10	Surface	61.34	Known[65]
PF3D7_1364100	*Pf*92	Surface	92.56	Known[65]
PF3D7_0508000	*Pf*38	Surface	40.56	Known[65, 70]
PF3D7_0612700	*Pf*12	Surface	39.41	Known[65]
PF3D7_1420700	*Pf*113	Surface	112.5	Predicted[14, 65, 74]
PF3D7_0405900	ASP	Rhoptry	85.41	Known[65]
PF3D7_0828800	GAMA	Microneme	85.20	Predicted[65]
PF3D7_0707300	RAMA	Rhoptry	103.58	Known[65]
PF3D7_0419700	*Pf*34	Rhoptry neck	38.81	Known[65, 90]
PF3D7_1136200	Conserved protein	Unknown	76.571	Predicted[65]
PF3D7_0606800	Probable protein	Surface/ Rhoptry	34.50	Predicted[65]

GPI-anchored proteins underwent different cleavages, modifications, while others remained unchanged (Figure 3.6). Changes were identified by the spectral count of the GPI-anchored protein within the respective mass fraction. MSP1 was the most abundant protein identified followed by *Pf*92, *Pf*113, RAMA, GAMA, *Pf*38, probable protein, ASP, *Pf*12, conserved protein, *Pf*34, MSP10 and MSP2 respectively. The analysis of the proteomic changes identified are discussed in Section 3.3.

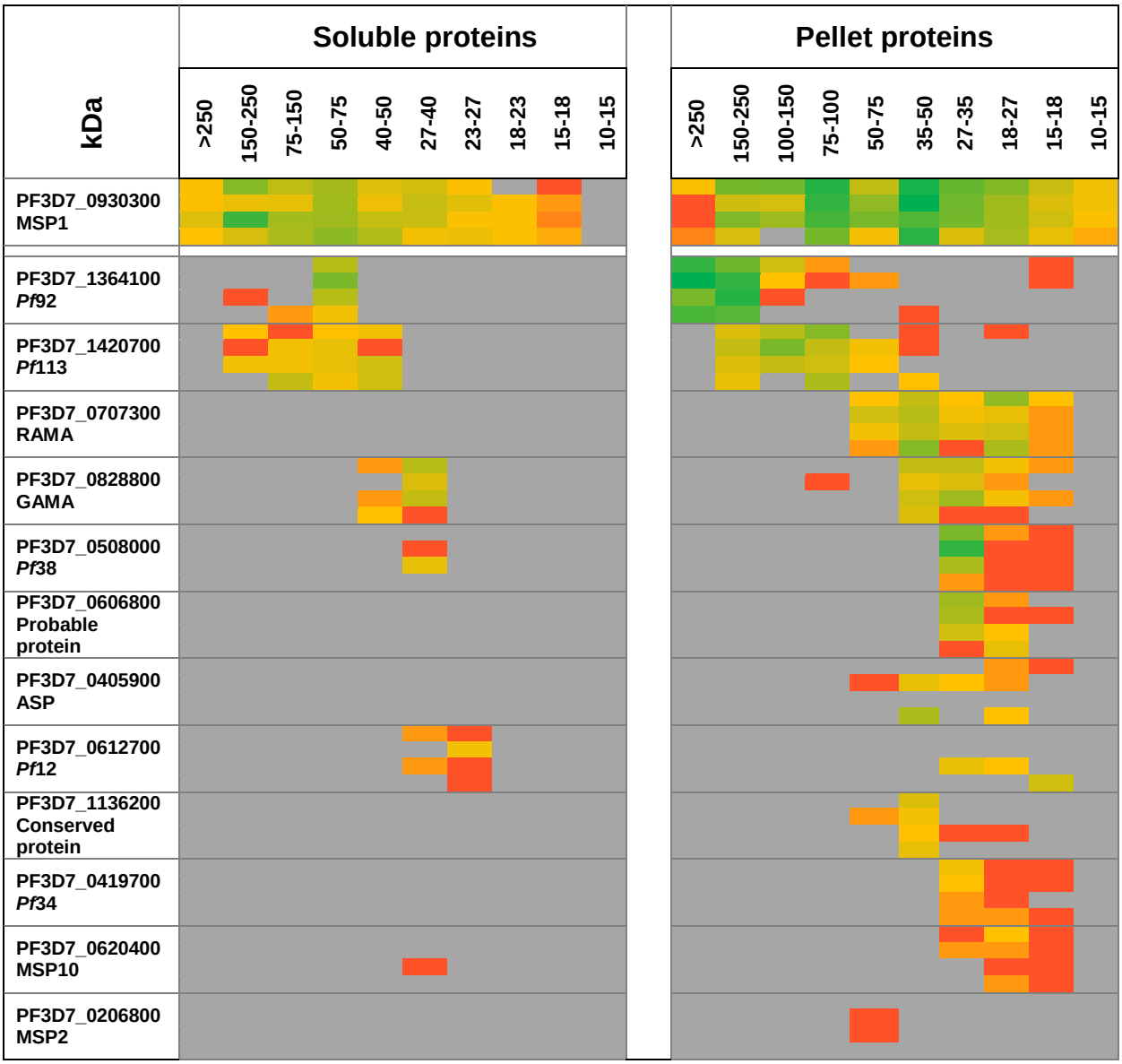

Figure 3.6: Heat map of the GPI-anchored proteins spectral count; identified by SDS-PAGE and mass spectrometry in untreated and edelfosine treated samples. Spectral count for GPI-anchored proteins listed in terms of spectral count identified in samples (top- most abundant). The spectral count of all proteins are compared against the fraction with highest GPI-anchored spectral count (excluding MSP1). The heat map of MSP1 was determined by comparison against its own mostly highly abundant fraction; this is due to the large abundance of MSP1 which would overshadow other proteins. Columns for each protein from top to bottom represent 5 min untreated, 120 min untreated, 5 min edelfosine, and 120 min edelfosine treated samples respectively. Spectral count is indicated by a colour scale ranging from highest to lowest: green- high; yellow- moderate; orange- low; grey- protein not identified in gel section.

3.3 Discussion

3.3.1 GPI-anchored protein identification and characterisation

MSP1 was found to be the most abundant protein on the merozoite in both pelleted samples and in soluble samples; this is consistent with what has previously been found in literature.[65] MSP1 is an 195 kDa protein which is essential to invasion where disruption of MSP1 cleavage renders the merozoite non-invasive.[173] While MSP1 is involved in the recognition and binding to erythrocytes and is cleaved by SUB1 into multiple fragments termed MSP1-83, MSP1-30, MSP1-38 and MSP1-42, where MSP1-42 is located at the C-terminal. The numbering of the subunits corresponds to their molecular masses.[173] In soluble samples, high abundances of MSP1 were found in fractions corresponding to the masses of approximately full length MSP1 and MSP1-83, with smaller amounts corresponding to masses of the smaller subunits. The highest abundance of MSP1 in pelleted samples corresponds to the mass of MSP1-42, indicating that MSP1-42 was not cleaved from the merozoite surface and remained attached to the GPI-anchor at the C-terminal end. During the invasion process MSP1-42 is processed by SUB2 into MSP1-19 and MSP1-33 subunits. MSP1-33 would then be cleaved and released while MSP1-19 is attached to a GPI-anchor. [174] The MSP1-19 subunit contains two epidermal growth factor (EGF) -like domains that are thought to be involved in binding to the erythrocyte, and gets carried into the erythrocyte during invasion.[174] However, the high abundance of MSP1-42 on pelleted samples suggests that SUB2 cleavage had not occurred, or only occurred to a small degree (otherwise the primary subunit on the pellet would be expected to be MSP1-19). This was the case with both 5 and 120 min samples, suggesting that total cleavage by SUB2 does not occur at egress, nor changes over time in the absence of invasion. In addition, SUB2 was not identified in samples possibly due to a combination of solubility, compartmentalisation or dilution during sample preparation. Large amounts of MSP1 at ~80 kDa was also found on pelleted samples. It has been reported that MSP1 cleavage occurs at specific sites referred to as 83/30, 30/38, and 38/42 (corresponding to the sites of cleavage and resulting subunit masses). The high abundance of MSP1 at ~80 kDa associated with the merozoite pellet suggests that not all 38/42 cleavage occurred by SUB1. The 38/42 cleavage has been confirmed to be a rate limiting processing step and that this cleavage takes longer than the other cleavages.[173] However, after the 120 min incubation period, the spectral count of this mass range did not significantly decrease. SUB1 was found predominantly in soluble samples at both 5 and 120 min and showed decreased spectral counts over time, corresponding to its activity prior to the commence of invasion events. Partial processing by SUB1 appeared to have occurred in the absence of erythrocytes with high abundances of MSP1-42+MSP1-38 remaining on the pellet, while SUB2 processing of MSP1-42 appeared not to have

occurred or have been limited. MSP1 was also found within the 150-250 kDa range in both pellet and supernatant fractions. The proteins with which MSP1 generally forms complexes (MSP6 and MSP7) were not present in this mass range, thus its presence was most likely not due to binding with its common partner proteins. A fractionation analysis (shown by protein mass range in Figure 3.6) showed that approximately full length of the MSP1 protein was identified in these fractions. This confirms that MSP1 or subunit complexes can be released from the merozoite in the absence of invasion, and confirms other suggestions that this does occur despite the observation that erythrocyte invasion is required for complete shedding.[69, 175, 176] After 120 min the spectral count of protein in the 150-250 kDa range decreased 5 fold for supernatant proteins and 3 fold in pelleted samples. SUB2 has not been implicated in the release of approximately full length MSP1 here, as SUB2 is involved with cleavage prior to entry into the erythrocyte, thus an additional protease or mechanism is expected to be involved here. In edelfosine treated samples there was an overall increase in spectral count for supernatant proteins in both time periods (140%), and a moderate decrease in spectral count for pelleted proteins (90% for 5 min and 50% for 120 min).

MSP2 is a ~25 kDa protein known to be the second most abundant protein on the merozoite surface in terms of copy number and is said to be an essential protein to invasion.[69] However, only small amounts of MSP2 were identified and were found in the 50-75 kDa fractions of pelleted samples. MSP2 has previously been found to have an observed weight of 40–50 kDa,[65] and has a tendency to self-associate to form dimers or crosslink to other proteins. It has been suggested to be responsible for the dense protein coat on the merozoite,[177] however, this was not observed based on the low MSP2 spectral count identified here. The low spectral count could be influenced by solubility issues. MSP2 was not found in supernatant samples at acceptable confidence levels, which corresponds to literature that MSP2 is not cleaved off the parasite and is carried into the erythrocyte without apparent shedding during invasion.[178-180]

MSP10 is a highly conserved protein[181] having both surface and apical distributions.[182, 183] However, the function of MSP10 is yet to be determined. MSP10 is expressed as an 80 kDa protein[183] and said to be processed to have a theoretical mass of 61 kDa.[184] MSP10 was found in gel bands found in the 18-35 kDa range in pelleted protein samples. Which is consistent with Black *et al.*[183] who noted that post-translational modifications result in a 36 kDa subunit that localises to the apical end of merozoites.[183] For the untreated samples the spectral count of MSP10 in the pellet samples was unchanged. In contrast for the edelfosine pellets there was a time related decrease to half the abundance of MSP10. This protein has two C-terminal EGF-like domains adjacent to the GPI-anchor attachment point.[183] With MSP10 being identified only at the

lower molecular masses in the pelleted samples suggests that the protein is cleaved at egress, or before invasion. The presence of EGF-like domains suggests that the 36 kDa subunit would remain on the merozoite surface during invasion,[184] although a potential erythrocyte receptor for MSP10 is yet to be identified.[69] Interestingly, some MSP10 in the range 27-40 kDa was identified in the 5 min edelfosine soluble fraction, with no MSP10 located in any other soluble fractions. This could indicate that the abundance of cleaved MSP10 was too low to be identified in other fractions, or had been further degraded, or that cleaved subunits remain pellet associated, or that edelfosine causes increased supernatant and decreased pelleted abundances as observed for MSP1.

The GPI-anchored Cys6 family of merozoite surface proteins include *Pf*12, *Pf*38, *Pf*92, and *Pf*113 who all have a conserved cysteine residue pattern that is repeated in two structurally similar domains although the proteins are different lengths and have varying characteristics. These proteins are closely associated with other surface proteins in raft-like lipid structures.[70, 184, 185] The Cys6 proteins are expected to be involved in initial reversible interactions with erythrocytes. Interestingly, *Pf*92 and *Pf*113 were found to be the second and third most abundant GPI-anchored proteins found in the samples respectively as determined by total spectral count. Besides the cysteine-rich domains these proteins contain no homology to other proteins.[70] *Pf*92 is 92 kDa protein which was found predominantly in gel bands with masses >150 and >250 kDa in pelleted samples. Considering that *Pf*92 has 14 cysteine residues, there is extensive disulfide-bonding likely causing random crosslinking to other proteins,[70] however, it would be expected that these disulfide-bonds would be reduced during sample preparation. In addition, *Pf*92 contains an array of cysteine rich high affinity binding peptides (HABPs) which are thought to be implicated in initial erythrocyte interactions by rolling over erythrocyte membrane and establishing multiple points of contact with the target cell.[185] These regions are implicated in forming complexes with erythrocyte proteins, but *Pf*92 was found at high molecular masses in the absence of target erythrocytes indicating possible non-specific crosslinkages, or formation of macromolecular complexes on the merozoite surface.[185] No interactions with other merozoite proteins have been reported to date.[185] In addition, *Pf*92 was identified in 50-75 kDa fractions in all soluble samples indicating that the protein underwent cleavage. The identified peptide was closest to the C-terminus, however, based on sequence coverage, it could not be confirmed whether any fragments remained on the pellet. *Pf*92 has been found in merozoite and ring stage, indicating that a subunit of *Pf*92 may enter the erythrocyte during invasion.[185]

*Pf*113 is not found in any other lifecycle stages of *P. falciparum* besides the merozoite.[70] The full length of *Pf*113 has a mass of 113 kDa; the protein was found in several gel sections indicating

multiple masses of this protein in both treated and untreated control samples. *Pf*113 was found at approximately its full length in both pellet and in soluble fractions, and in smaller cleaved units between 40 and 100 kDa. The protein is classified as an adhesion molecule[186] and has recently been considered as an important invasion protein as it may function as an alternative to MSP1.[185] *Pf*113 was found in fractions of 150-250 kDa in both pellet and soluble protein fractions. As with *Pf*92, it could be participating in the formation of macromolecular complexes on the merozoite surface,[185] as it has been found to complex with unknown proteins to result in complexes of masses >400 kDa in native samples.[185] *Pf*113 has multiple binding sites for low-affinity molecular interactions. The binding sites crosslink with erythrocyte receptors, thus the presence at higher molecular masses may be due to non-specific crosslinking.

*Pf*38 is considered a non-essential protein[187] located on the merozoite surface with increasing concentrations towards the apical region.[70, 182] *Pf*38 was found in fractions relating to its full molecular mass in both soluble and pelleted fractions. *Pf*38 has uncharacterised functions and potential modifications have not been identified.[69]

The Cys6 proteins *Pf*92, *Pf*113, and *Pf*38 demonstrated no significant changes in the spectral count over time in soluble samples (Figure 3.6). In edelfosine treated samples, a trend was observed where *Pf*92, *Pf*113, and *Pf*38 showed decreased spectral counts in pelleted protein samples, *Pf*113 and *Pf*38 showed increases in soluble samples compared to untreated samples, and *Pf*92 showed limited change in abundance in the soluble fractions.

*Pf*12 is a 40 kDa surface protein[188] showing an increased concentration towards the apical region.[70, 188] *Pf*12 forms a heterodimer with non-GPI-anchored Cys6 protein *Pf*41 through disulphide bonds[69, 184] which should have been reduced during preparation as these proteins eluted separately (based on the mass range where they were found). *Pf*12 is shed from the merozoite as two smaller subunits.[188] Interestingly, *Pf*12 appeared to be present at its full length in the 5 min soluble protein samples, however, after 120 min incubation, the protein was found at 23-27 kDa fractions, which was seen in both treated and untreated samples. This modification appeared to be unique to *Pf*12 indicating a possible truncation over time. In contrast to other Cys6 proteins, *Pf*12 was not found in untreated pelleted protein samples, while it was found in treated pelleted protein samples. In the 5 min treated pelleted protein samples the mass appeared to be consistent with full length *Pf*12, while found at 15-18 kDa in 120 min fractions. The modification of *Pf*12 would indicate cleavage by two separate mechanisms, one at time of egress with a second modification that occurs over time, although a reason for this would need to be identified. *Pf*12 cleavage by SUB2 has been speculated,[188] however, the early cleavage of *Pf*12 could render this

unlikely as SUB2 is involved with the final processing of the merozoite protein prior to entry into the erythrocyte which was not assessed here.

GAMA is micronemal protein involved in the binding of merozoites to erythrocytes. GAMA is said to migrate to the surface of merozoites where it undergoes primary and secondary processing events.[182, 189] The 85 kDa protein has been found to migrate as 80 kDa, 49 kDa, 42 kDa, and 37 kDa subunits in SDS-PAGE.[187] GAMA forms two different heterodimers, P37+P49 and P37+P42.[187] In this study, GAMA was found in soluble fractions corresponding to the 37 and 42 or 49 kDa subunits. GAMA did not appear to migrate as its full length mass. Peptide coverage analysis of soluble protein samples showed that peptides towards N-terminal (37 kDa) and C-terminal (42 or 49 kDa) were found in soluble protein samples in their respective mass fractions. The subunits are bound together most likely by a sulphide bond[182] as they elute together in native gels while in this study sulphide bonds were reduced and subunits were found separately in these samples. GAMA is said to be cleaved off the merozoite leaving a short GPI anchored ‘stub’ left bound to the surface.[187] Thus it can expected that the cleaved subunits are the P37+P42 dimer,[69] although this could not be confirmed here as both 42 and 49 subunits would be found in the same gel section. GAMA was also found in pelleted fractions with both N- and C- terminal subunits at their expected masses. The significance of the initial processing into the P37 and P49 subunits remain unclear, although it could be hypothesised that such a cleavage could serve to “activate” GAMA by exposing a functional domain. The identity of the parasite protease responsible for the cleavages is unknown, however, one could be involved causing the early 37/49 cleavage, with an additional protease causing the cleavage of 49 into 42 to release it from the merozoite. In previous literature, GAMA has been found to be in supernatant protein samples only after merozoite invasion. However, some cleavage did occur in the absence of entry into erythrocyte, thus may be caused by a mechanism with at least partial cross reactivity. With the apical concentration of GAMA and the non-specificity of SUB2 cleavage, it cannot be ruled out that SUB2 could cause the release of GAMA at the tight junction, however, action of an additional protease has been predicted.[182] With the presence of GAMA on pellet samples, and apical concentrations of the protein[182] this is consistent with the concept that GAMA is required for invasion. Interestingly, GAMA was found at significantly lower spectral counts after 120 min in all fractions, with no obvious changes caused by edelfosine treatment.

ASP is an 85 kDa rhoptry neck protein containing sushi domains (also known as short complement repeats (SCRs)).[190] The function of ASP is unknown, however, the SCRs may be involved in the regulation of complement ligands.[90] ASP was found only in pelleted protein

fractions, with a ~3 fold higher spectral count at 120 min compared to 5 min. Cleavage fractions of ASP were identified in the pellet protein fractions at 25-50 kDa. ASP is reported to be cleaved into a 30 kDa N-terminal and a 50 kDa C-terminal subunit.[190] The two subunits are attached by a disulfide bond,[190] and remain associated with the pellet over time in the absence of invasion. No subunits were identified in soluble protein samples at their respective masses. ASP is thought to be involved in tight junction formation thus would not be cleaved during invasion, or only released towards the erythrocyte binding phase of invasion, which would therefore not be identified in this study. ASP is reported to interact with other proteins, such as *Pf*Rh4, but no crosslinking was identified in this study. Limited differences were identified between treated and untreated sample in terms of spectral count, however, treated samples were found to separate into more defined mass ranges on the SDS-PAGE gel.

RAMA is conserved amongst *Plasmodium* species, and is essential in *P. falciparum.*[71, 191] RAMA forms non-covalent macromolecular complexes in lipid rafts with RAP-1, RAP-2, RAP-3, RhopH3.[184] RAMA is a rhoptry protein associated with the rhoptry membranes.[191] It is synthesised as an 170 kDa precursor in early trophozoites and is proteolytically processed to yield a smaller 60 kDa form that is bound to the inner membrane of the rhoptry via a C-terminal GPI-anchor.[191] The 60 kDa subunit was found in pelleted protein samples. Further processing of RAMA was not seen, with C-terminal fraction showing no changes over time or with edelfosine treatment. However, RAMA binds to unknown erythrocyte receptors during invasion and has been found in soluble fractions of invaded erythrocytes.[191] This suggests that the signals or interactions required for its release had not yet occurred in the conditions used in this study.

*Pf*34 is a rhoptry neck protein which remains to be functionally characterised.[90] The full length of *Pf*34 has a mass of 38 kDa; and was identified in pelleted protein samples, showing no significant changes over time or with edelfosine treatment, showing a similar response to that of RAMA. *Pf*34 may play a role similar to that of RAMA, by forming complexes with proteins involved in invasion.[90] Like RAMA, *Pf*34 was not cleaved in any protein samples analysed in this study.

The conserved protein with unknown localisation was found in pelleted protein samples with none in supernatant protein samples. This protein showed similar distribution patterns to rhoptry neck proteins RAMA and *Pf*34. This a 76 kDa protein found at 35-50 kDa possibly indicating a pre-processing step which would need to further assessed. A pre-processing step can be hypothesised with no cleaved subunits being identified in soluble protein fractions after egress or in the absence of invasion. No significant changes were caused by edelfosine treatment. This

protein has been shown to be important to invasion as antibodies against this protein has resulted in significant reductions of erythrocyte invasion.[192]

The probable protein is a 34 kDa protein predicted to be associated with the merozoite surface and/or rhoptry organelles. This protein also showed patterns similar to that of rhoptry proteins. The probable protein was identified only in pellet protein samples at its full molecular weight, with no protein identified in soluble fractions. The protein did not appear to be processed or have smaller subunits in any of the protein fractions. In addition, the probable protein showed negligible differences between 5 and 120 min samples, with a moderate decrease in spectral count of samples from edelfosine treatment.

A number of known or predicted GPI-anchored proteins expected to be found in these samples were not identified in any of the fractions analysed. These are MSP4, MSP5, MSP8, CyPRA and AARP. MSP4 is found on the merozoite surface, and is carried into the erythrocyte during invasion, for unknown functions within the new parasite.[178] MSP4 was expected to be identified in pellet samples, but not in the soluble fraction. Although its role is unknown MSP4 contains two EGF-like domains adjacent to their C-terminal GPI-anchor attachment points, which are highly immunogenic and thus most likely located at apical end possibly for involvement in erythrocyte invasion.[14, 183, 193] Not finding the MSP4 is thus suspected to be caused by solubility issues. MSP5 also contains EGF-like domains and is thus most likely also to be involved in invasion. In *P. falciparum,* MSP5 can be disrupted with no apparent growth defect.[14, 71] Its function and potential processing are unknown, or whether it is carried into the erythrocyte is yet to be determined.[69] MSP8 was previously thought to be involved in invasion, but this protein appears to play a more prominent role in early PV function and appears to dominate in the ring stage,[70] and is most likely carried into the erythrocyte during invasion. CyRPA is a conserved protein expressed at 35 kDa in the micronemes. It subsequently migrates to the apical end of the merozoite surface[194] and when inhibited, marked invasion reduction is observed.[194] CyPRA interacts with two non-GPI linked proteins (Reticulocyte binding-like homologous protein 5 (*Pf*Rh5) and PfRH5-interacting protein (*Pf*Ripr)) to form a ~200 kDa complex that attaches to the erythrocyte antigen, Basigin, during invasion. *Pf*Ripr was not found and only small amounts of RH5, indicating that the complex may remain in insoluble components or other mechanisms at play. Apical asparagine rich protein (*Pf*AARP) is expressed with ASP and also localised to the rhoptry neck,[195] and remains to be functionally characterised,[90] its absence may be related to solubility.

3.3.2 Electrophoresis on the merozoite proteome

Whole organism analyses was conducted on SDS-PAGE gels and the complete lanes were analysed by LC-MS/MS thus a large number of proteins were identified. Using whole organism analysis, proteins of varying mass ranges and characteristics were present. Supernatant proteins had predominantly well resolved narrow bands with sharp edges, which are characteristic of soluble and extrinsic membrane associated proteins (excluding the very highly abundant 13 and 26 kDa bands associated with haemoglobin). Although pelleted proteins showed many proteins with these same characteristics there was an increased number of bands present in pelleted samples with broader and less defined edges. The less resolved bands could indicate the presence of hydrophobic side chains (hydrophobic sections of the protein may undergo incomplete denaturing); or this could indicate that multiple proteins of similar masses are present in the band. Both scenarios would have the individual molecules running separately giving a distribution of molecular masses within the band making it visually less resolved. SDS-PAGE techniques can be adjusted to account for the characteristics of the proteins present, or the proteins of interest in the samples so that protein identification can be optimal. The gel concentration used here was ideal to visualise proteins between 10-250 kDa, which was the mass range where the majority of merozoite proteins were found. The polyacrylamide concentration of the gel effects the separation of protein bands according to their respective apparent masses, thus to visualise the full mass range of proteins, or to better visualise more narrow mass ranges, the concentration of polyacrylamide could be altered. The relationship between mass and relative mobility is logarithmic thus a different concentration would alter separation patterns. This would assist with identifying same protein subunits with similar masses. For example, GAMA has subunits of similar masses of which would not be differentiated here due to migration within the same band with limited mass resolution. A higher polyacrylamide concentration could be selected to better separate proteins within specific mass ranges. Upon assessment of protein bands showing high abundance, multiple proteins were present in many cases. This would prevent the ability to definitively state that a GPI-anchor protein or subunit was located in a specific band and could only be identified to a mass range within gel fractions after LC-MS/MS analysis.

Band clarity and resolution can be affected by the voltage used to run gels. Low mass proteins (<70kDa) show improved resolution at high voltages, while high mass proteins (>70kDa) show better resolutions at low voltages.[196] Considering both low and high mass proteins, gels were run at a low voltage through the stacking gel and increased to a medium voltage for the remainder of the run. A higher voltage gives better resolution for smaller size proteins as smaller molecules are

more prone to diffusion, the higher voltage enables the proteins to remain in compact sharp bands. Larger proteins need to find their lowest energy form and conformation, before moving through the gel, thus large proteins need lower voltages to give them the additional time. Gels were run at 60 V through the stacking gel, followed by 120 V through the remainder of the gel. The mid-range voltage enabled well resolved bands (accounting for the number of protein bands visualised) and prevented gels from swelling or forming a curved pattern towards the bottom of the gel which would occur if over heated by voltages that are too high, thus indicating a good choice in voltage for merozoite proteins. Coomassie is considered the standard for staining gels in proteomic work as it is sensitive to low mass proteins and is compatible with mass spectrometric analyses. Coomassie is more sensitive to some proteins depending on their chemistry and composition. Alternative stains such as the silver stain is known to be more sensitive than Coomassie and would be valuable in cases where specific bands would be cut out of the gel, however, silver stain is not compatible with mass spectrometry and thus was not required here as whole lane analyses was conducted.

3.3.2 Unidentified GPI-anchored proteins

Some GPI-anchored proteins were found in relatively low abundances in both supernatant and pelleted protein samples with several known GPI-anchored proteins not being identified in this study. This could be due to a number of reasons. Insoluble material remained in pelleted protein sample wells after SDS-PAGE gels were run. Products that remained in the wells would typically be products too large to penetrate the gel such as large crosslinked proteins or proteins bound to DNA, nucleic acids, carbohydrates, or lipid products.[197] The merozoites are equipped with large volumes of DNA for the commencement of a new lifecycle, thus it is expected that significant amounts of the remaining product would be DNA. The merozoite proteins are predominantly within 10-250 kDa range, hence only smaller proportions of this product would be large merozoite proteins, with remaining protein then being crosslinked proteins or proteins that were not sufficiently solubilised. Full SDS-PAGE lanes were excised and analysed by means of highly sensitive LC-MS/MS equipment. DDA was used to analyse samples where only selected highly abundant proteins showing large signal intensity and proteins with multiple charges were selected for further MS/MS analysis. Using this technique a large range of proteins were identified. However, as only selected proteins were fragmented for spectral analysis proteins of lower intensity would not have been recorded. This could result in the non-identification of several GPI-anchored proteins. In addition, it is normal that not all proteins are found by LC-MS/MS. MSP5, for example, is non-essential which could result in its absence. More complete proteome

identification could be obtained with additional LC-MS/MS replicates. High concentrations of TCA followed by acetone washing would have removed lipids but could also reduce proteins that may be associated with large lipids. SDS has excellent solubilising qualities,[198] and samples appeared to have complete solubilisation after preparation in sample buffer. An additional explanation for low abundances of GPI-anchored proteins in pelleted samples may be due to an association with lipid rafts on the merozoite surface.[85, 199] Lipid rafts are highly hydrophobic in nature. The association with lipid rafts could have resulted in the under-reporting GPI-anchored proteins.[200] Some proteins associated with lipid rafts may aggregate when heated with SDS through strong hydrophobic interactions leading to selective protein loss, or these peptides may resist digestion or resist elution from the gel.[200] The rafts are largely composed of sphingolipids and cholesterol which stabilise to form larger microdomains and restrict free diffusion of membrane proteins.[201] The restriction of protein movement may be important for protein specific roles in invasion. Proteins involved in initial interactions with erythrocytes are localised over the merozoite exterior surface, while proteins involved in tight junction formation should be localised to apical regions.[70] Proteins on the merozoite exterior surface such as MSP1, Cys6 proteins (specifically *Pf*92 and *Pf*113) were found in high abundance, and have surface fluidity aiding their role in initial rolling and attachment to erythrocytes. Several apically localised proteins such as MSP4, CyRPA, AARP were not identified. The different composition of the lipid rafts on basal and apical regions could be speculated as influencing the detection rates. This is suggested based on recent finding that lipid rafts influence the selection of proteins and lipids for incorporation into the PVM during entry into erythrocytes.[201] Enrichment using a non-ionic detergent such as Triton X-100 or Triton X-114 at low temperature could be used in order to better characterise GPI-anchored proteins associated with lipid rafts in detergent resistant localisations.[201] In this study, raft association is expected to affect abundance of pelleted proteins and not the soluble cleaved proteins in these samples, as lower abundances in soluble samples would be caused by separate mechanisms (discussed below). Although sample temperatures were maintained at 4ºC or below until solubilisation in sample buffer, some protein degradation was expected to have occurred causing background peptides to be identified and lead to inaccurate assumptions about the relative abundance. The use of multiple protease inhibitors or EDTA should be included in future analyses in order to prevent protein degradation.[202] In addition, proteins diffuse out of the gel over time if left for too long before processing for LC-MS/MS analyses, proteins were cut from the gel and analysed by LC-MS/MS within one week of running the gel, thus it was not expected that protein loss from gels would have had a major impact on abundances found.

3.3.3 GPI-anchored protein cleavage

For successful invasion, it is essential that merozoite proteins undergo specific cleavages and proteomic modifications. Early analyses of the merozoite found that GPI-anchored proteins line the surface of the merozoite and are cleaved to enable the parasite to enter into the erythrocyte. However, it was later found that there was not a universal cleavage pattern of GPI-anchored proteins and it has since been determined that proteins are processed differently in some cases. Many surface proteins are cleaved and shed from the surface of the merozoite during invasion; yet, not all surface proteins are cleaved or processed, with some proteins or subunits being retained on the surface during invasion. SUB1 is required for the maturation of SERA proteins, MSP1, and other merozoite surface proteins prior to release from schizonts.[143, 203, 204] This proteolytic modification primes and/or activates the proteins for their role in egress or invasion. SUB1 is discharged from exonemes at the apical end of the protein into the parasitophorous vacuolar space,[205] where it cleaves the target proteins along the length of the protein and not at the anchor, thus would not be responsible for release of soluble proteins found at their full length. Here, the abundance of secreted SUB1 decreased over time indicating the early activity of the protease by preparing proteins for their functions. This corresponds to the concept that serine proteases are activated for the brief periods during which their activity is required.[60] Although large amounts of MSP1-42 was abundant on the merozoite surface, the high abundance of MSP1-42+MSP1-38 suggests that MSP1 exhibited only partial cleavage by SUB1. The cleavage to the 38/42 form takes longer to occur.[173] However, merozoites had egressed for 120 min with limited release of these truncated protein subunits. This could suggest that there is an additional level of control preventing complete processing.

After merozoite egress the SUB2 protease is secreted from micronemes/dense granules onto the merozoite surface.[69] After the release of SUB2 but prior to invasion, the SUB2 protease remains associated to the merozoite surface in regions most likely associated to the apical regions. SUB2 is involved in the shedding of the merozoite coat, so during the invasion process SUB2 is said to rapidly translocate from the apex to the posterior of the merozoite causing protein shedding.[206, 207] The SUB2 protease cleaves MSP1 and other merozoite surface proteins from the merozoite surface.[173, 203, 208] SUB2 cleaves MSP1-42 leaving MSP1-19 on the surface. The lack of cleavage of MSP1-42 suggests that this processing does not occur with time after egress and that control is required in this mechanism, most likely linked to a signal that would be associated with a step in invasion that this required prior to the commencement of entry into the erythrocyte. The lack of

SUB2 identified suggests that the protease may be crosslinked prior to its activity in cleaving the surface coat, or missing due to technical implications.

GPI-anchored proteins on most eukaryotic cells including mammalian and other protozoan species such as *Trypanosoma brucei* or *Toxoplasma gondii* are cleaved at the phosphatidylinositol of the GPI-anchor by PI-PLC.[84] However, *P. falciparum* merozoite GPI-anchored proteins have been found to be PI-PLC insensitive. This insensitivity is due to an additional acyl group attached onto the phosphatidylinositol of the GPI-anchor. This may provide an important control mechanism for the merozoite by preventing GPI-anchored proteins from being cleaved by host PI-PLC. The acylation would ensure that only parasite enzyme would be involved in GPI-anchor protein cleavage. In this way the parasite is in control of which proteins are cleaved and reduces the possibility of GPI-anchor cleavage being host driven. By the parasite controlling the enzymatic involvement in protein cleavage the parasite would then also be able to control the timing of cleavage during invasion.

In contrast to other *P. falciparum* merozoite GPI-anchored proteins the P76 merozoite serine protease is said to be susceptible to PI-PLC cleavage.[60] The P76 merozoite serine protease is found to be active only on merozoite stages of the lifecycle, and is associated with either the merozoite surface or rhoptry organelles,[209, 210] with half its abundance found in soluble fractions.[89] P76 is involved in invasion with its soluble form showing proteolytic activity on merozoites.[60] The cleavage of P76 on intact merozoites is inhibited by an inhibitor of *T. brucei* PI-PLC[60] (edelfosine inhibits *T. brucei* PI-PLC). However, both P76 and PI-PLC were not identified in samples. This prevented the effect of edelfosine from being determined on PI-PLC and potential successive activities of P76 from being assessed. As the P76 protease is PI-PLC sensitive, the GPI-anchor of P76 is then expected to be without the additional acylation. However, this would need to be further researched due to the reported conserved structure of *P. falciparum* GPI-anchors. *P. falciparum* parasites have been found to possess GPI-anchors that do not contain the additional acylation, however, these are generally thought to be GPI precursors and intermediates.[20] The presence of non-acylated GPI-anchors associated with proteins is yet to be characterised.

3.3.4 Loss of merozoite invasive capacity

Merozoites have a short period in which they retain invasive capacity. The previous understanding is that merozoites loose ability to invade by two possible mechanisms: either due to spontaneous shedding of GPI-anchored proteins and premature release of rhoptry and microneme proteins; or that merozoites loose invasive capacity as a result of a loss of metabolic activity.[211, 212] These were both suggested to occur within several minutes of egress from schizonts. The spontaneous

cleavage of merozoite GPI-anchored proteins would cause loss of invasive capacity by preventing the merozoite from having the initial low-affinity, reversible interactions with erythrocytes. Some GPI-anchored protein can be released in the absence of invasion, as shown in these results and in literature.[63, 175, 176] Previous analyses observed that the GPI-anchored proteins are cleaved off the merozoite surface prior to entry into the erythrocyte, and that increasing amounts are lost the longer the non-invaded merozoite is outside of the schizont.[12] For example, large quantities of MSP1 was found in supernatant fractions 5 min after egress as near full length MSP1 and in the various MSP1 subunits. The most significant change was noted in the spectral count of near full length MSP1 which decrease by 5 fold between 5 min and 120 min after egress. The Cys6 proteins (*Pf*12, *Pf*38, *Pf*92, *Pf*113), showed cleavage in the absence of invasion with insignificant changes in soluble proteins over extended times as used in this study. Micronemal protein, GAMA, showed partial release with some protein identified in the soluble fractions, while no rhoptry or rhoptry neck proteins were identified in soluble samples. The absence of conserved protein in soluble sample may indicate that it is associated with rhoptry organelles. The loss of MSP1, Cys6 proteins and micronemal proteins during the first five minutes after egress could be associated with a loss or decrease of invasive capacity, however, GPI-anchored rhoptry proteins appeared to not be involved in this process. Not all merozoite proteins are lost in the absence of invasion, with invasion being required for full cleavage, implying that the merozoite probably has significant control over cleavage of GPI-anchored and other proteins involved in the invasion process.

The merozoite is designed for invasion, thus is could be suggested that the merozoite contains only enough energy reserves for the short period in which it maintains invasive capacity and thereafter would require the utilisation erythrocyte contents for energy and proliferation. Another suggestion is that energy usage has changed, whereby energy stored in the mitochondria is no longer being used for invasion and energy consumption is shifted to the production of proteins and compounds necessary for the survival of the ring. Proteins involved in glycolysis were identified with high spectral count in untreated samples and showed a slight decrease over time. Interestingly, the treated samples showed increases in glycolysis proteins over time in both pellet and soluble protein fractions (not shown here). This increase in glycolysis enzymes contrasts what has been seen following edelfosine treatment in *Leishmania*.[213] This does however, suggest that the merozoite retains capacity for metabolic activity at 120 min after egress. In addition, merozoites can maintain invasive capacity after their release from E64 treated parasites, this coupled with the evidence that some merozoites maintain invasive capacity greater than an hour after egress suggests that merozoites may not be programmed to invade directly after egress and

require additional signals to trigger invasion.[72] Suggesting that merozoites do possess levels of intrinsic control over their viability.

3.3.5 Pathological effects of GPIs and implications

The *Plasmodium* merozoite invests heavily in its surface proteins which are antigenically diverse and exposed directly to the host's immune system components. A possible reason for this is that some surface proteins modulate host responses to assist in merozoite survival after release from the infected erythrocyte.[79] This may be done by the released and cleaved proteins acting as an immunological "smoke screen" or by blocking activity of the complement pathway.[214] It is likely that *Plasmodium* parasites have developed mechanisms to protect the merozoite against complement and other innate host responses, with extrinsic proteins being prime candidates for this function.[74, 215] Typically GPI-anchored proteins are cleaved at different places by different enzymes, and in some cases, leaving the GPI-anchor itself attached to the merozoite. However, the GPI-anchor has been implicated as a major cause of the pathological symptoms of malaria (particularly in uncomplicated malaria as other major pathologies contribute to severe malaria). The pathological section of the GPI-anchor has been found to be the additional acylation on the phosphatidylinositol of the GPI-anchor. This differs to mammalian host GPI-anchors which are not acylated. The additional acylation causes cytokine induction and causes an immunological response.[23, 216] Previous studies have indicated that the removal of the acylation of the GPI anchor prevents the immunological response.[20] In addition, merozoites are known to contain a "fuzzy" material that lines the surface. While the merozoite contains large amounts of GPI-anchored anchored proteins, it has also been found to accumulate large amounts of non-anchored protein free GPIs on the merozoite surface.[217] With 2-5 fold the required amounts of GPI being synthesised in *P. falciparum* merozoites than what is required for GPI-anchoring, and this excess is thought to accumulate on the plasma membrane.[217] A large proportion of these GPIs contain the acylation and thus would be involved in pathogenesis during the release of merozoites.[84, 217] Targeting non-anchored protein free GPIs could potentially provide new avenues of disease control.

3.3.6 Potential of GPI-anchored proteins to be used as a drug or vaccine target

In support of the above, epidemiological studies observed that immunity to disease precedes the ability to control parasite densities. This is demonstrated in the fact that protective immunity is acquired and develops in three sequential phases: first, immunity to life-threatening disease; second, immune development that results in a reduction in symptom severity (here the symptoms are reduced while parasitisation is not reduced); and third, partial immunity to parasitisation.[25]

This was also demonstrated where antibodies to GPIs reduce the symptomatic profile but not the invasion events. By exposing mice to acylated GPIs, the pathological response has been sufficient to result in death.[23] Thus a GPI based vaccine might only prevent clinical symptoms whereas an enzyme inhibitor may prevent cleavage of GPI-anchored proteins, thereby reduce the number of merozoites invading erythrocytes, while also reducing the clinical severity.[87] Polyclonal antibody studies against MSP1 and separate Cys6 proteins (*Pf*92 and *Pf*113) have shown high success when targeting multiple merozoite invasion proteins, while attempts to inhibit a single protein have shown only moderate success.[65, 218] However, these results and other literature indicate that multiple proteases are involved in the release of portions or complete GPI-anchored proteins. Thus in order for complete invasion blockade a mutli-targeted response would need to be incorporated, where multiple specific inhibitors are used to prevent invasion-required protein cleavage, and prevent the merozoite from utilising alternative pathways of erythrocyte entry. As SUB1 had shown the majority of its activity prior to release from schizonts, compounds that inhibit cleavage would need to focus on GPI-release post merozoite egress. These post egress targets could prevent activity of SUB2 or inhibition of triggers that initiate cleavage during invasion. The structure of the GPI-anchor in *Plasmodium* appears to be well conserved across all the strains[74] while the proteins themselves show lower levels conservation.[185] This again suggests that the plasmodial GPI is a valuable target for both vaccine and drug studies.[184]

3.3.7 Possible triggers to erythrocyte invasion by merozoites

The cleavage, release, and other modifications made to the GPI-anchored proteins do not occur at the same time, thus multiple processes would be implicated in the control of GPI-anchored protein modifications. The proteins have different roles during the invasion process. Thus despite the similarity that these are all attached via a GPI-anchor, different factors should cause and trigger protein cleavages, release and modifications. These different triggers would need to be well coordinated in accordance with the protein function and phase of invasion where the GPI-anchored protein is active. For example, SUB1 is activated prior to egress and causes the priming of MSP1 and other specific proteins. The cleavage by SUB1 allows the protein subunits to form other multi-protein complexes that are involved in recognition of erythrocytes or early invasion. Once the merozoite is released form the schizont initial interactions occur with new target erythrocytes mostly thought to occur by Cys6 proteins. Interactions with erythrocytes were not measured in these experiments possibly limiting the visualisation of further GPI-anchored protein cleavages and release. It has been reported that the trigger to invasion could be environmental changes such as low potassium ion concentrations. This is suggested as during the time of egress

cytosolic calcium levels are increased resulting in low potassium levels. This occurs through a phospholipase C mediated pathway where the liberation of diacylglycerol act as a second messenger and activates protein kinases.[72, 219] It has been suggested that other rhoptry processes may be regulated within the same biochemical cascade.[89] The release of calcium activates the secretion of adhesion and invasion proteins from the micronemes onto the parasite surface,[72, 220] as demonstrated by the partial release of GAMA. External calcium is required for the release of SUB2 and other proteases from micronemes onto the parasite surface.[60, 72, 220] This then initiates modification of GPI-anchored proteins. However, the lack of SUB2 and its cleavage subunits may indicate that although external calcium may be required, additional triggers are needed for cleavage by SUB2 and other proteases. The release of microneme and rhoptry proteins possibly do not occur all at once, with subgroups released at different times, allowing some to be translocated before or during egress in the case of the partial release of GAMA or AMA1.[221, 222]

Full release or complete cleavage would then only occur after establishment of a tight junction and would involve additional release of proteins from the micronemes and rhoptry organelles.[14] Only partial cleavages of GPI-anchored proteins were identified in protein samples assayed in this study where invasion was blocked by providing no target erythrocytes, thus it can be suggested that invasion events or additional signalling events would need to occur for the complete processing of GPI-anchored proteins. This complete process would thus only occur in the presence of erythrocytes. In addition, as the different GPI-anchored proteins are processed differently, the signals required for cleavage are probably not identical and may be different for cleavage by different proteases. The separate mechanisms of GPI-anchored protein degradation may be an important mechanism for the regulation of invasion and evading host immune responses. A cell might express many different GPI-anchored proteins, and it seems unlikely that simultaneous release of all of them would be advantageous to the cell, implying control of their release may be important to the survival.[86] GPI-anchored protein cleavage is not a uniform process thus these additional triggers would then be needed for synchronised cleavages that are in alignment with the invasion process. Cleavage and shedding of proteins is a selective process that requires specific protein cleavage of GPI-anchored or other membrane anchored proteins.

3.3.8 Edelfosine effects on GPI-anchored processes and potential as an antimalarial

Edelfosine did appear to affect some GPI-anchored proteins, causing more protein in soluble samples and less in pellet samples for certain proteins e.g. MSP1 or MSP10. However, this appeared to be specific to certain proteins and unrelated to enzymes SUB1, SUB2, or PI-PLC.

This suggests that the primary effect is expected to be on the merozoite surface, plasma membrane lipid rafts or other uncharacterised enzymes/proteases that can affect some GPI-anchored proteins. Edelfosine does accumulate at the cell surface,[103] and has a number of effects including increasing membrane fluidity (seen in neoplastic cells),[158] produces morphological changes in membranes, modifies plasma membrane lipid composition causing selective association or/and displacement of proteins associated with lipid rafts. Edelfosine does not have a direct detergent-like effect but rather a metabolically or physically based influence on the plasma membrane.[104, 158] Merozoites were exposed to edelfosine (100 µM) from egress when merozoites would still demonstrate invasive capacity, and this induced a ~60% inhibition of invasion. It cannot be excluded that if a greater level of inhibition had been attained that a greater alteration of the proteome would have been demonstrated. In order to observe a more complete drug effect on protein cleavage the experimental drug may need to be present before or at the time of merozoite egress to account for early processing of GPI-anchored proteins. GPI-anchored proteins were the primary focus in this research, and proteomic analyses was conducted primarily on the GPI-anchored proteome. However, it is likely that edelfosine inhibited invasion through additional pathways not assessed which should be assessed in further analyses. In addition to edelfosine's effect on plasma membranes, *in vivo* effects of edelfosine would be beneficial to study in terms of both inhibition of invasion and pathogenesis. Edelfosine causes the activation of macrophages[105] and displays anti-inflammatory activity.[102] Edelfosine has been shown to cause up regulation of IL-10 at early post-infection times in schistosomias, thus potentiating anti-inflammatory actions; followed by a down-regulation of IL-10 at late post-infection times, and reductions in both IFN-γ and IL-2 production.[102] Thus in addition to decreasing invasion events, edelfosine has the potential of reducing clinical symptoms.

Chapter 4: Conclusions and Recommendations

4.1 Concluding discussion

This project followed specific aims and objectives that were each successfully completed using optimised approaches and powerful analytical techniques. The purpose of this study was to characterise glycophosphatidylinositol (GPI) -anchored merozoite surface proteins during the invasive phase, while exploring the use of these proteins as potential targets against intraerythrocytic malaria. Merozoites and invasive processes are considered as promising areas for drug and vaccine development. While many merozoite proteins have been identified the receptor-ligand associations, exact functions and relative contributions to invasion are not well established with very few invasion inhibiting compounds having been identified to date.[68] This has previously been due to a lack of optimised techniques for producing large numbers of highly synchronised merozoites for analytical studies.

Large volumes of tightly synchronised cultures were required for analytical merozoite studies due to the small size and short invasive life-span of the merozoite. Parasite culturing techniques were successfully optimised from standard culturing methods to specifically isolate tightly synchronised merozoite populations. Parasite culturing was optimised using several key initiatives: The Malarwheel was developed as part of this study and was an incredibly valuable tool that was used to determine the times for sorbitol synchronisation and magnetic activated cell sorting (MACs) isolation. This tool provided the means to improve culture synchronicity to a narrow 2-3 hr window by using optimised techniques. A formula was used to determine culture media volumes required for a 24 hr period.[119] This was combined with frequent culture splitting to improve replication rates, parasite wellness and reduced parasite recuperation periods after isolations in order to increase the frequency of experiments. Synchronisation techniques were improved by combining sorbitol treatment with MACs isolations to obtain the narrow synchronous window. In addition to this, MACs isolations were optimised by passing already synchronised cultures through a MACs column 3 times which increased parasite and proteomic yield.

Potential inhibitory compounds were successfully screened using a modified Malaria SYBR green I-based fluorescence (MSF) assay to determine inhibitory potential and stage specific effects on *P. falciparum* intraerythrocytic stages. The merozoite invasion assay (MIA) was successfully used to determine the potential inhibitory effect of the selected compounds on merozoite invasion of erythrocytes. The results described here are some of the first MIAs conducted on *P. falciparum* 3D7 strain parasites. The MIA differs from other methods by allowing accurate research

specifically on the invasion phase[63]; when combined with the optimised culturing techniques discussed here the MIA can be used for semi-high throughput drug screening to significantly widen the pool of known anti-invasive compounds.

Compounds were successfully screened based on their potential to inhibit intraerythrocytic parasite stages and invasive merozoites. Four compounds were screened these being vanadate, edelfosine, dioctyl sodium sulfosuccinate (DSS) and gentamicin. The inhibitor effect of vanadate is influenced by its redox state which is concentration dependent in solution. Monomeric vanadate was assessed for its potential inhibitory activity against serine proteases, however, the compound also exhibits activity against ATPases and several other enzymes, while tetrameric vanadate was assessed for its inhibitory potential against PI-PLC. Monomeric vanadate demonstrated antimalarial activity by inhibition of intraerythrocytic stages which was assessed using the MSF assay and showed a stage specific inhibition for ring and early trophozoites stages of the lifecycle. Monomeric vanadate showed some anti-invasive activity, while tetrameric vanadate inhibited invasion to the greatest extent. However, the concentrations required to promote tetrameric vanadate were higher than what would be physiologically acceptable and it was expected that inhibition at these concentrations would be caused by various phosphate metabolising inhibition effects resulting in the toxic effects measured. The inhibitory effects of vanadate were thus expected to be related to inhibition of enzymes involved in intraerythrocytic stages with a secondary or indirect inhibition on invasion. DSS has been shown to have an inhibitory effect on proteolytic enzymes and was screened by MSF and merozoite invasion assays, however, although showing inhibition against intraerythrocytic stages, DSS showed no invasion inhibition and demonstrated a haemolytic effect at higher concentrations. In addition to gentamicin's antibacterial effect, the compound has shown inhibitory effects against PI-PLC and phospholipase A2. However, gentamicin showed limited inhibitory effect against intraerythrocytic stages and none against merozoite invasion. Edelfosine demonstrated antimalarial and anti-invasive activity and inhibited invasion to the greatest extent of those assessed at physiologically applicable concentrations. Edelfosine caused ~60% inhibition of invasion at 100 µM, and was used for treatments where the changes in the proteome were assessed by mass spectrometric analysis. The effects of physiologically relevant concentrations of edelfosine on the expression of GPI-anchored proteins were then assessed with the goal of providing new insight and extending existing knowledge pertaining to the potential use of anti-GPI-anchored compounds as treatment against malaria.

Merozoites were isolated, treated and incubated for defined time points and successful protein separation was carried out using sodium dodecyl sulphate-polyacrylamide gel electrophoresis (SDS-PAGE). The resulting protein fingerprints showed high quality protein bands with reproducible protein mass separations. Parasite protein alterations were visualised by assessing protein expression during the time that merozoites were invasive and again after they had lost invasive capacity in both untreated and 100 µM edelfosine treated samples. Lanes of interest were excised, in-gel trypsinised and successful peptide sequencing was carried out using liquid chromatography tandem mass spectrometry (LC-MS/MS). High quality sequence data was obtained and searching against human and *Plasmodium* sequence databases, where a large number of merozoite proteins of varying abundances were identified with high confidence. Proteomic analysis was successfully conducted using ProteinPilot and PeptideShaker. The difference in protein abundance between 5 min and 120 min demonstrates the importance of working with merozoites that have invasive capacity as previous merozoite research would have been conducted on merozoites proteins which are no longer invasive. This study highlights the importance to optimise and reassess previous work as new methods become available - as new important proteins may now be visualised and better characterised. In these experiments merozoites were not exposed to erythrocytes and thus differences in identification of cleaved or released GPI-anchored proteins into the soluble fraction in comparison to proteins remaining associated to the merozoite (recovered as a pellet) highlight important factors concerning the release, processing, triggers and timing involved in the GPI-anchor and GPI-anchored protein's role in invasion. The assessment of relative abundance of proteins was carried out using spectral counting which correlated to protein abundance by using the number of peptide to spectrum matches obtained from the single LC-MS/MS run. Samples were run in triplicate on SDS-PAGE gels while were analysed in a single run by LC-MS/MS. As one gel was analysed by LC-MS/MS in this research, the lack of replicates analysed infers that these results can be used to indicate trends and patterns without definitive conclusions. Label-free analysis by means of spectral counting was used to assess proteomic alterations in terms of the presence, abundance, and cleavages of GPI-anchored proteins on the merozoite. Label-free analysis is adequate for total protein identification and spectral counting can be used to assess relative changes in abundance. However, technical and biological variation can significantly affect both protein identification and protein abundance, thus spectral counting after using data-dependent acquisition (DDA) mass spectrometric techniques would not be sensitive enough to measure small proteomic changes induced by the treatment or changes that over a relatively short time where protein synthesis is

not expected to contribute to the major changes taking place. Thus protein abundance comparisons would be considered significant only where a multi-fold change is identified.

This study did further characterise GPI-anchored proteins and suggestions concerning the processing of these proteins can be proposed. Merozoite invasion is a finely coordinated process. GPI-anchored protein cleavage occurs in a complicated and synchronised step wise manner. Proteases such as SUB1 are involved in the priming of some merozoite proteins. The complete processing by SUB1 was not identified, where rate limiting cleavage steps appeared to have not been completed in the absence of invasion. The SUB1 rate limiting cleavages did not significantly change over time or with treatment which indicates that the cleavage is dependent on an additional trigger for complete processing. Some GPI-anchored proteins can be released in the absence of erythrocytes and in the absence of invasion. While other GPI-anchored proteins remain associated to the merozoite surface after invasive capacity has been lost. The loss of merozoite invasive capacity has been suggested to be caused by a loss or release of GPI-anchored merozoite surface proteins after egress. However, this was not universally found. For example, large amounts of MSP1 was released from the merozoite surface but a significant amount remained pellet associated over time. Other GPI-anchored surface proteins showed limited change over time: the spectral count of micronemal proteins was unchanged over time, and rhoptry proteins appeared not to have been released. This suggests that the merozoite can control the full release of GPI-anchored proteins, and that changes in these GPI-anchored proteins may not be responsible for the loss of invasive capacity. The lack of complete release of merozoite proteins also indicates that further triggers are required for protein release and cleavage, which could be coordinated after recognition of erythrocytes, and formation of tight junction.

The merozoite proteins were distinctively processed in preparation for invasion. The distinct processing of individual proteins, and families of proteins during the invasive phase until the time that the merozoite loses invasive capacity highlights the complexity of the malaria parasite, and indicates the diversity of the proteins involved in this process. In some cases, modification events and proteases involved are well defined. In other cases, the precise mechanisms, cleavages and proteases involved are still not identified. The analysis of merozoite proteins over time was conducted to gain a better understanding of functions and biology of the merozoite. The findings of this study was in agreement with the known understanding of GPI-anchored proteins, while some less explored GPI-anchored proteins and processes were further characterised. The findings of this study can be used for improved merozoite specific studies in terms of optimised

culturing, antimalarial and anti-invasive drug screening techniques and lay a foundation for further merozoite studies on invasion and GPI-anchored proteome with the aim to develop novel antimalarial drugs and vaccines against this rampant disease.

4.2 Improvements and future perspectives

Despite the fact that the aims and objectives were achieved, the analysis of the merozoite proteome and the effects of drugs on the levels of expressed protein is increasing and therefore improvements to these methods should be incorporated to improve future studies:

- *P. falciparum* strains differ in terms of virulence and kinetic proteins, thus culturing techniques could be improved by further strain specific optimisation. Characterisation of the strain specific half-life, optimum temperatures for invasion, and optimum ratios of merozoites to erythrocytes could improve culturing, results from merozoite invasion assays, and improve proteomic results.

- After forced egress from schizonts, the merozoites suspensions contained haemozoin crystals, these should be removed in certain experimental applications such as assays of immune responses. It has not been determined if the crystals provide some hindrance to invasion even as mechanical obstructions[63]. Further analyses for MIAs and proteomics could remove the crystals by passage through a magnetic column or separation with magnetic beads or column-free immunomagnetic separation methods can be used.

- Proteomic analyses could be conducted on merozoite soluble proteins that are exposed to target erythrocytes. In association with the study conducted here, this would give an indication of triggers and additional protein cleavages that occur in the presence of target erythrocytes.

- GPI-anchored merozoite proteins are associated with lipid rafts. Enrichment of these proteins using compounds such as Triton X-100 or Triton X-114 could increase the total abundance of the proteins identified which would aid in the analysis of the GPI-anchored proteome.

- The inclusion of a protease inhibitor cocktail added at specific time points after egress could improve the validity of changes in proteomic abundances identified.

- Haemoglobin was a highly abundant contaminant that significantly influenced protein abundance in quantitative assays and lowered the absolute amount of merozoite protein loaded onto gels. Future research could incorporate a method to remove haemoglobin from protein samples, thereby increasing the amount of merozoite protein that would be

loaded into wells. This would improve clarity at the lower mass region of the SDS-PAGE gels for better analysis of low molecular mass proteins. The increase in merozoite protein concentration would be of benefit for visualisation of proteins present on SDS-PAGE and allow for better identification of less abundant merozoite proteins, and reduce masking of proteins at similar masses on SDS-PAGE and LC-MS/MS.

- The SDS-PAGE gel was cut into fractions which may have contained several bands, thus it was not always possible to identify the exact mass at which a protein was found. This is an issue particularly with proteins that cleave into closely matched mass fragments. Further analyses could then cut gel lanes into more gel fractions for more accurate mass identification. In addition, increasing the number of LC-MS/MS analytical runs from additional SDS-PAGE gels would improve identification of proteins and aid in statistical analyses. This would however, increase the cost and the required analysis time on the LC-MS/MS substantially and must be considered an experimental limitation.

- LC-MS/MS techniques such as data-independent acquisition (DIA) could be used in place of DDA in further analyses. DIA has improved sensitivity and claims to analyse the full set of peptides present in a sample, where DDA analyses selected peptides based on predefined parameters such as abundance and charge. This would increase the number of peptides identified and their respective quantification.

- Two-dimensional electrophoresis (2DE) is considered to be a more sensitive approach and is known for its higher resolving ability over SDS-PAGE. Further proteomic analyses and characterisations could be carried out using 2DE. 2DE does contain its own limitations especially with respect to lipid associated proteins due to solubility and difficulty in obtaining reproducible gels however, once optimised it could be used to better characterise changes that occur to the GPI-anchored proteome.

- Bioinformatic analyses was only conducted on selected proteins associated with the GPI-anchored proteome. However, multiple proteins were affected by edelfosine which would have been overlooked during the selective analysis. Further analyses could include an improved global analysis using software such as Perseus that identifies trends and is well suited for novel discoveries which may highlight potential biological pathways that may be up-regulated or down-regulated.

4.3 Concluding statements

There is a reason as to why malaria still exists today, even after its first known descriptions dating back tens of thousands of years and after the countless initiatives aimed at ridding it from the globe. This is because the malaria parasite is an incredibly intelligent, complex and adaptive disease causing organism. Throughout modern research numerous proteins and pathways have claimed to be the Achilles heel of the malaria disease, including GPI-anchored proteins. However, history and the most recent developments in antimalarial drug resistance re-emphasises the concept that there is no single cure to this disease. With each potential new “cure” used against malaria the parasite adapts to cause resistance to this over time. The parasite is invested in multiple proteins and protein families. One of these families are the GPI-anchored proteins. These proteins have a major similarity which would typically infer that they would be controlled by the same mechanism. However, in *P. falciparum* merozoites it is shown here they the proteins are controlled by multiple enzymes, triggers and control points. The merozoite is known use separate sialic acid dependent and independent pathways for erythrocyte entry after the initial attachment; the utilisation of these pathways can be altered based on environmental aspects that could hinder the parasites ultimate goal of invading the erythrocyte to continue into a new stage of reproduction. The separate mechanisms involved in GPI-anchored protein control suggests that the parasite has the options of utilising multiple mechanisms in GPI-anchored processes as well. This could reason as to why previous studies have found that blockage of single proteins or pathways do not cause complete inhibition of invasion or disease progression. These results along with what has previously been reported in literature and history strongly suggest that a multi-targeted strategy that focuses on multiple processes and pathways is required in order to truly have success in conquering malaria on a large scale.

References

1. Roll Back Malaria. *2001-2010 United Nations Decade to Roll Back Malaria: Economic costs of malaria.* Geneva, Switzerland: Roll Back Malaria, World Health Organization, 2010.

2. Singh B, Kim Sung L, Matusop A, Radhakrishnan A, Shamsul SS, Cox-Singh J, Thomas A and Conway DJ. A large focus of naturally acquired Plasmodium knowlesi infections in human beings. *Lancet.* 2004; 363: 1017-24.

3. Snow RW. Global malaria eradication and the importance of Plasmodium falciparum epidemiology in Africa. *BioMed Central.* 2015; 13: 23.

4. World Health Organization. *World Malaria Report 2015.* 2015 ed. Geneva, Switzerland: World Health Organization, 2015.

5. Harper JF and Harmon A. Plants, symbiosis and parasites: a calcium signalling connection. *Nature Reviews: Molecular Cell Biology.* 2005; 6: 555-66.

6. Rosenberg R and Rungsiwongse J. The number of sporozoites produced by individual malaria oocysts. *American Journal of Tropical Medicine and Hygiene.* 1991; 45: 574-7.

7. Gerald N, Mahajan B and Kumar S. Mitosis in the human malaria parasite Plasmodium falciparum. *Eukaryotic cell.* 2011; 10: 474-82.

8. Haldar K, Kamoun S, Hiller NL, Bhattacharje S and van Ooij C. Common infection strategies of pathogenic eukaryotes. *Nature Reviews: Microbiology.* 2006; 4: 922-31.

9. Orjih AU, Ryerse JS and Fitch CD. Hemoglobin catabolism and the killing of intraerythrocytic Plasmodium falciparum by chloroquine. *Experientia.* 1994; 50: 34-9.

10. Chugh M, Sundararaman V, Kumar S, et al. Protein complex directs hemoglobin-to-hemozoin formation in Plasmodium falciparum. *Proceedings of the National Academy of Sciences of the United States of America.* 2013; 110: 5392-7.

11. Bannister LH. Looking for the exit: How do malaria parasites escape from red blood cells? *Proceedings of the National Academy of Sciences of the United States of America.* 2001; 98: 383-4.

12. Bannister LH, Mitchell GH, Butcher GA, Dennis ED and Cohen S. Structure and development of the surface coat of erythrocytic merozoites of Plasmodium knowlesi. *Cell and Tissue Research.* 1986; 245: 281-90.

13. Bannister LH, Hopkins JM, Fowler RE, Krishna S and Mitchell GH. A brief illustrated guide to the ultrastructure of Plasmodium falciparum asexual blood stages. *Parasitology Today.* 2000; 16: 427-33.

14. Cowman AF and Crabb BS. Invasion of red blood cells by malaria parasites. *Cell.* 2006; 124: 755-66.

15. Lew VL. Malaria: surprising mechanism of merozoite egress revealed. *Current Biology.* 2011; 21: R314-6.

16. Baker DA. Malaria gametocytogenesis. *Molecular and Biochemical Parasitology.* 2010; 172: 57-65.

17. Duffy S and Avery VM. Identification of inhibitors of Plasmodium falciparum gametocyte development. *Malaria Journal.* 2013; 12: 408.

18. Reader J, Botha M, Theron A, Lauterbach SB, Rossouw C, Engelbrecht D, Wepener M, Smit A, Leroy D, Mancama D, Coetzer TL and Birkholtz LM. Nowhere to hide: interrogating different metabolic parameters of Plasmodium falciparum gametocytes in a transmission blocking drug discovery pipeline towards malaria elimination. *Malaria Journal.* 2015; 14: 213.

19. Dixon MW, Thompson J, Gardiner DL and Trenholme KR. Sex in Plasmodium: a sign of commitment. *Trends in Parasitology.* 2008; 24: 168-75.

20. Schofield L and Hackett F. Signal transduction in host cells by a glycosylphosphatidylinositol toxin of malaria parasites. *The Journal of Experimental Medicine.* 1993; 177: 145-53.

21. Ropert C and Gazzinelli RT. Signaling of immune system cells by glycosylphosphatidylinositol (GPI) anchor and related structures derived from parasitic protozoa. *Current Opinion in Microbiology.* 2000; 3: 395-403.

22. Gowda DC and Davidson EA. Protein glycosylation in the malaria parasite. *Parasitology Today.* 1999; 15: 147-52.

23. Schofield L, Hewitt MC, Evans K, Siomos MA and Seeberger PH. Synthetic GPI as a candidate anti-toxic vaccine in a model of malaria. *Nature.* 2002; 418: 785-9.

24. Clark IA, Virelizier JL, Carswell EA and Wood PR. Possible importance of macrophage-derived mediators in acute malaria. *Infection and Immunity.* 1981; 32: 1058-66.

25. Schofield L and Grau GE. Immunological processes in malaria pathogenesis. *Nature Reviews: Immunology.* 2005; 5: 722-35.

26. Murphy GS and Oldfield EC, 3rd. Falciparum malaria. *Infectious disease clinics of North America.* 1996; 10: 747-75.

27. Suh IB, Lee KH, Kim YR, et al. Comparison of immunological responses to the various types circumsporozoite proteins of Plasmodium vivax in malaria patients of Korea. *Microbiology and Immunology.* 2004; 48: 119-23.

28. World Health Organization. Severe Malaria. *Tropical Medicine and International Health.* 2014; 19 (Suppl. 1): 7 - 131.

29. Hotez PJ, Molyneux DH, Fenwick A, Ottesen E, Ehrlich Sachs S and Sachs JD. Incorporating a rapid-impact package for neglected tropical diseases with programs for HIV/AIDS, tuberculosis, and malaria. *PLoS Medicine.* 2006; 3: e102.

30. World Health Organization. *World Malaria Report 2014*. Geneva, Switzerland: World Health Organization, 2014.

31. World Health Organization. *Management of severe malaria: a practical handbook.* Geneva, Switzerland: World Health Organization, 2012.

32. Murray CJ, Rosenfeld LC, Lim SS, Andrews KG, Foreman KJ, Haring D, Fullman N, Naghavi M, Lozano R and Lopez AD. Global malaria mortality between 1980 and 2010: a systematic analysis. *Lancet*. 2012; 379: 413-31.

33. Bloland PB. *Drug resistance in malaria.* Switzerland: World Health Organization. 2001.

34. Klein EY. Antimalarial drug resistance: a review of the biology and strategies to delay emergence and spread. *International Journal of Antimicrobial Agents.* 2013; 41: 311-7.

35. Petersen I, Eastman R and Lanzer M. Drug-resistant malaria: molecular mechanisms and implications for public health. *FEBS Letters.* 2011; 585: 1551-62.

36. Foley M and Tilley L. Quinoline antimalarials: mechanisms of action and resistance. *International Journal for Parasitology.* 1997; 27: 231-40.

37. Krogstad DJ, Gluzman IY, Herwaldt BL, Schlesinger PH and Wellems TE. Energy dependence of chloroquine accumulation and chloroquine efflux in Plasmodium falciparum. *Biochemical Pharmacology.* 1992; 43: 57-62.

38. Atroosh WM, Al-Mekhlafi HM, Mahdy MA and Surin J. The detection of Pfcrt and Pfmdr1 point mutations as molecular markers of chloroquine drug resistance, Pahang, Malaysia. *Malaria Journal.* 2012; 11: 251.

39. Chaijaroenkul W, Wisedpanichkij R and Na-Bangchang K. Monitoring of in vitro susceptibilities and molecular markers of resistance of Plasmodium falciparum isolates from Thai-Myanmar border to chloroquine, quinine, mefloquine and artesunate. *Acta Tropica.* 2010; 113: 190-4.

40. O'Neill PM, Barton VE, Ward SA and Chadwick J. 4-Aminoquinolines: Chloroquine, Amodiaquine and Next-Generation Analogues. *Treatment and Prevention of Malaria.* Basel Springer, 2012: 19 - 43.

41. Hall AP, Segal HE, Pearlman EJ, Phintuyothin P and Kosakal S. Amodiaquine resistant falciparum malaria in Thailand. *American Journal of Tropical Medicine and Hygiene.* 1975; 24: 575-80.

42. Croft SL, Duparc S, Arbe-Barnes SJ, Craft JC, Shin CS, Fleckenstein L, Borghini-Fuhrer I and Rim HJ. Review of pyronaridine anti-malarial properties and product characteristics. *Malaria Journal*. 2012; 11: 270.

43. Wang H, Bei ZC, Wang JY and Cao WC. Plasmodium berghei K173: selection of resistance to naphthoquine in a mouse model. *Experimental Parasitology.* 2011; 127: 436-9.

44. Schlitzer M. Antimalarial drugs - what is in use and what is in the pipeline. *Archiv der Pharmazie.* 2008; 341: 149-63.

45. Warhurst DC and Duraisingh MT. Rational use of drugs against Plasmodium falciparum. *Transactions of the Royal Society of Tropical Medicine and Hygiene.* 2001; 95: 345-6.

46. Le Bras J and Durand R. The mechanisms of resistance to antimalarial drugs in Plasmodium falciparum. *Fundamentals and Clinical Pharmacology.* 2003; 17: 147-53.

47. Price RN, Uhlemann AC, van Vugt M, Brockman A, Hutagalung R, Nair S, Nash D, Singhasivanon P, Anderson TJ, Krishna S, White NJ and Nosten F. Molecular and pharmacological determinants of the therapeutic response to artemether-lumefantrine in multidrug-resistant Plasmodium falciparum malaria. *Clinical Infectious Diseases.* 2006; 42: 1570-7.

48. Sisowath C, Stromberg J, Martensson A, Msellem M, Obondo C, Bjorkman A and Gil JP. In vivo selection of Plasmodium falciparum pfmdr1 86N coding alleles by artemether-lumefantrine (Coartem). *Journal of Infectious Diseases.* 2005; 191: 1014-7.

49. Adekunle AI, Pinkevych M, McGready R, Luxemburger C, White LJ, Nosten F, Cromer D and Davenport MP. Modeling the dynamics of Plasmodium vivax infection and hypnozoite reactivation in vivo. *PLoS Neglected Tropical Diseases.* 2015; 9: e0003595.

50. Ashley EA, Dhorda M, Fairhurst RM, Amaratunga C, Lim P, Suon S, Sreng S, Anderson JM, Mao S, Sam B, Sopha C, Chuor CM, Nguon C, Sovannaroth S, Pukrittayakamee S, Jittamala P, Chotivanich K, Chutasmit K, Suchatsoonthorn C, Runcharoen R, Hien TT, Thuy-Nhien NT, Thanh NV, Phu NH, Htut Y, Han KT, Aye KH, Mokuolu OA, Olaosebikan RR, Folaranmi OO, Mayxay M, Khanthavong M, Hongvanthong B, Newton PN, Onyamboko MA, Fanello CI, Tshefu AK, Mishra N, Valecha N, Phyo AP, Nosten F, Yi P, Tripura R, Borrmann S, Bashraheil M, Peshu J, Faiz MA, Ghose A, Hossain MA, Samad R, Rahman MR, Hasan MM, Islam A, Miotto O, Amato R, MacInnis B, Stalker J, Kwiatkowski DP, Bozdech Z, Jeeyapant A, Cheah PY, Sakulthaew T, Chalk J, Intharabut B, Silamut K, Lee SJ, Vihokhern B, Kunasol C, Imwong M, Tarning J, Taylor WJ, Yeung S, Woodrow CJ, Flegg JA, Das D, Smith J, Venkatesan M, Plowe CV, Stepniewska K, Guerin PJ, Dondorp AM, Day NP, White NJ and Tracking Resistance to Artemisinin C. Spread of artemisinin resistance in Plasmodium falciparum malaria. *New England Journal of Medicine.* 2014; 371: 411-23.

51. White NJ. Malaria: a molecular marker of artemisinin resistance. *Lancet.* 2014; 383: 1439-40.

52. Siregar JE, Kurisu G, Kobayashi T, Matsuzaki M, Sakamoto K, Mi-ichi F, Watanabe Y, Hirai M, Matsuoka H, Syafruddin D, Marzuki S and Kita K. Direct evidence for the atovaquone action on the Plasmodium cytochrome bc1 complex. *Parasitology International.* 2015; 64: 295-300.

53. Cobbard SA, Chua HH, Nijagel B, Creek DJ, Ralph SA and McConville MJ. Metabolic Dysregulation Induced in Plasmodium falciparum by Dihydroartemisinin and Other Front-Line Antimalarial Drugs. *Journal of Infectious Diseases.* 2015.

54. White NJ. Assessment of the pharmacodynamic properties of antimalarial drugs in vivo. *Antimicrobial Agents and Chemotherapy.* 1997; 41: 1413-22.

55. Chotivanich K, Tripura R, Das D, Yi P, Day NP, Pukrittayakamee S, Chuor CM, Socheat D, Dondorp AM and White NJ. Laboratory detection of artemisinin-resistant Plasmodium falciparum. *Antimicrobial Agents and Chemotherapy.* 2014; 58: 3157-61.

56. O'Meara WP, Smith DL and McKenzie FE. Potential impact of intermittent preventive treatment (IPT) on spread of drug-resistant malaria. *PLoS Medicine*. 2006; 3: e141.

57. Amaratunga C, Lim P, Suon S, Sreng S, Mao S, Sopha C, Sam B, Dek D, Try V, Amato R, Blessborn D, Song L, Tullo GS, Fay MP, Anderson JM, Tarning J and Fairhurst RM. Dihydroartemisinin-piperaquine resistance in Plasmodium falciparum malaria in Cambodia: a multisite prospective cohort study. *Lancet Infectious Diseases.* 2016.

58. World Health Organization. *World Malaria Report 2013.* Geneva, Switzerland: World Health Organization, 2013.

59. Wilson DW, Langer C, Goodman CD, McFadden GI and Beeson JG. Defining the timing of action of antimalarial drugs against Plasmodium falciparum. *Antimicrobial Agents and Chemotherapy.* 2013; 57: 1455-67.

60. Braun-Breton C, Rosenberry TL and da Silva LP. Induction of the proteolytic activity of a membrane protein in Plasmodium falciparum by phosphatidyl inositol-specific phospholipase C. *Nature.* 1988; 332: 457-9.

61. Kilejian A. Stage-specific proteins and glycoproteins of plasmodium falciparum: identification of antigens unique to schizonts and merozoites. *Proceedings of the National Academy of Sciences of the United States of America.* 1980; 77: 3695-9.

62. Boyle MJ, Wilson DW and Beeson JG. New approaches to studying Plasmodium falciparum merozoite invasion and insights into invasion biology. *International Journal for Parasitology.* 2013; 43: 1-10.

63. Boyle MJ, Wilson DW, Richards JS, Riglar DT, Tetteh KK, Conway DJ, Ralph SA, Baum J and Beeson JG. Isolation of viable Plasmodium falciparum merozoites to define erythrocyte invasion events and advance vaccine and drug development. *Proceedings of the National Academy of Sciences of the United States of America.* 2010; 107: 14378-83.

64. Boyle MJ, Richards JS, Gilson PR, Chai W and Beeson JG. Interactions with heparin-like molecules during erythrocyte invasion by Plasmodium falciparum merozoites. *Blood.* 2010; 115: 4559-68.

65. Gilson PR, Nebl T, Vukcevic D, Moritz RL, Sargeant T, Speed TP, Schofield L and Crabb BS. Identification and stoichiometry of glycosylphosphatidylinositol-anchored membrane proteins of the human malaria parasite Plasmodium falciparum. *Molecular and Cellular Proteomics.* 2006; 5: 1286-99.

66. Koch M and Baum J. The mechanics of malaria parasite invasion of the human erythrocyte - towards a reassessment of the host cell contribution. *Cellular Microbiology.* 2015.

67. Gilson PR and Crabb BS. Morphology and kinetics of the three distinct phases of red blood cell invasion by Plasmodium falciparum merozoites. *International Journal for Parasitology.* 2009; 39: 91-6.

68. Weiss GE, Gilson PR, Taechalertpaisarn T, Tham WH, de Jong NW, Harvey KL, Fowkes FJ, Barlow PN, Rayner JC, Wright GJ, Cowman AF and Crabb BS. Revealing the sequence and resulting cellular morphology of receptor-ligand interactions during Plasmodium falciparum invasion of erythrocytes. *PLoS Pathogens.* 2015; 11: e1004670.

69. Beeson JG, Drew DR, Boyle MJ, Feng G, Fowkes FJ and Richards JS. Merozoite surface proteins in red blood cell invasion, immunity and vaccines against malaria. *FEMS Microbiology Reviews.* 2016; 40: 343-72.

70. Sanders PR, Gilson PR, Cantin GT, Greenbaum DC, Nebl T, Carucci DJ, McConville MJ, Schofield L, Hodder AN, Yates JR, 3rd and Crabb BS. Distinct protein classes including novel merozoite surface antigens in Raft-like membranes of Plasmodium falciparum. *Journal of Biological Chemistry*. 2005; 280: 40169-76.

71. Sanders PR, Kats LM, Drew DR, O'Donnell RA, O'Neill M, Maier AG, Coppel RL and Crabb BS. A set of glycosylphosphatidyl inositol-anchored membrane proteins of Plasmodium falciparum is refractory to genetic deletion. *Infection and Immunity*. 2006; 74: 4330-8.

72. Singh S, Alam MM, Pal-Bhowmick I, Brzostowski JA and Chitnis CE. Distinct external signals trigger sequential release of apical organelles during erythrocyte invasion by malaria parasites. *PLoS Pathogens.* 2010; 6: e1000746.

73. Riglar DT, Richard D, Wilson DW, Boyle MJ, Dekiwadia C, Turnbull L, Angrisano F, Marapana DS, Rogers KL, Whitchurch CB, Beeson JG, Cowman AF, Ralph SA and Baum J. Super-resolution dissection of coordinated events during malaria parasite invasion of the human erythrocyte. *Cell Host Microbe.* 2011; 9: 9-20.

74. Cowman AF, Berry D and Baum J. The cellular and molecular basis for malaria parasite invasion of the human red blood cell. *Journal of Cell Biology*. 2012; 198: 961-71.

75. Duraisingh MT, Triglia T, Ralph SA, Rayner JC, Barnwell JW, McFadden GI and Cowman AF. Phenotypic variation of Plasmodium falciparum merozoite proteins directs receptor targeting for invasion of human erythrocytes. *EMBO Journal.* 2003; 22: 1047-57.

76. Baum J, Richard D, Healer J, Rug M, Krnajski Z, Gilberger TW, Green JL, Holder AA and Cowman AF. A conserved molecular motor drives cell invasion and gliding motility across malaria life cycle stages and other apicomplexan parasites. *Journal of Biological Chemistry.* 2006; 281: 5197-208.

77. Haldar K and Mohandas N. Erythrocyte remodeling by malaria parasites. *Current Opinion in Hematology.* 2007; 14: 203-9.

78. Bannister LH, Butcher GA, Dennis ED and Mitchell GH. Structure and invasive behaviour of Plasmodium knowlesi merozoites in vitro. *Parasitology.* 1975; 71: 483-91.

79. Oeuvray C, Bouharoun-Tayoun H, Gras-Masse H, Bottius E, Kaidoh T, Aikawa M, Filgueira MC, Tartar A and Druilhe P. Merozoite surface protein-3: a malaria protein inducing antibodies that promote Plasmodium falciparum killing by cooperation with blood monocytes. *Blood.* 1994; 84: 1594-602.

80. Naik RS, Branch OH, Woods AS, Vijaykumar M, Perkins DJ, Nahlen BL, Lal AA, Cotter RJ, Costello CE, Ockenhouse CF, Davidson EA and Gowda DC. Glycosylphosphatidylinositol anchors of Plasmodium falciparum: molecular characterization and naturally elicited antibody response that may provide immunity to malaria pathogenesis. *Journal of Experimental Medicine.* 2000; 192: 1563-76.

81. Cova M, Rodrigues JA, Smith TK and Izquierdo L. Sugar activation and glycosylation in Plasmodium. *Malaria Journal.* 2015; 14: 427.

82. Smith TK, Sharma DK, Crossman A, Dix A, Brimacombe JS and Ferguson MA. Parasite and mammalian GPI biosynthetic pathways can be distinguished using synthetic substrate analogues. *The EMBO Journal.* 1997; 16: 6667-75.

83. Gerold P, Dieckmann-Schuppert A and Schwarz RT. Glycosylphosphatidylinositols synthesized by asexual erythrocytic stages of the malarial parasite, Plasmodium falciparum. Candidates for plasmodial glycosylphosphatidylinositol membrane anchor precursors and pathogenicity factors. J*ournal of Biological Chemistry*. 1994; 269: 2597-606.

84. Tsai YH, Liu X and Seeberger PH. Chemical biology of glycosylphosphatidylinositol anchors. *Angewandte Chemie. International Ed. In English.* 2012; 51: 11438-56.

85. Paulick MG and Bertozzi CR. The glycosylphosphatidylinositol anchor: a complex membrane-anchoring structure for proteins. *Biochemistry.* 2008; 47: 6991-7000.

86. Low MG. Glycosyl-phosphatidylinositol: a versatile anchor for cell surface proteins. *Federation of American Societies for Experimental Biology*. 1989; 3: 1600-8.

87. Fotoran WL, Santangelo RM, Medeiros MM, Colhone M, Ciancaglini P, Barboza R, Marinho CR, Stabeli RG and Wunderlich G. Liposomes loaded with P. falciparum merozoite-derived proteins are highly immunogenic and produce invasion-inhibiting and anti-toxin antibodies. *Journal of Controlled Release.* 2015; 217: 121-7.

88. Dreyer AM, Matile H, Papastogiannidis P, Kamber J, Favuzza P, Voss TS, Wittlin S and Pluschke G. Passive Immunoprotection of Plasmodium falciparum-Infected Mice Designates the CyRPA as Candidate Malaria Vaccine Antigen. *The Journal of Immunology.* 2012; 188: 6225-37.

89. Braun-Breton C and Pereira da Silva L. Activation of a Plasmodium falciparum protease correlated with merozoite maturation and erythrocyte invasion. *Biologie Cellulaire.* 1988; 64: 223-31.

90. Counihan NA, Kalanon M, Coppel RL and de Koning-Ward TF. Plasmodium rhoptry proteins: why order is important. *Trends Parasitology.* 2013; 29: 228-36.

91. Berridge MJ and Irvine RF. Inositol phosphates and cell signalling. *Nature.* 1989; 341: 197-205.

92. Raabe A, Berry L, Sollelis L, Cerdan R, Tawk L, Vial HJ, Billker O and Wengelnik K. Genetic and transcriptional analysis of phosphoinositide-specific phospholipase C in Plasmodium. *Experimental Parasitology.* 2011; 129: 75-80.

93. Wichroski MJ and Ward GE. Biosynthesis of glycosylphosphatidylinositol is essential to the survival of the protozoan parasite Toxoplasma gondii. *Eukaryotic cell.* 2003; 2: 1132-6.

94. Smilkstein M, Sriwilaijaroen N, Kelly JX, Wilairat P and Riscoe M. Simple and inexpensive fluorescence-based technique for high-throughput antimalarial drug screening. *Antimicrobial Agents and Chemotherapy.* 2004; 48: 1803-6.

95. Bianco AE, Battye FL and Brown GV. Plasmodium falciparum: rapid quantification of parasitemia in fixed malaria cultures by flow cytometry. E*xperimental Parasitology.* 1986; 62: 275-82.

96. Guerrieri N, Cerletti P, De Vincentiis M, Salvati A and Scippa S. Vanadium inhibition of serine and cysteine proteases. *Comparative Biochemistry and Physiology: Molecular and Integrative Physiology.* 1999; 122: 331-6.

97. Cantley LC, Cantley LG and Josephson L. A characterization of vanadate interactions with the (Na,K)-ATPase. Mechanistic and regulatory implications. *Journal of Biological Chemistry.* 1978; 253: 7361-8.

98. McCallum-Deighton N and Holder AA. The role of calcium in the invasion of human erythrocytes by Plasmodium falciparum. *Molecular and Biochemical Parasitology.* 1992; 50: 317-23.

99. Vizitiu D, Kriste AG, Campbell AS and Thatcher GR. Inhibition of phosphatidylinositol-specific phospholipase C: studies on synthetic substrates, inhibitors and a synthetic enzyme. *Journal of Molecular Recognition.* 1996; 9: 197-209.

100. Crans DC and Schelble SM. Vanadate dimer and tetramer both inhibit glucose-6-phosphate dehydrogenase from Leuconostoc mesenteroides. *Biochemistry.* 1990; 29: 6698-706.

101. Azzouz S, Maache M, Garcia RG and Osuna A. Leishmanicidal activity of edelfosine, miltefosine and ilmofosine. *Basic and Clinical Pharmacology and Toxicology.* 2005; 96: 60-5.

102. Yepes E, Varela MR, Lopez-Aban J, Rojas-Caraballo J, Muro A and Mollinedo F. Inhibition of Granulomatous Inflammation and Prophylactic Treatment of Schistosomiasis with a Combination of Edelfosine and Praziquantel. *PLoS Neglected Tropical Diseases.* 2015; 9: e0003893.

103. Hoffman DR, Hoffman LH and Snyder F. Cytotoxicity and Metabolism of Alkyl Phospholipid Analogues in Neoplastic Cells. *Cancer Research.* 1986; 46: 5803-9.

104. Busto JV, Sot J, Goni FM, Mollinedo F and Alonso A. Surface-active properties of the antitumour ether lipid 1-O-octadecyl-2-O-methyl-rac-glycero-3-phosphocholine (edelfosine). *Biochimica et Biophysica Acta*. 2007; 1768: 1855-60.

105. Modolell M, Andreesen R, Pahlke W, Brugger U and Munder PG. Disturbance of Phospholipid Metabolism during the Selective Destruction of Tumor Cells Induced by Alkyl-lysophospholipids. *Cancer Research.* 1979; 39: 4681-86.

106. Powis G, Seewald MJ, Gratas C, Melder D, Riebow J and Modest EJ. Selective inhibition of phosphatidylinositol phospholipase C by cytotoxic ether lipid analogues. *Cancer Research.* 1992; 52: 2835-40.

107. Seewald MJ, Olsen RA, Sehgal I, Melder DC, Modest EJ and Powis G. Inhibition of growth factor-dependent inositol phosphate Ca^{2+} signaling by antitumor ether lipid analogues. *Cancer Research.* 1990; 50: 4458-63.

108. Jodhka GS, Gouda MW, Medora RS and Knalil SA. Inhibitory effect of dioctyl sodium sulfosuccinate on trypsin activity. *Journal of Pharmaceutical Sciences.* 1975; 64: 1858-62.

109. Tam VH, Kabbara S, Vo G, Schilling AN and Coyle EA. Comparative Pharmacodynamics of Gentamicin against Staphylococcus aureus and Pseudomonas aeruginosa. *Antimicrobial Agents and Chemotherapy.* 2006; 50: 2626-31.

110. Schacht J. Interaction of neomycin with phosphoinositide metabolism in guinea pig inner ear and brain tissues. *Annals of Otology, Rhinology and Laryngology.* 1974; 83: 613-8.

111. Schibeci A and Schacht J. Action of neomycin on the metabolism of polyphosphoinositides in the guinea pig kidney. *Biochemical Pharmacology.* 1977; 26: 1769-74.

112. Krugliak M, Waldman Z and Ginsburg H. Gentamicin and amikacin repress the growth of Plasmodium falciparum in culture, probably by inhibiting a parasite acid phospholipase. *Life Sciences.* 1987; 40: 1253-7.

113. Lipsky JJ and Lietman PS. Aminoglycoside inhibition of a renal phosphatidylinositol phospholipase C. *Journal of Pharmacology and Experimental Therapeutics.* 1982; 220: 287-92.

114. Carlier MB, Laurent G, Claes PJ, Vanderhaeghe HJ and Tulkens PM. Inhibition of lysosomal phospholipases by aminoglycoside antibiotics: in vitro comparative studies. *Antimicrobial Agents and Chemotherapy.* 1983; 23: 440-49.

115. Laurent G, Carlier M-B, Rollman B, Van Hoof Fi and Tulkens P. Mechanism of aminoglycoside-induced lysosomal phospholipidosis: In vitro and in vivo studies with Gentamicin and Amikacin. *Biochemical Pharmacology.* 1982; 31: 3861-70.

116. Kuss C, Gan CS, Gunalan K, Bozdech Z, Sze SK and Preiser PR. Quantitative proteomics reveals new insights into erythrocyte invasion by Plasmodium falciparum. *Molecular and Cellular Proteomics.* 2012; 11: M111 010645.

117. Moll K, Kaneko A, Scherf A and Wahlgren M. *Methods in Malaria Research.* Manassas, 2013.

118. Cranmer SL, Magowan C, Liang J, Coppel RL and Cooke BM. An alternative to serum for cultivation of Plasmodium falciparum in vitro. *Transactions of the Royal Society of Tropical Medicine and Hygiene.* 1997; 91: 363-5.

119. Radfar A, Mendez D, Moneriz C, Linares M, Marin-Garcia P, Puyet A, Diez A and Bautista JM. Synchronous culture of Plasmodium falciparum at high parasitemia levels. *Nature Protocols.* 2009; 4: 1899-915.

120. Lambros C and Vanderberg JP. Synchronization of Plasmodium falciparum erythrocytic stages in culture. *Journal of Parasitology.* 1979; 65: 418-20.

121. Salmon BL, Oksman A and Goldberg DE. Malaria parasite exit from the host erythrocyte: a two-step process requiring extraerythrocytic proteolysis. *Proceedings of the National Academy of Sciences of the United States of America.* 2001; 98: 271-6.

122. Reilly HB, Wang H, Steuter JA, Marx AM and Ferdig MT. Quantitative dissection of clone-specific growth rates in cultured malaria parasites. *International Journal for Parasitology.* 2007; 37: 1599-607.

123. Le Manach C, Scheurer C, Sax S, Schleiferbock S, Cabrera DG, Younis Y, Paquet T, Street L, Smith P, Ding XC, Waterson D, Witty MJ, Leroy D, Chibale K and Wittlin S. Fast in vitro methods to determine the speed of action and the stage-specificity of anti-malarials in Plasmodium falciparum. *Malaria Journal.* 2013; 12: 424.

124. Johnson JD, Dennull RA, Gerena L, Lopez-Sanchez M, Roncal NE and Waters NC. Assessment and continued validation of the malaria SYBR green I-based fluorescence assay for use in malaria drug screening. *Antimicrobial Agents and Chemotherapy.* 2007; 51: 1926-33.

125. Jensen JB. In vitro culture of Plasmodium parasites. *Methods in Molecular Medicine.* 2002; 72: 477-88.

126. Rovira-Graells N, Gupta AP, Planet E, Crowley VM, Mok S, Ribas de Pouplana L, Preiser PR, Bozdech Z and Cortés A. Transcriptional variation in the malaria parasite Plasmodium falciparum. *Genome Research.* 2012; 22: 925-38.

127. Maier AG, Cooke BM, Cowman AF and Tilley L. Malaria parasite proteins that remodel the host erythrocyte. *Nature Reviews: Microbiology*. 2009; 7: 341-54.

128. Sigma Aldrich. Dioctyl sulfosuccinate sodium salt. Safety Data Sheet. Version 5.4 ed.: sigma-aldrich.com, 2015, p. Safety Data Sheet.

129. Tocris Biosciences. Edelfosine Cat. No. 3022. Tocris Bioscience, 2015

130. Santos NC, Figueira-Coelho J, Martins-Silva J and Saldanha C. Multidisciplinary utilization of dimethyl sulfoxide: pharmacological, cellular, and molecular aspects. *Biochemical Pharmacology.* 2003; 65: 1035-41.

131. Murata Y, Watanabe T, Sato M, Momose Y, Nakahara T, Oka S and Iwahashi H. Dimethyl sulfoxide exposure facilitates phospholipid biosynthesis and cellular membrane proliferation in yeast cells. *Journal of Biological Chemistry.* 2003; 278: 33185-93.

132. Walters GO, Miller FM and Worwood M. Serum ferritin concentration and iron stores in normal subjects. *Journal of Clinical Pathology.* 1973; 26: 770-2.

133. Fairhurst RM, Fujioka H, Hayton K, Collins KF and Wellems TE. Aberrant development of Plasmodium falciparum in hemoglobin CC red cells: implications for the malaria protective effect of the homozygous state. *Blood.* 2003; 101: 3309-15.

134. Mata-Cantero L, Lafuente MJ, Sanz L and Rodriguez MS. Magnetic isolation of Plasmodium falciparum schizonts iRBCs to generate a high parasitaemia and synchronized in vitro culture. *Malaria Journal.* 2014; 13: 112.

135. Bates AH, Mu J, Jiang H, Fairhurst RM and Su XZ. Use of magnetically purified Plasmodium falciparum parasites improves the accuracy of erythrocyte invasion assays. *Experimental Parasitology.* 2010; 126: 278-80.

136. Deponte M and Becker K. Plasmodium falciparum-do killers commit suicide? *Trends Parasitology.* 2004; 20: 165-9.

137. Mutai BK and Waitumbi JN. Apoptosis stalks Plasmodium falciparum maintained in continuous culture condition. *Malaria Journal.* 2010; 9: S6.

138. Fivelman QL, McRobert L, Sharp S, Taylor CJ, Saeed M, Swales CA, Sutherland CJ and Baker DA. Improved synchronous production of Plasmodium falciparum gametocytes in vitro. *Molecular and Biochemical Parasitology.* 2007; 154: 119-23.

139. Saul A, Myler P, Mangan T and C. K. Plasmodium falciparum: Automated Assay of Erythrocyte Invasion Using Flow Cytometry. *Experimental Parasitology.* 1981; 54: 8.

140. Trager W, Zung J and Tershakovec M. Initial extracellular development in vitro of erythrocytic stages of malaria parasites (Plasmodium falciparum). *Proceedings of the National Academy of Sciences of the United States of America.* 1990; 87: 5618-22.

141. Childs RA, Miao J, Gowda C and Cui L. An alternative protocol for Plasmodium falciparum culture synchronization and a new method for synchrony confirmation. *Malaria Journal.* 2013; 12: 386-86.

142. Reed MB, Caruana SR, Batchelor AH, Thompson JK, Crabb BS and Cowman AF. Targeted disruption of an erythrocyte binding antigen in Plasmodium falciparum is associated with a switch toward a sialic acid-independent pathway of invasion. *Proceedings of the National Academy of Sciences of the United States of America.* 2000; 97: 7509-14.

143. Arastu-Kapur S, Ponder EL, Fonovic UP, Yeoh S, Yuan F, Fonovic M, Grainger M, Phillips CI, Powers JC and Bogyo M. Identification of proteases that regulate erythrocyte rupture by the malaria parasite Plasmodium falciparum. *Nature Chemical Biology.* 2008; 4: 203-13.

144. Glushakova S, Mazar J, Hohmann-Marriott MF, Hama E and Zimmerberg J. Irreversible effect of cysteine protease inhibitors on the release of malaria parasites from infected erythrocytes. *Cellular Microbiology.* 2009; 11: 95-105.

145. Hill DL, Eriksson EM and Schofield L. High yield purification of Plasmodium falciparum merozoites for use in opsonizing antibody assays. *Journal of Visualized Experiments.* 2014.

146. Lyon JA, Haynes JD, Diggs CL, Chulay JD, Haidaris CG and Pratt-Rossiter J. Monoclonal antibody characterization of the 195-kilodalton major surface glycoprotein of Plasmodium falciparum malaria schizonts and merozoites: identification of additional processed products and a serotype-restricted repetitive epitope. *Journal of Immunology.* 1987; 138: 895-901.

147. Bergmann-Leitner ES, Duncan EH, Mullen GE, Burge JR, Khan F, Long CA, Angov E and Lyon JA. Critical evaluation of different methods for measuring the functional activity of antibodies against malaria blood stage antigens. *American Journal of Tropical Medicine and Hygiene.* 2006; 75: 437-42.

148. Woehlbier U, Epp C, Kauth CW, Lutz R, Long CA, Coulibaly B, Kouyate B, Arevalo-Herrera M, Herrera S and Bujard H. Analysis of antibodies directed against merozoite surface protein 1 of the human malaria parasite Plasmodium falciparum. *Infection and Immunity.* 2006; 74: 1313-22.

149. Chulay JD, Haynes JD and Diggs CL. Plasmodium falciparum: Assessment of in vitro growth by [^{3}H]hypoxanthine incorporation. *Experimental Parasitology.* 1983; 55: 138-46.

150. Arnot DE and Gull K. The Plasmodium cell cycle: facts and questions. *Annals of Tropical Medicine and Parasitology.* 1998; 92: 361.

151. Yayon A, Vande Waa JA, Yayon M, Geary TG and Jensen JB. Stage-dependent effects of chloroquine on Plasmodium falciparum in vitro. *Journal of Protozoology.* 1983; 30: 642-7.

152. Eckstein-Ludwig U, Webb RJ, van Goethem IDA, East JM, Lee AG, Kimura M, O'Neill PM, Bray PG, Ward SA and Krishna S. Artemisinins target the SERCA of Plasmodium falciparum. *Nature.* 2003; 424: 957-61.

153. Krishna S, Woodrow C, Webb R, Penny J, Takeyasu K, Kimura M and East JM. Expression and functional characterization of a Plasmodium falciparum Ca^{2+}-ATPase (PfATP4) belonging to a subclass unique to apicomplexan organisms. *Journal of Biological Chemistry.* 2001; 276: 10782-7.

154. Spillman NJ, Allen RJ, McNamara CW, Yeung BK, Winzeler EA, Diagana TT and Kirk K. Na(+) regulation in the malaria parasite Plasmodium falciparum involves the cation ATPase PfATP4 and is a target of the spiroindolone antimalarials. *Cell Host and Microbe.* 2013; 13: 227-37.

155. Ginsburg H, Kutner S, Krugliak M and Ioav Cabantchik Z. Characterization of permeation pathways appearing in the host membrane of Plasmodium falciparum infected red blood cells. *Molecular and Biochemical Parasitology.* 1985; 14: 313-22.

156. Campbell SA, Thatcher GR. Tetravanadate is an inhibitor of phoshatidyl inositol-specific phospholipase C. *Bioorganic and Medicinal Chemistry Letters.* 1992; 2: 665-58.

157. Crans DC, Willging EM, Butler SR. Vanadate Tetramer as the Inhibiting Species in Enzymes Reactions in Vitro and in Vivo. *Journal of the American Chemical Society.* 1990;112: 428-32

158. Wagner BA, Buettner GR, Oberley LW and Burns CP. Sensitivity of K562 and HL-60 cells to edelfosine, an ether lipid drug, correlates with production of reactive oxygen species. *Cancer Research.* 1998; 58: 2809-16.

159. Rajalingam D, Loftis C, Xu JJ and Kumar TK. Trichloroacetic acid-induced protein precipitation involves the reversible association of a stable partially structured intermediate. *Protein Science.* 2009; 18: 980-93.

160. Paulo JA, Lee LS, Wu B, Repas K, Banks PA, Conwell DL and Steen H. Optimized sample preparation of endoscopic collected pancreatic fluid for SDS-PAGE analysis. *Electrophoresis.* 2010; 31: 2377-87.

161. Nandakumar MP, Shen J, Raman B and Marten MR. Solubilization of trichloroacetic acid (TCA) precipitated microbial proteins via naOH for two-dimensional electrophoresis. *Journal of Proteome Research*. 2003; 2: 89-93.

162. Smith PK, Krohn RI, Hermanson GT, Mallia AK, Gartner FH, Provenzano MD, Fujimoto EK, Goeke NM, Olson BJ and Klenk DC. Measurement of protein using bicinchoninic acid. *Analytical Biochemistry.* 1985; 150: 76-85.

163. Thermo Fisher Scientific. Protein assay compatibility table. In: Thermo Fisher Scientific, (ed.). Online. Thermo Fisher Scientific, Pierce Biotechnology, 2012.

164. Wiechelman KJ, Braun RD and Fitzpatrick JD. Investigation of the bicinchoninic acid protein assay: identification of the groups responsible for color formation. *Analytical Biochemistry.* 1988; 175: 231-7.

165. De St. Groth SF, Webster RG and Datyner A. Two new staining procedures for quantitative estimation of proteins on electrophoretic strips. *Biochimica et Biophysica Acta.* 1963; 71: 377-91.

166. Dyballa N and Metzger S. Fast and Sensitive Coomassie Staining in Quantitative Proteomics. In: Marcus K, (ed.). *Quantitative Methods in Proteomics.* Totowa, NJ: Humana Press, 2012, p. 47-59.

167. Shevchenko A, Tomas H, Havlis J, Olsen JV and Mann M. In-gel digestion for mass spectrometric characterization of proteins and proteomes. *Nature Protocols.* 2006; 1: 2856-60.

168. Egertson JD, MacLean B, Johnson R, Xuan Y and MacCoss MJ. Multiplexed Peptide Analysis using Data Independent Acquisition and Skyline. *Nature Protocols.* 2015; 10: 887-903.

169. Gillette MA and Carr SA. Quantitative analysis of peptides and proteins in biomedicine by targeted mass spectrometry. *Nature Methods.* 2013; 10: 28-34.

170. Aebersold R and Mann M. Mass spectrometry-based proteomics. *Nature.* 2003; 422: 198-207.

171. Zhang B, VerBerkmoes NC, Langston MA, Uberbacher E, Hettich RL and Samatova NF. Detecting differential and correlated protein expression in label-free shotgun proteomics. *Journal of Proteome Research.* 2006; 5: 2909-18.

172. Richards JS, Arumugam TU, Reiling L, Healer J, Hodder AN, Fowkes FJ, Cross N, Langer C, Takeo S, Uboldi AD, Thompson JK, Gilson PR, Coppel RL, Siba PM, King CL, Torii M, Chitnis CE, Narum DL, Mueller I, Crabb BS, Cowman AF, Tsuboi T and Beeson JG. Identification and prioritization of merozoite antigens as targets of protective human immunity to Plasmodium falciparum malaria for vaccine and biomarker development. *Journal of Immunology.* 2013; 191: 795-809.

173. Child MA, Epp C, Bujard H and Blackman MJ. Regulated maturation of malaria merozoite surface protein-1 is essential for parasite growth. *Molecular Microbiology.* 2010; 78: 187-202.

174. Gilson PR, O'Donnell RA, Nebl T, Sanders PR, Wickham ME, McElwain TF, de Koning-Ward TF and Crabb BS. MSP1(19) miniproteins can serve as targets for invasion inhibitory antibodies in Plasmodium falciparum provided they contain the correct domains for cell surface trafficking. *Molecular Microbiology*. 2008; 68: 124-38.

175. Blackman MJ, Heidrich HG, Donachie S, McBride JS and Holder AA. A single fragment of a malaria merozoite surface protein remains on the parasite during red cell invasion and is the target of invasion-inhibiting antibodies. *Journal of Experimental Medicine.* 1990; 172.

176. Blackman MJ. Purification of Plasmodium falciparum merozoites for analysis of the processing of merozoite surface protein-1. *Methods in Cell Biology.* 1994; 45: 213-20.

177. Low A, Chandrashekaran IR, Adda CG, et al. Merozoite surface protein 2 of Plasmodium falciparum: expression, structure, dynamics, and fibril formation of the conserved N-terminal domain. *Biopolymers.* 2007; 87: 12-22.

178. Low A, Chandrashekaran IR, Adda CG, Yao S, Sabo JK, Zhang X, Soetopo A, Anders RF and Norton RS. Merozoite surface protein 2 of Plasmodium falciparum: expression, structure, dynamics, and fibril formation of the conserved N-terminal domain. *Biopolymers.* 2007; 87: 12-22.

179. Ramasamy R. Studies on glycoproteins in the human malaria parasite Plasmodium falciparum. Identification of a myristilated 45kDa merozoite membrane glycoprotein. *Immunology and Cell Biology*. 1987; 65 Pt 5: 419-24.

180. Clark JT, Donachie S, Anand R, Wilson CF, Heidrich HG and McBride JS. 46-53 kilodalton glycoprotein from the surface of Plasmodium falciparum merozoites. *Molecular and Biochemical Parasitology.* 1989; 32: 15-24.

181. Maskus DJ, Bethke S, Seidel M, Kapelski S, Addai-Mensah O, Boes A, Edgü G, Spiegel H, Reimann A, Fischer R, Barth S, Klockenbring T and Fendel R. Isolation, production and characterization of fully human monoclonal antibodies directed to Plasmodium falciparum MSP10. *Malaria Journal.* 2015; 14: 276.

182. Hinds L, Green JL, Knuepfer E, Grainger M and Holder AA. Novel putative glycosylphosphatidylinositol-anchored micronemal antigen of Plasmodium falciparum that binds to erythrocytes. *Eukaryotic cell.* 2009; 8: 1869-79.

183. Black CG, Wang L, Wu T and Coppel RL. Apical location of a novel EGF-like domain-containing protein of Plasmodium falciparum. *Molecular and Biochemical Parasitology.* 2003; 127: 59-68.

184. Rodriguez LE, Curtidor H, Urquiza M, Cifuentes G, Reyes C and Patarroyo ME. Intimate molecular interactions of P. falciparum merozoite proteins involved in invasion of red blood cells and their implications for vaccine design. *Chemical Reviews.* 2008; 108: 3656-705.

185. Obando-Martinez AZ, Curtidor H, Arevalo-Pinzon G, Vanegas M, Vizcaino C, Patarroyo MA and Patarroyo ME. Conserved high activity binding peptides are involved in adhesion of two detergent-resistant membrane-associated merozoite proteins to red blood cells during invasion. *Journal of Medicinal Chemistry.* 2010; 53: 3907-18.

186. Ansari FA, Kumar N, Bala Subramanyam M, Gnanamani M and Ramachandran S. MAAP: malarial adhesins and adhesin-like proteins predictor. *Proteins.* 2008; 70: 659-66.

187. Arumugam TU, Takeo S, Yamasaki T, Thonkukiatkul A, Miura K, Otsuki H, Zhou H, Long CA, Sattabongkot J, Thompson J, Wilson DW, Beeson JG, Healer J, Crabb BS, Cowman AF, Torii M and Tsuboi T. Discovery of GAMA, a Plasmodium falciparum merozoite micronemal protein, as a novel blood-stage vaccine candidate antigen. *Infection and Immunity.* 2011; 79: 4523-32.

188. Taechalertpaisarn T, Crosnier C, Bartholdson SJ, Hodder AN, Thompson J, Bustamante LY, Wilson DW, Sanders PR, Wright GJ, Rayner JC, Cowman AF, Gilson PR and Crabb BS. Biochemical and functional analysis of two Plasmodium falciparum blood-stage 6-cys proteins: P12 and P41. *PloS One.* 2012; 7: e41937.

189. Haase S, Cabrera A, Langer C, Treeck M, Struck N, Herrmann S, Jansen PW, Bruchhaus I, Bachmann A, Dias S, Cowman AF, Stunnenberg HG, Spielmann T and Gilberger TW. Characterization of a conserved rhoptry-associated leucine zipper-like protein in the malaria parasite Plasmodium falciparum. *Infection and Immunity.* 2008; 76: 879-87.

190. Srivastava A, Singh S, Dhawan S, Mahmood Alam M, Mohmmed A and Chitnis CE. Localization of apical sushi protein in Plasmodium falciparum merozoites. *Molecular and Biochemical Parasitology.* 2010; 174: 66-69.

191. Topolska AE, Lidgett A, Truman D, Fujioka H and Coppel RL. Characterization of a membrane-associated rhoptry protein of Plasmodium falciparum. *Journal of Biological Chemistry.* 2004; 279: 4648-56.

192. Osier FH, Mackinnon MJ, Crosnier C, Fegan G, Kamuyu G, Wanaguru M, Ogada E, McDade B, Rayner JC, Wright GJ and Marsh K. New antigens for a multicomponent blood-stage malaria vaccine. *Science Translational Medicine.* 2014; 6: 247ra102.

193. Gaur D, Mayer DC and Miller LH. Parasite ligand-host receptor interactions during invasion of erythrocytes by Plasmodium merozoites. *International Journal for Parasitology.* 2004; 34: 1413-29.

194. Reddy KS, Amlabu E, Pandey AK, Mitra P, Chauhan VS and Gaur D. Multiprotein complex between the GPI-anchored CyRPA with PfRH5 and PfRipr is crucial for Plasmodium falciparum erythrocyte invasion. *Proceedings of the National Academy of Sciences of the United States of America.* 2015; 112: 1179-84.

195. Wickramarachchi T, Devi YS, Mohmmed A and Chauhan VS. Identification and characterization of a novel Plasmodium falciparum merozoite apical protein involved in erythrocyte binding and invasion. *PloS One.* 2008; 3: e1732.

196. Thermo Fisher Scientific. Overview of Protein Electrophporesis. In: Thermo Fisher Scientific, (ed.). Protein Biology Resource Library. Thermo Fisher Scientific 2017.

197. Hao R, Adoligbe C, Jiang B, Zhao X, Gui L, Qu K, Wu S and Zan L. An Optimized Trichloroacetic Acid/Acetone Precipitation Method for Two-Dimensional Gel Electrophoresis Analysis of Qinchuan Cattle Longissimus Dorsi Muscle Containing High Proportion of Marbling. *PloS One*. 2015; 10: e0124723.

198. Seddon AM, Curnow P and Booth PJ. Membrane proteins, lipids and detergents: not just a soap opera. *Biochimica et Biophysica Acta - Biomembranes.* 2004; 1666: 105-17.

199. Sharom FJ and Lehto MT. Glycosylphosphatidylinositol-anchored proteins: structure, function, and cleavage by phosphatidylinositol-specific phospholipase C. *Biochemistry and Cell Biology.* 2002; 80: 535-49.

200. Li N, Shaw AR, Zhang N, Mak A and Li L. Lipid raft proteomics: analysis of in-solution digest of sodium dodecyl sulfate-solubilized lipid raft proteins by liquid chromatography-matrix-assisted laser desorption/ionization tandem mass spectrometry. *Proteomics.* 2004; 4: 3156-66.

201. Yam XY, Birago C, Fratini F, Di Girolamo F, Raggi C, Sargiacomo M, Bachi A, Berry L, Fall G, Curra C, Pizzi E, Breton CB and Ponzi M. Proteomic analysis of detergent-resistant membrane microdomains in trophozoite blood stage of the human malaria parasite Plasmodium falciparum. *Molecular & Cellular Proteomics.* 2013; 12: 3948-61.

202. Yasui K, Uegaki M, Shiraki K and Ishimizu T. Enhanced solubilization of membrane proteins by alkylamines and polyamines. *Protein Science.* 2010; 19: 486-93.

203. Koussis K, Withers-Martinez C, Yeoh S, Child M, Hackett F, Knuepfer E, Juliano L, Woehlbier U, Bujard H and Blackman MJ. A multifunctional serine protease primes the malaria parasite for red blood cell invasion. *EMBO Journal.* 2009; 28: 725-35.

204. Silmon de Monerri NC, Flynn HR, Campos MG, Hackett F, Koussis K, Withers-Martinez C, Skehel JM and Blackman MJ. Global identification of multiple substrates for Plasmodium falciparum SUB1, an essential malarial processing protease. *Infection and Immunity.* 2011; 79: 1086-97.

205. Yeoh S. Subcellular discharge of a serine protease mediates release of invasive malaria parasites from host erythrocytes. *Cell.* 2007; 131: 1072-83.

206. Harris PK, Yeoh S, Dluzewski AR, O'Donnell RA, Withers-Martinez C, Hackett F, Bannister LH, Mitchell GH and Blackman MJ. Molecular identification of a malaria merozoite surface sheddase. *PLoS Pathogens.* 2005; 1: 241-51.

207. Child MA, Harris PK, Collins CR, Withers-Martinez C, Yeoh S and Blackman MJ. Molecular determinants for subcellular trafficking of the malarial sheddase PfSUB2. *Traffic.* 2013; 14: 1053-64.

208. Barale JC, Blisnick T, Fujioka H, Alzari PM, Aikawa M, Braun-Breton C and Langsley G. Plasmodium falciparum subtilisin-like protease 2, a merozoite candidate for the merozoite surface protein 1-42 maturase. *Proceedings of the National Academy of Sciences of the United States of America.* 1999; 96: 6445-50.

209. Clark JT, Anand R, Akoglu T and McBride JS. Identification and characterisation of proteins associated with the rhoptry organelles of Plasmodium falciparum merozoites. *Parasitology Research.* 1987; 73: 425-34.

210. Schofield L, Bushell GR, Cooper JA, Saul AJ, Upcroft JA and Kidson C. A rhoptry antigen of Plasmodium falciparum contains conserved and variable epitopes recognized by inhibitory monoclonal antibodies. *Molecular and Biochemical Parasitology.* 1986; 18: 183-95.

211. Langreth SG, Nguyen-Dinh P and Trager W. Plasmodium falciparum: merozoite invasion in vitro in the presence of chloroquine. *Experimental Parasitology.* 1978; 46: 235-8.

212. Johnson JG, Epstein N, Shiroishi T and Miller LH. Identification of Surface Proteins on Viable Plasmodium knowlesi Merozoites. *Journal of Eukaryotic Microbiology.* 1981; 28: 160-4.

213. Azzouz S, Maache M, Sánchez-Moreno M, Petavy AF and Osuna A. Effect of alkyl-lysophospholipids on some aspects of the metabolism of Leishmania donovani. *Journal of Parasitology.* 2007; 93: 1202-07.

214. Saul A. Kinetic constraints on the development of a malaria vaccine. *Parasite Immunology.* 1987; 9: 1-9.

215. Olivieri A, Collins CR, Hackett F, Withers-Martinez C, Marshall J, Flynn HR, Skehel JM and Blackman MJ. Juxtamembrane shedding of Plasmodium falciparum AMA1 is sequence independent and essential, and helps evade invasion-inhibitory antibodies. *PLoS Pathogens.* 2011; 7: e1002448.

216. Tachado SD, Gerold P, McConville MJ, Baldwin T, Quilici D, Schwarz RT and Schofield L. Glycosylphosphatidylinositol toxin of Plasmodium induces nitric oxide synthase expression in macrophages and vascular endothelial cells by a protein tyrosine kinase-dependent and protein kinase C-dependent signaling pathway. *Journal of Immunology.* 1996; 156: 1897-907.

217. Moran A, Holst O, Brennan PJ and von Itzstein M. *Microbial Glycobiology: Structures, Relevance and Applications.* First Edition ed. London: Elservier, 2009.

218. Baum J, Maier AG, Good RT, Simpson KM and Cowman AF. Invasion by P. falciparum merozoites suggests a hierarchy of molecular interactions. *PLoS Pathogens.* 2005; 1: e37.

219. Berridge MJ and Irvine RF. Inositol trisphosphate, a novel second messenger in cellular signal transduction. *Nature*. 1984; 312: 315-21.

220. Srinivasan P, Beatty WL, Diouf A, Herrera R, Ambroggio X, Moch JK, Tyler JS, Narum DL, Pierce SK, Boothroyd JC, Haynes JD and Miller LH. Binding of Plasmodium merozoite proteins RON2 and AMA1 triggers commitment to invasion. *Proceedings of the National Academy of Sciences of the United States of America.* 2011; 108: 13275-80.

221. Healer J, Crawford S, Ralph S, McFadden G and Cowman AF. Independent translocation of two micronemal proteins in developing Plasmodium falciparum merozoites. *Infection and Immunity*. 2002; 70: 5751-8.

222. Mitchell GH, Thomas AW, Margos G, Dluzewski AR and Bannister LH. Apical membrane antigen 1, a major malaria vaccine candidate, mediates the close attachment of invasive merozoites to host red blood cells. *Infection and Immunity.* 2004; 72: 154-8.

Appendix

Letter of ethical approval

The Research Ethics Committee, Faculty Health Sciences, University of Pretoria complies with ICH-GCP guidelines and has US Federal wide Assurance.
- FWA 00002567, Approved dd 22 May 2002 and Expires 20 Oct 2016.
- IRB 0000 2235 IORG0001762 Approved dd 22/04/2014 and Expires 22/04/2017.

UNIVERSITEIT VAN PRETORIA
UNIVERSITY OF PRETORIA
YUNIBESITHI YA PRETORIA

Faculty of Health Sciences Research Ethics Committee

05/05/2014

Approval Certificate
New Application

Ethics Reference No.: 141/2014

Title: Characterisation of the pre-invasion glycophosphatidylinositol-anchored surface proteins of Plasmodium falciparum merozoites

Dear Miss Tarryn TL Venter

The **New Application** as supported by documents specified in your cover letter for your research received on the 04/04/2014, was approved, by the Faculty of Health Sciences Research Ethics Committee on the 05/05/2014.

Please note the following about your ethics approval:
- Ethics Approval is valid for 2 year
- Please remember to use your protocol number (**141/2014**) on any documents or correspondence with the Research Ethics Committee regarding your research.
- Please note that the Research Ethics Committee may ask further questions, seek additional information, require further modification, or monitor the conduct of your research.

Ethics approval is subject to the following:
- The ethics approval is conditional on the receipt of 6 monthly written Progress Reports, and
- The ethics approval is conditional on the research being conducted as stipulated by the details of all documents submitted to the Committee. In the event that a further need arises to change who the investigators are, the methods or any other aspect, such changes must be submitted as an Amendment for approval by the Committee.

We wish you the best with your research.

Yours sincerely

Dr R Sommers; MBChB; MMed (Int); MPharMed.
Deputy Chairperson of the Faculty of Health Sciences Research Ethics Committee, University of Pretoria

The Faculty of Health Sciences Research Ethics Committee complies with the SA National Act 61 of 2003 as it pertains to health research and the United States Code of Federal Regulations Title 45 and 46. This committee abides by the ethical norms and principles for research, established by the Declaration of Helsinki, the South African Medical Research Council Guidelines as well as the Guidelines for Ethical Research: Principles Structures and Processes 2004 (Department of Health).

♦ Tel:012-3541330 ♦ Fax:012-3541367 Fax2Email: 0866515924 ♦ E-Mail: fhsethics@up.ac.za
♦ Web: //www.healthethics-up.co.za ♦ H W Snyman Bld (South) Level 2-34 ♦ Private Bag x 323, Arcadia, Pta, S.A., 0007